I. A STUDY OF THE CATALYTIC DECOMPOSITION OF NITRIC OXIDE

II. A CHROMATOGRAPHIC APPARATUS AND TECHNIQUE FOR THE ANALYSIS OF NITRIC OXIDE IN NITROGEN

III. KINETICS AND MECHANISM OF THE AIR OXIDATION OF THE DITHIONITE ION ($S_2O_4^{=}$) IN AQUEOUS SOLUTION

Thesis by

Roy Ryosuke Sakaida

In Partial Fulfillment of the Requirements

For the Degree of

Doctor of Philosophy

California Institute of Technology

Pasadena, California

1960

ACKNOWLEDGMENT

Professor William H. Corcoran supervised the work presented in this thesis. His invaluable suggestions and his continued encouragement directed this work to a successful conclusion.

My sincere appreciation goes to Professors William N. Lacey, Paul A. Longwell and Bruce H. Sage for their active interest in the progress of my work and studies and their helpful assistance during my years at the Institute.

Dr. Robert G. Rinker and Yui Loong Wang were instrumental in the completion of my thesis. They assisted me continuously during the course of my work. During thesis preparation, Dr. Rinker reviewed the manuscript and assisted in the preparation of figures and tables, while Mr. Wang assisted in the correlation of experimental data. To these colleagues, I am indebted.

The members of the Chemical Engineering machine shop, Willard DeWitt, George Griffith and Seichi Nakawatase, were very helpful in the construction of the apparatus.

I am grateful to Evelyn Anderson, who typed both the rough and the final draft of the thesis. She worked many long hours in order to expedite its completion.

Financial assistance was received from the California Institute of Technology in the form of Institute Scholarships and Teaching Assistantships and from the Union Carbide Fellowship Fund. Research funds were made available by the Air Pollution Control District of

Los Angeles County. I am grateful for their assistance.

Finally, I sincerely appreciate the patience and understanding of my wife and family, especially during the experimentation program and the final few months of thesis preparation.

ABSTRACT

I. The study of the catalytic decomposition of nitric oxide at a concentration of 0.5% by volume in nitrogen was conducted over a packed bed in a tubular flow reactor. The packed bed was in the form of alumina pellets impregnated with 0.1% by weight of platinum oxide and 3.0% by weight of nickel oxide. Tests which were conducted at pressures of 1 to 15 atm and temperatures of 800 to 1000°F showed that the rate is second-order with respect to the nitric oxide and is retarded by the adsorption of atomic oxygen on the surface of the catalyst.

II. In conjunction with the decomposition studies, a gas chromatographic technique for the analysis of nitric oxide at a concentration of less than 0.5% by volume in nitrogen was developed. The chromatograph column with a length of 8 ft contained silica gel and was operated in a temperature range of 65 to 85°C. Helium was used as the carrier gas, and the eluted components were measured by means of a thermal conductivity cell with dual thermistors.

III. A study of the air oxidation of sodium dithionite in aqueous solution was made. A mechanism was proposed in which the SO_2^- free-radical ion was the reactive intermediate. The rate of oxidation was found to be half-order with respect to the dithionite ion and first-order with respect to molecular oxygen.

TABLE OF CONTENTS

Part I

A STUDY OF THE CATALYTIC DECOMPOSITION OF NITRIC OXIDE

INTRODUCTION

In many industrial or heavily populated areas, the air-pollution problem is acute because natural processes of purification are inadequate. Thus, during the past few years there has arisen considerable interest in the prevention and removal of pollutants from the atmosphere. Although these pollutants consist mainly of carbon and sulfur compounds, the presence of nitric oxide, which is produced in high compression engines, power plants, furnaces and other high-temperature equipment, is of extreme importance in contributing to an unhealthful and corrosive atmosphere.

One method of minimizing the addition of nitric oxide to the atmosphere is by catalytic decomposition to its elements, nitrogen and oxygen. Thermodynamic considerations show that the decomposition of nitric oxide is feasible since its equilibrium concentration in air is extremely low. For example, the equilibrium concentration of nitric oxide in air is 0.003% by volume at 1300°F and 0.0002% by volume at 1000°F. The rate of the uncatalyzed reaction, however, is so low at temperatures below 2700°F that the equilibrium concentration is not readily attained.

Although the decomposition of nitric oxide is of both practical and theoretical interest, there is very little information on this subject in the literature. The bulk of the experimental studies on catalytic decomposition occurred during the period between 1923 and 1934 (1,2,3,4,5,6,7,8). During this time, efforts were primarily

directed toward decomposing pure nitric oxide at pressures of one atmosphere or less and at temperatures from 1100 to 2500°F. With the exception of Muller (4) and Schwab (5), who used a variety of metals and metal oxides for catalysts, the experimentalists generally used platinum catalysts. On the basis of these experiments it was generally assumed (3,4,5,7,8) that the reaction was first-order in nitric oxide and was retarded by adsorbed oxygen:

$$r = - \frac{dP_{NO}}{d\theta} = k \frac{P_{NO}}{P_{O_2}} \tag{1}$$

or

$$r = - \frac{dP_{NO}}{d\theta} = \frac{kP_{NO}}{1 + k'P_{O_2}} \tag{2}$$

Bachman (1), however, from his studies in the temperature range of 1900 to 2500°F, proposed that the reaction was second-order with respect to nitric oxide but was also retarded by oxygen:

$$r = - \frac{dP_{NO}}{d\theta} = \frac{k(P_{NO})^2}{P_{O_2}} \tag{3}$$

In 1956, the Armour Research Foundation (9) screened a large number of catalysts to determine their effectiveness in decomposing nitric oxide which was present in nitrogen at a concentration of 0.2% by volume. The conditions of these tests simulated those which are found in automobile exhaust manifolds.

In 1958, Fraser (10) studied the catalytic decomposition of diluted nitric oxide over metal oxides with low surface areas. In this work the temperature was varied from 1700 to 1900°F, and helium was used to dilute the nitric oxide to 10% by volume. A zero-order reaction rate was obtained, and this was attributed to the saturation of active sites on the catalysts.

These earlier studies seemed to confirm the hypothesis that the decomposition of nitric oxide was not affected by the addition of either nitrogen or helium to the reactant stream.

Some work has also been done on the high-pressure decomposition (11,12,13,14,15) of pure nitric oxide. Studies were made at pressures up to 800 atm and temperatures up to 575°F. Products of the decomposition were found to be nitrogen, oxygen and various oxides of nitrogen (N_2O, N_2O_3, NO_2, N_2O_4). Mechanism and rate studies were not made, but it was ascertained qualitatively that the rate of decomposition was increased with increases in either or both temperature and pressure.

Present Work

The purpose of the present work was to develop further knowledge of the kinetics of the catalytic decomposition of nitric oxide. A tubular, flow reactor which contained a packed bed was constructed for use at temperatures up to 1000°F and pressures up to 30 atm. For analysis of the molecular species, a gas chromatography column suitable for separating nitric oxide and nitrogen was developed. Finally, experiments were conducted at temperatures of 800, 900, and 1000°F

and at pressures of 1, 8 and 15 atm over a platinum-nickel catalyst. The feed stream consisted of nitric oxide diluted with nitrogen to a concentration of approximately 0.5% by volume

SUMMARY

A reactor was constructed for the study of the catalytic decomposition of nitric oxide. Several preliminary experiments were conducted in the reactor in order, first, to determine the magnitude of wall effects on the decomposition reaction and, secondly, to select a suitable catalyst for use in extensive kinetic studies of the reaction.

Tests on the wall effects were conducted by filling the reactor tube with turnings of type-304 stainless-steel described in Table 1A in Appendix I. This material was chemically similar to practically all of the surface in the reactor assembly which the nitric oxide contacted at the elevated temperatures and pressures. In later experiments, the tests on wall effects were repeated using an empty reactor. From these studies the minimum feed rate of the reactant was established so that the kinetic study of the catalytic decomposition of nitric oxide could be accomplished with negligible wall effects or homogeneous reactions.

Catalyst evaluation experiments were conducted in order to select a catalyst for the final tests. Girdler's G-43, nickel-platinum catalyst was not only among the most effective of the catalysts tested but also gave the most reproducible results. The description and results of these preliminary experiments are given in Appendix I.

With the G-43 catalyst, studies were made at nine operating conditions, which were combinations of the three temperatures of 800, 900 and 1000°F and the three pressures of 1, 8 and 15 atm. Each of these

operating conditions was repeated using 9.0, 18.0 and 36.0 gm of the catalyst.

Data for each feed rate were tabulated in terms of fractional conversion of nitric oxide. They are presented as functions of temperature and pressure versus the ratio of catalyst weight to molar feed rate. The resulting curves were then analyzed on the basis of rate equations which are presented in Appendix II.

The rate equation which gave the best fit to the data is

$$r = \frac{A(P_{NO})^2}{(1 + B\sqrt{P_{O_2}})^2}$$

For the above rate equation, it was found theoretically that the coefficient A should be a function of both temperature and pressure but that the coefficient B should be a function only of temperature. For this reason, A was correlated empirically as a function of both temperature and pressure and B as a function only of temperature. The correlations apply to the temperature range of 800 to 1000°F and the pressure range of 1 to 15 atm.

APPARATUS

General

A flow diagram of the reactor assembly is shown in Figure 1. Included in the assembly were input and output sample ports to which were attached 12/5 glass ball joints, preheater for the feed stream, the reactor, a manifold and gauges for pressure measurement, a cooler for the product stream, a back-pressure valve, interchangeable Fischer and Porter Tri-flat rotameters and a means of absorbing NO and NO_2 from the exit gases. The reactor and accessory equipment necessary for sample preparation, regulation of temperature, pressure and flow, and measurement of pressure and flow were located inside or mounted on the outside of the reactor bay as shown in Figures 2 and 3.

The reactor bay with approximate dimensions of 9 ft x 30 in. x 30 in. consisted of a steel superstructure covered on three sides respectively with two panels and a double door made of 3/16-in. steel and on the fourth side with a panel made of 1/8-in. aluminum for the mounting of instruments. Two brackets were mounted inside the bay to assist in the support of the reactor and to support the feed-stream preheater and the product-stream cooler.

An instrument bench, which is shown in Figure 4, was located adjacent to the reactor bay and contained the potentiometers for temperature measurement.

A gas-chromatography unit, which was constructed for the kinetics laboratory as a general analytical tool, was used for the analysis of

the feed and product streams. A detailed description of this unit is given in Part II of this thesis.

Reactor

The reactor which is shown in Figure 5 was constructed from a 5/8-in. tube of type-304 stainless-steel with a length of 46 in. and an inside diameter of 0.495 in. A bed of catalyst, supported by perforated metal discs and risers, was packed in the central portion of the reactor to a maximum depth of 15.5 in. A uniform temperature was maintained in the catalyst bed for all lengths up to the maximum.

Six equally-spaced pressure taps were installed on the reactor tube to allow measurement of pressures and differences of pressures in the reactor. The taps consisted of 1/32-in. holes drilled through the wall at 8-in. intervals along one side of the reactor. These were connected to a pressure manifold by means of type-304 stainless-steel tubing having an outside diameter of $\frac{1}{4}$ in.

A thermocouple well was located 90° from each pressure tap and on alternate sides of the taps. Each of the wells consisted of a 0.4-in. length of type-304 stainless-steel rod welded to the reactor and threaded to receive a $\frac{1}{4}$-28 NF fitting. A 0.078-in. hole was drilled through the center of the rod to within 0.010 in. of the inside wall of the reactor and was lined at the bottom with a piece of mica having a thickness of 0.001 in. The mica provided insulation between the reactor and the thermocouple junction. A Stupakoff tube with an outside diameter of 0.078 in. and with double holes was placed in each

of the wells to support and insulate the thermocouple wires. It was held tightly in place by means of a knurled cap which screwed onto the threaded rod. A detailed drawing of a thermocouple well is shown in Figure 5.

Perforated discs, introduced through each end of the reactor to support the catalyst, were made from type-304 stainless-steel stock with a diameter of 0.485 in. and a length of 0.50 in. The center of the stock was bored out along the longitudinal axis to form a thimble with 0.10-in. walls and bottom. On the bottom were drilled as many 0.08-in. holes as possible. The riser for the bottom disc was simply a length of the $\frac{1}{4}$-in., type-304 stainless-steel tube flared and grooved at both ends.

For connections to the feed and output lines the reactor was flared at both ends to fit 37° flare connectors. The reducing unions, also of type-304 stainless-steel, connected the 5/8-in. reactor tube to the $\frac{1}{4}$-in. type-304 stainless-steel tubing. The bulk of the gas-carrying lines in the reactor assembly was made from the $\frac{1}{4}$-in. tubing with a wall thickness of 0.035 in.

For electrical insulation of the reactor from its heater wires, the tube was first coated over its entire length with a 0.3-in. layer of zirconium oxide cement. Over this were wound four sections of Nichrome V resistance wire, each with a resistance of 38 ohms. These were then covered with successive layers of 1/32-in. asbestos tape, 3/16-in. Micro-Quartz insulation, aluminum foil, $\frac{1}{2}$-in. Glass Micro-

Fiber insulation, and finally with an outside covering of aluminum foil. The overall diameter of the completed reactor was slightly under $4\frac{1}{2}$ in. Separate sections of insulation were wrapped at the ends to allow easy access to the end fittings for insertion or removal of catalyst.

The reactor was mounted vertically in the center of the reactor bay and was held stationary by means of the input and output lines and the six pressure-tap lines.

Reactor Accessories

Although gas mixtures were obtained commercially, a sample preparation system for making binary gas mixtures was available in the reactor assembly. As shown in Figure 1, three cylinders of gas could be attached to the system, two of them containing pure gases and one containing the reactant mixture. In preparing a mixture of known composition, the entire system was evacuated with a Duo-Seal vacuum pump. Pure gases were then added to the cylinder for the gas mixture. As the gases were added, the pressure in the cylinder could be measured from less than one micron to 1500 psig by successive use of a McLeod gauge, a mercury manometer and a Bourdon gauge. All lines and connections which were required to withstand greater than one atmosphere pressure were made of type-304 stainless-steel.

The preheater section consisted of a 15-ft length of the $\frac{1}{4}$-in. stainless-steel tubing, coiled to a length of about 9 in., with the outflow leg passing through the center of the coil. This coil fitted

snugly inside a brass tube having an O.D. of $3\frac{1}{2}$ in., a wall thickness of 1/16 in. and a length of 10 in. Over the zirconium oxide cement which was used to insulate the outflow leg was wrapped Nichrome V wire which, with variac control, allowed a variable energy input of up to 700 watts. Between the outflow leg and the inner surface of the coil was a McDanel porcelain tube having an I.D. of $1\frac{1}{2}$ in. and a length of 12 in. Two lengths of Nichrome V wire with a resistance of 15 ohms each were spiraled in $\frac{1}{4}$-in. O.D. coils, which in turn were wound around the McDanel tube. This assembly was located inside a cylindrical shield which was made from a McDanel porcelain tube closed at the top. Vertical slits were cut $\frac{1}{2}$ in. apart around the circumference at both ends of the shield which had a length of 13 in. and an O.D. of 5 in. A heater with 20 ohms resistance was wrapped vertically on the shield by passing the heater wire through the slotted holes in the closed top end and the slits at the base. This assembled preheater, which is partially visible in the lower right of Figure 3, rested on a 9-in. x 9-in. base formed by placing together two $2\frac{1}{2}$-in. x $4\frac{1}{2}$-in. x 9-in. bricks. The preheater was insulated with Micro-Quartz and Fiber-Glas and then covered with aluminum foil.

From the reactor, the gas flowed to the cooler which was a short length of the $\frac{1}{4}$-in. stainless-steel tubing coiled and submerged in a water bath. The bath contained both hot and cold water lines, and the water level was controlled by means of an overflow drain line.

Exit gas which passed through the back-pressure valve expanded to atmospheric pressure and flowed through a Fischer and Porter Tri-flat

rotameter whose calibration was corrected for use with nitrogen because it was originally based on air. The gas then passed through a bed of 60-80 mesh silica gel coated with a solution of H_2SO_4 and CrO_3 for removal of oxides of nitrogen. This stripped gas was then piped into a drain with running water.

Control and Measurement of Pressure and Temperature

The pressure and flow rate in the reactor were controlled by the adjustment of a Matheson Automatic High-Pressure Regulator No. 3, which was attached to the gas cylinder containing the feed mixture, and by the simultaneous adjustment of a $\frac{1}{4}$-in., stainless-steel needle valve which was used as the back-pressure valve.

Pressures above 10 psig were measured with a Bourdon gauge which had a 400 psi scale and was located at the exit of the reactor. For pressures below 10 psig, a Barton No. 199 differential pressure gauge was used. This gauge was connected to the pressure taps on the reactor via a manifold system as shown in Figure 6. For this purpose, instead of measuring the difference in pressure between taps, one measured the pressure difference between a tap and the manifold vent. These pressure gauges were stipulated to be accurate to within 0.5% of the full scale reading by the manufacturers, and these accuracies were confirmed by checks with a pressure balance and mercury manometer. Readings on the Bourdon gauge were consistently between 1 and 2 psi high for the range of 100 to 250 psi.

As mentioned previously the temperatures in the preheater, the feed line leaving the preheater, and the reactor were maintained by

use of resistance-wire heaters. Several 1000-watt fixed heaters were present in the preheater, but its temperature was controlled by two heaters which were connected to variacs. Seven variacs were mounted on the aluminum panel of the reactor bay along the top and on the left side as shown in Figure 2. From right to left, the first four controlled the voltage input into the reactor heaters; the top two on the left controlled the variable heaters in the preheater; and the seventh variac, located on the same vertical line and beneath the battery of fixed-heater switches, controlled the heater voltage to the feed-line between the preheater and the reactor.

At present the voltage input to the reactor equipment is regulated to 115 $\pm$ 1 volts by means of a 10 KVA Stabiline EMT4115 Voltage Regulator. A comparison of the voltage to the reactor equipment before and after installation of the regulator can be made from the charts shown in Figure 2A of Appendix III.

Temperatures in the preheater, the feed-line connecting the preheater to the reactor, and the reactor were measured by means of ten chromel-alumel thermocouples; one was located in the middle of the preheater, another at the exit of the preheater, two in the feed-line and six in the thermocouple wells of the reactor. The calibration of these thermocouples, which were made of 28-gauge chromel P and alumel wires is discussed under Experimental Procedure.

The emfs produced by the thermocouples were measured by means of a Type K-3 Universal Potentiometer. A six-point Micromax recorder was

also used to check attainment of steady-state temperatures. The thermocouple leads could be connected to either or both of the potentiometers by means of a multiple-contact rotary switch and/or by use of jumpers on a plug board.

EXPERIMENTAL PROCEDURE

Calibration of Equipment

As discussed under Apparatus, all of the thermocouples in the reactor assembly were fabricated from the same sources of chromel P and alumel wires. For calibration of the thermocouples, several of them were compared with a standard platinum--platinum-10% rhodium thermocouple which had been calibrated by the National Bureau of Standards. The thermocouples were compared directly with the standard in a variac-controlled furnace. The emfs produced at various temperatures were recorded only after steady state had been attained with respect to each temperature. The difference between the actual temperatures as measured by the N.B.S. thermocouple and the tabulated temperature (N.B.S. Circular 561) for a corresponding emf of a chromel-alumel thermocouple was plotted versus the tabulated temperature. These residual temperature calibrations are presented in Figure 1A and Table 8A in Appendix III. Temperatures in the reactor assembly could then be obtained by converting the emfs of the measuring thermocouples to the tabulated temperatures and then adding the residual temperatures from the plot. The nominal deviation from the curve was approximately $3^{\circ}F$.

The chromatography column was calibrated during each run by using the feed-stream gas which was purchased from Matheson. Mixtures of approximately 0.5% nitric oxide in nitrogen were prepared and calibrated by Matheson. These mixtures were further calibrated by chemical analyses according to ASTM specification No. D-1608-58-T. Since the

range of nitric oxide concentrations was small (from 0.1% to 0.45%), it was assumed that the response of the chromatograph detector was linear with respect to concentration. These calibrations were performed without amplification; but when the detector response was amplified, a 0.25% mixture of nitric oxide in nitrogen was used. In this case, samples were analyzed with and without amplification in order to compute a correction factor for the amplified signal. The circuits of the attenuation and amplification networks, however, were calibrated with a Leeds and Northrup Type K-3 Potentiometer. The detailed operational procedure of the chromatograph is given in Part II of the thesis.

The Tri-flat rotameters, for measuring the reactor exit gas and the chromatograph carrier-gas, were received from the manufacturer with calibration for air. Corrections were made according to the manufacturer's recommendations (16) for use with nitrogen and helium at the approximate temperature and pressure in the rotameter.

Catalyst Data

Eighty of the Girdler G-43 catalyst pellets were measured with a micrometer to obtain their average dimensions. A sample of pellets was sent to the Union Oil Company at Brea, California, for area measurements by means of nitrogen adsorption. Other properties of the G-43 as well as its chemical composition were obtained from the Chemical Products Division of the Chemetron Corporation. These data are tabulated in Table 1.

For each charge of catalyst, the pellets added to and removed from

the reactor were counted and weighed. Also the catalyst bed heights were recorded. Among these measurements listed in Table 2, the weight of removed catalyst was of particular importance because of its use in correlating conversion with kinetic mechanisms.

Before conducting tests with a new charge of catalyst, it was activated at 1050 - 1100°F with a low flow of Linde Hi Purity Dry nitrogen at atmospheric pressure. The drying time usually extended over a period of 2 or 3 days.

Reactor

When not in use, the reactor was usually kept under a slight pressure of nitrogen and at a temperature of approximately 800°F. Prior to a run, each variac was set at a voltage which gave approximately the desired temperature of operation. The thermocouple in the preheater, a thermocouple in the feed line and the four central thermocouples in the reactor were connected to a Micromax recording potentiometer. By observing the continuous record of the thermocouple emfs, the approach to steady state and to the final operating temperature was regulated by adjusting the variacs. Meanwhile the feed-stream gas was passed through the reactor at the desired pressure of operation. Two to three hours were generally required for the system to reach steady state.

About one hour before the first sample was taken, the flow of the product stream was adjusted to a predetermined setting on the rotameter by means of a regulator valve on the cylinder of the reactant gas and

a back-pressure valve on the reactor exit. The valve for the product-sampling port was opened with the sample valve attached. The product stream then passed through the sampler to a nitric oxide scrubber and was subsequently expelled into the atmosphere. During this time, the temperature and pressure in the reactor and the flow rate of the product stream were measured and recorded. If all the variables were steady, a sample was taken. The sampler was then removed from the sample port and attached to the entrance section of the chromatograph column. A second sampler was then placed on the sample port of the reactor. After the air had been flushed through the chromatograph column and the base line had become steady, the contents of the first sampler were analyzed. At the appearance of the final elution peak, a second sample was taken from the reactor. In this manner, at least three samples were taken under identical operating conditions from the reactor. The time interval between samples was 20 to 35 min and was governed by both the analysis time and the degree of fluctuations in the operating conditions. If the three samples were found to agree satisfactorily by inspection of the elution peaks, the feed rate was adjusted to a new value. Thus, a series of runs in a given experiment was conducted at identical temperatures and pressures but each at a different feed rate. In general, $1\frac{1}{2}$ hr were allowed to elapse after a change in feed rate so that steady state could be re-established.

When a series of runs had been completed, the reactor was put on standby condition by adjusting its variacs to give a temperature of

approximately 800°F. All other variacs were turned off. The pressure in the reactor was reduced to atmospheric and calibration samples were withdrawn from the feed-stream sampling port. After the feed-stream samples had been withdrawn, the exit valves on the reactor were closed, and the entire system was pressurized to about 50 psig with nitrogen. After a series of experiments had been completed on a particular bed of catalyst, the reactor was allowed to cool. The top was then opened, and the depth of the void space above the catalyst bed was measured. Finally, the catalyst was emptied from the reactor into a vial and weighed.

THEORY

The general material balance for a component in a reacting system is the basis for designing reactors or for interpreting kinetics data and is represented as follows:

$$\begin{bmatrix}\text{Rate of reactant}\\ \text{added in}\\ \text{feed stream}\end{bmatrix} - \begin{bmatrix}\text{Rate of reactant}\\ \text{lost in}\\ \text{exit stream}\end{bmatrix} - \begin{bmatrix}\text{Rate of reactant}\\ \text{converted}\\ \text{in reactor}\end{bmatrix} = \begin{bmatrix}\text{Rate of reactant}\\ \text{accumulated}\\ \text{in reactor}\end{bmatrix} \tag{4}$$

When a reaction proceeds in a tubular, flow reactor, and the conversion of a reactant varies from point to point, the material balance must be applied to a differential element of the reactor. In a reactor containing a bed of catalyst, the differential element is based on the weight of catalyst.

To simplify the rather complex processes which occur in a flow system, particularly in a catalytic reactor, the one in the present studies was operated isothermally and at steady state. Longitudinal mixing by diffusion and lateral variations of concentration, pressure and velocity were neglected.

Since fouling of the catalyst did not occur, the material balance equation reduces to the following form:

$$\text{Input} - \text{Output} = \text{Conversion} \tag{5}$$

or

$$F(1 - X) - \left[F(1 - X) + \frac{\partial F(1 - X)}{\partial x} dx\right] = rdW \qquad (6)$$

which reduces to

$$FdX = rdW \qquad (7)$$

where:

F = constant feed rate, $\frac{\text{moles A}}{\text{hr}}$

X = fractional conversion of A

dW = weight of catalyst in the differential element

r = net rate of conversion, $\frac{\text{moles A converted}}{(\text{hr})(\text{wt catalyst})}$

There are two types of tubular flow-reactors of interest in experimental studies. One is differential and the other is integral. The discussion here, however, will be limited to the analysis of data for an integral reactor, since this was the type used in the present studies.

Kinetic studies from an engineering standpoint are generally conducted to find rate equations in terms of X so that Equation 7 in its integrated form

$$\frac{W}{F} = \int \frac{dX}{r} \qquad (8)$$

can be used in the design of reactors. With use of an integral reactor, it is necessary to obtain a series of X values as a function of W/F under isothermal conditions. From a plot of X versus W/F, instantaneous

rates can be obtained as a function of X since

$$r = \frac{dX}{d(W/F)} \tag{9}$$

which is the slope of the curve. Based upon the assumptions involved in deriving Equation 8, r is invariant for a fixed W/F regardless of variations in F.

These values of r as a function of X can then be used to find an empirical relationship between r and X or to test a series of postulated rate equations which can be directly inserted into Equation 8. By performing graphical or analytical integrations, values of X vs W/F are obtained. The final test of a selected rate equation, in either case, is to compare the results of the integration of Equation 8 with experimental data.

When using an integral reactor, therefore, knowledge of feed and product compositions, feed rates, weight of catalyst in the reactor and temperature of the reacting system is necessary and sufficient to test proposed rate equations or to find correlations between rate and conversion for use in reactor design.

RESULTS

The discussions of the chromatographic analysis, its results and its sources of error are located in Part II of this thesis. The results of the preliminary studies with the reactor, which included wall effects and choice of catalyst are presented in Appendix I. The results of the catalytic decomposition of nitric oxide on the surface of the G-43 platinum-nickel catalyst are discussed under this section. The computed results of the experimental data are listed in Tables 3, 4 and 5.

Temperature Control

The main source of difficulty in conducting the experiments was the control of temperature. The temperatures in the preheat section and the reactor were maintained by the adjustment of variacs. When the reactor was operated in the temperature range of 800 to 1000°F a difference in setting of approximately five volts was required to change the temperature by 100°F. Once the operating temperature was attained for a given pressure, the temperature could generally be controlled to $\pm$ 2°F if no fluctuation in line voltage occurred. During the hours from 6 a.m. to 9 p.m., however, changes in line voltage up to 10 volts often occurred. This required continuous measurement of temperatures during certain periods of the day in order to compensate for these changes by the adjustment of variacs. To avoid this difficulty, experiments were conducted in such a manner that the periods of time from 9 p.m. to 6 a.m. and weekends were

utilized as much as possible. With installation of the electro-mechanical voltage regulator on the final day of experimentation, a temporary connection between the reactor and regulator was made and tests were conducted. These tests and subsequent tests with the chromatograph confirmed the desirability of having regulated voltage for electrically-heated systems which have non-automatic control.

For unregulated voltage, temperature fluctuations in time intervals between samples were often as great as 10°F. When temperatures fluctuated to such an extent, samples were not taken until the operating temperature was steady for at least 10 min.

Temperature differences in the catalyst bed did not exceed 3°F according to thermocouple readings. The temperature profile was assumed linear between thermocouples; hence the temperature of the catalyst bed was obtained by an arithmetic average.

Pressure Control

The total pressure in the reactor, which was measured with a Bourdon gauge when above 1 atm, could be controlled to within $\pm$ 0.1 atm. For the studies at atmospheric pressure, the differential manometer was used, and for the maximum flow rate at this pressure, the pressure drop was less than 0.007 atm. Since the absolute pressure of the surroundings varied from 0.968 to 0.974 atm, the average pressure for the atmospheric runs was taken as 0.975 $\pm$ 0.01 atm.

For all other conditions of temperature, pressure and flow rate used in this study, the maximum pressure drop through the reactor was less than 0.01 atm, and this was neglected.

Feed Rate

The maximum errors in the feed rate measurements varied from ± 3% at the lower rates to ± 1% at the higher flow rates. These errors were largely due to uncertainties in reading the rotameter scale.

Feed and Product Composition

The composition of the feed gases, which were mixed by the Matheson Company, were either 0.404% or 0.432% nitric oxide in nitrogen to within 4%. Analyses of the mixtures by chromatography positively showed the absence of water and other impurities which would be separable from nitrogen or nitric oxide. Impurities which were not separable from nitrogen or nitric oxide were considered negligible or inconsequential.

The chromatographic analyses of the product gases were interpreted on the basis of calibrations with the feed stream gases. The results of an analysis were used to calculate the percent of nitric oxide in the product mixture and to determine from this, by a material balance, the amount of oxygen present. This approach was sound even though nitrogen and oxygen were eluted simultaneously from the chromatograph column. The maximum amount of oxygen present could not exceed 0.2%. Therefore its contribution to the nitrogen peak was negligible. For perfect gases at a total pressure π and with an initial pressure $(P_{NO})_0$ of nitric oxide, the following relationships were used to compute the conversion and the partial pressures of the gaseous components.

$$P_{NO} = (\%\ NO \text{ from analysis}) \frac{\pi}{100} \tag{10}$$

$$\frac{(P_{NO})_0 - P_{NO}}{(P_{NO})_0} = X \tag{11}$$

$$P_{O_2} = \frac{(P_{NO})_O \, X}{2} \tag{12}$$

$$P_{N_2} = (P_{N_2})_O + \frac{(P_{NO})_O \, X}{2} = \pi - (P_{NO})_O \left(1 - \frac{X}{2}\right) \tag{13}$$

$$\pi = P_{NO} + P_{O_2} + P_{N_2} \tag{14}$$

Weight of Catalyst

The catalyst pellets which were packed into the reactor were weighed and counted before and after use. These values are listed in Table 2. For any specific number of pellets the weights after use were found to reproduce to within 0.2% and were used to calculate the W/F ratio for use in Equation 8.

Data Correlation

Two distinct curves were obtained when X vs W/F was plotted for constant temperature and pressure and thus were treated separately. Figures 7, 8 and 9 are plots of representative samples of data from studies with 9.0 or 18.0 gm of catalyst in the reactor. Figures 10, 11 and 12 show plots of representative samples of data from the studies with 36.0 gm of catalyst. The studies with the 36.0 gm of catalyst bed gave the lower conversion figures, and this is believed to be due to incomplete activation of the catalyst before use. These figures are separated according to pressure, with isotherms plotted for each of the pressures. For convenience, Tables 3, 4 and 5 which contain the tabulated data were divided according to catalyst weight

and further subdivided according to pressure and feed-stream composition.

Several methods were used in an attempt to correlate the data with rate equations which were based on the assumptions listed in Appendix II and which are presented in Tables 6A and 7A of that Appendix. The method of using initial rates proved to be inconclusive because of an insufficient number of operating pressures. Trial-and-error calculations were then made by substituting the simpler rate equations in Tables 6A and 7A into Equation 8 and testing the integrated equations with the data. These calculations were made for one set of data curves at 1000°F and as a result eliminated all of the simpler rate equations except for the following:

$$r = \frac{A(P_{NO})^2}{(1 + B\sqrt{P_{O_2}})^2} \tag{15}$$

In order to check the trial-and-error calculations and the remaining rate equations, a second approach involved the use of the least squares method for which a Burroughs 220 digital computer was utilized. The integrated equations for W/F as a function of X contained transcendental terms which were complex, and the general least squares method was found to be inapplicable. To circumvent this problem, the several rate equations were linearized. For example, Equation 15 when linearized became

$$\frac{P_{NO}}{\sqrt{r}} = \frac{1}{\sqrt{A}} + \frac{B}{\sqrt{A}}\sqrt{P_{O_2}} \tag{16}$$

where P_{NO} and P_{O_2} are functions of conversion as given by Equations 11 and 12. Least squares operations were then performed on equations of this form by using rate and conversion values taken off of smoothed plots of X vs W/F.

These calculations were made, initially, by using individual curves as well as combinations of curves from the data at 1000°F. The constants obtained were substituted into their respectively integrated equations and the resulting curves compared with the data points. Equations which obviously did not fit the data were eliminated from further consideration. A continuation of this procedure confirmed that Equation 15 was the only rate equation to fit all of the curves individually. Since the rates had been measured using smoothed curves which may not have been the best curves for the data, it was necessary to use further trial-and-error calculations to correlate the coefficients of Equation 15 as orderly functions of temperature and pressure.

Correlation of the Constants of Equation 15

The following integrated equation, which resulted from substituting Equation 15 into Equation 8, was used to test and correlate the coefficients of Equation 15.

$$\frac{W}{F} = \frac{1}{A(P_{NO})_O^2}\left[\frac{X}{1-X} + B\sqrt{2(P_{NO})_O}\left(\frac{\sqrt{X}}{1-X} - \frac{1}{2}\ln\frac{1+\sqrt{X}}{1-\sqrt{X}}\right)\right.$$
$$\left. + \frac{B^2(P_{NO})_O}{2}\left(\ln|1-X| + \frac{X}{1-X}\right)\right] \qquad (17)$$

The equations of Appendix II, which were obtained from general methods of deriving rate expressions for catalytic reactions, were used in the interpretation of the coefficients of Equations 15 and 17. As a result A was found to be related functionally to the specific rate constant, the concentration of active sites available on the catalyst surface, and other equilibrium type constants. Likewise, B was related to the adsorption equilibrium constant of atomic oxygen. From these interpretations, A and B were defined as follows:

$$A = k(L - C_{N_2})^2 K' \tag{18}$$

$$B = \left(\frac{C_O}{C_s\sqrt{P_{O_2}}}\right)_{eq} \tag{19}$$

where:

k = specific reaction rate constant

L = concentration of active sites on the catalyst surface

C_{N_2} = concentration of active sites with adsorbed nitrogen

K' = equilibrium type constants

C_O = concentration of active sites with adsorbed atomic oxygen

C_s = concentration of empty active sites

Based on the above stipulations, trial-and-error calculations were carried out to correlate the experimental data with Equation 17 so that B was a function of temperature only and that A was an orderly function of temperature for constant pressures as well as an orderly function of pressure for constant temperatures.

Using the X vs W/F plots as guides, a range of B's was selected for each temperature and the corresponding A's calculated for each curve by use of Equation 17. These ranges of B were estimates based on results of the least squares analyses, and numerically were 50-110 for 800°F, 20-80 for 900°F and 0-70 for 1000°F. By assuming that log B was a consistent function of 1/T, the values of log A were plotted versus 1/T for each pressure, where T is in °R. It was found that with continuous adjustment of B, log A and also log B became almost linear with respect to 1/T for parameters of constant pressure. These functions are shown in Figures 13 and 14. Plots of A versus pressure as shown in Figure 15 gave reasonable loci for parameters of temperature. These were then taken as the final empirically correlated coefficients and are tabulated in Table 6.

The following equations were found to correlate the coefficients A and B as functions of temperature and/or pressure. The pressure range was 0.98 to 15 atm and the temperature range was 800 to 1000°F.

$$A_1 = 39.7\, e^{-3080/T} - 17.32\, e^{-2740/T} \sqrt{P_{N_2}} + 3.18\, e^{-3010/T} P_{N_2} \qquad (20)$$

$$A_2 = 17.33\, e^{-3080/T} - 7.50\, e^{-2740/T} \sqrt{P_{N_2}} + 1.394\, e^{-3010/T} P_{N_2} \qquad (21)$$

$$B = 0.01348\, e^{11160/T} \qquad (22)$$

Values of A_1 or A_2 calculated from Equation 20 or 21 are within 1% of those initially obtained from data for 9.0 and 18.0 gm of catalyst or

36.0 gm of catalyst, respectively. A_2 may also be obtained from Equation 20 after multiplying by an effectiveness factor E. This was necessary because the conversion for 36.0 gm of catalyst was lower than that predicted from the data for 9.0 and 18.0 gm of catalyst. Such an anomaly may possibly be attributed to differences in the conditioning process and in the packing arrangement of the catalyst bed. Values of E are plotted as a function of pressure in Figure 16 and give values of A_2 which may deviate as much as 6% from those tabulated in Table 6.

The values of A and B listed in Table 6 were used in Equation 17 to obtain curves for W/F vs X. These curves are plotted in Figures 7 to 12 for comparison with the experimental data. Although data beyond W/F of 20,000 in Figures 7 to 9 and beyond 32,000 in Figures 10 to 12 were not plotted, they were nevertheless used in the correlations. This omission was intentional because it was convenient for plotting and, in addition, the data of importance were below these limits.

DISCUSSION

Assumptions

Several items were neglected in the derivation of the rate equations presented in the thesis, namely, catalyst fouling, diffusion and the reverse reaction. Experimental data indicated that fouling did not occur for use of the catalyst up to 48 days.

Rough estimates of diffusion in a reacting flow system were made by using the methods presented in Smith (17). These showed that the effect of diffusion on the partial pressure of oxygen was less than 1%. The experimental data also showed that the effects of diffusion were negligible in the range of operating conditions tested.

Overall equilibrium constants for the decomposition of nitric oxide to its elements were calculated for the temperatures 800, 900 and 1000°F from available thermodynamic data of nitric oxide (18). Calculations were also made to determine the equilibrium partial pressure of nitric oxide at each of these temperatures and at 1 atm for an initial mixture of 0.5% nitric oxide in nitrogen. The results of these calculations as presented in Table 9A of Appendix III showed that the reverse reaction was negligible.

Accuracy of Data

One of the major sources of error in the rate studies was the lack of good temperature control because of large fluctuations in line voltage. As discussed under Results, this affected the maintenance of

steady state in the reactor. In fact, on some occasions, temperature fluctuations in the reactor were as high as $\pm$ 10°F over a 10-min period. Undoubtedly, the scattering in the data as shown in Figures 7 to 12 is partially attributable to the temperature fluctuations.

A potential source of error was in the sampling of the reaction products. Although a complete discussion of the sampling procedure for analysis by gas chromatography is given in Part II, it is pertinent to this section to discuss the magnitude of the error resulting from the oxidation of unreacted nitric oxide. Although reactor samples were usually analyzed within 15 min, it was occasionally necessary to store a sample in the glass sampler for as long as 20 min. This was sufficient time for oxygen, which was a product of the decomposition reaction, to react with the remaining nitric oxide to form nitrogen dioxide. Calculations showed that up to 5% of the nitric oxide would be oxidized in a period of 30 min at room temperature. Thus, the samples were analyzed as rapidly as possible to minimize this error.

In general, the overall error which occurred in the chromatographic analysis was magnified in terms of conversion and could be excessively high at lower conversions. As an example, when an error of $\pm$ 5% was obtained in the product analysis, an uncertainty of $\pm$ 45% resulted for a 10% conversion of nitric oxide, and an uncertainty of $\pm$ 20% resulted for a 20% conversion. The scatter in the data, especially for the pressure of 1 atm, was partly attributable to these uncertainties because of low conversion. With sufficient data, however, the overall

uncertainties in drawing curves through plotted data should be substantially reduced.

Initial Rates

The data points near the origin of the X vs W/F plots were subject to the error magnification, as discussed above, because of low conversion. This led to inaccuracies in taking slopes at the origin to obtain initial rates. Other methods, therefore, were used to find these rates. In one method, slopes of the curves were measured as functions of W/F, and the resultant points were plotted and extrapolated to W/F = 0. In a second method X/(W/F) vs W/F was plotted and extrapolated to W/F = 0. The study of these initial rates as proposed by Yang (19) proved to be inconclusive, however, because of an insufficient number of operating pressures.

Correlation of Data by Least Squares

In using least-square methods to correlate the data with integrated rate equations, it was found, as stated under Results, that such methods were not applicable. The least squares method is generally used to find the best correlation of data for straight-line functions and for polynomials in which the functional variations of data are simply related by an equation of the form:

$$y = ax + bx^2 + \ldots + nx^N$$

Typical integrated forms of the rate equations, however, were similar to Equation 17, in which the terms on the right-hand side are

complex functions of x instead of the simpler functions illustrated in the above equation. No general procedure for applying least squares analysis to these types of functions was available.

Pressure Effects

An increase in pressure proportionately increased the concentrations of the gases in the reactor. It also caused an increased adsorption of the gases on the catalyst surface. The amount of each component adsorbed in competition with other components was a function of its relative concentration and adsorptivity. Nitrogen constituted the main bulk of the reaction mixture and was a "pseudo" inert in the sense that a part of it was a product of the nitric oxide decomposition. With its preponderance of concentration over the nitric oxide and oxygen, the nitrogen was adsorbed on the catalyst in greater amounts as the pressure was increased above atmospheric. As a result, it blocked active sites. This process continued until a monomolecular layer of nitrogen was deposited at a pressure which is termed here as the "saturation pressure". At the saturation pressure, the nitrogen began adsorbing in a multimolecular layer on the catalyst, and this reduced the amount of additional adsorption on the active sites. On the other hand, the amount of nitric oxide and oxygen adsorbed on the active sites was continually increasing due to increased pressure above the saturation pressure of nitrogen. By having a higher adsorptivity on the catalyst, these components forced nitrogen off the sites. If the pressure were sufficiently high to build up to the saturation amount

of nitric oxide and oxygen, the decomposition reaction would then become zero-order.

The above qualitative discussion could partially explain the behavior of the coefficient A in Equation 15, which initially decreased in magnitude with increasing pressure and then, after leveling out, began to increase at the higher pressures. It is very probable that at the point of increase the saturation pressure for nitrogen had been attained. From Figure 14, the increase in A began at approximately 12 atm.

Log A vs 1/T

For a homogeneous reaction, the coefficient A would be the specific rate constant of the reaction, and a plot of log A vs 1/T would give an Arrhenius activation energy. In the study of catalysis, A is usually more complex and contains several components such as adsorption constants which may decrease with increase in temperature. Therefore, unless these constants and their values are known, an Arrhenius activation energy cannot be obtained.

An empirical activation energy for the reaction between two adsorbed nitric oxide molecules is given by the slope of Log A_0 vs 1/T. The coefficient A_0 is the first term in Equation 20. A value of 6.1 kcal/gm mole obtained from the slope is considerably less than the values of 40 to 60 kcal/gm mole presented by experimentalists for the homogeneous decomposition of nitric oxide (20).

CONCLUSIONS

The rate of the heterogeneous catalytic decomposition of nitric oxide over a platinum-nickel catalyst supported on activated alumina was found to be second-order with respect to nitric oxide, retarded by atomic oxygen and further retarded by the excess nitrogen in the system. This retardation was due to the components being adsorbed on active catalyst sites, thus, decreasing the number of sites available for the catalysis of the decomposition of nitric oxide.

The rate equation, which was obtained as follows,

$$r = \frac{A(P_{NO})^2}{(1 + B\sqrt{P_{O_2}})^2} \qquad (15)$$

is applicable for the decomposition of nitric oxide present in nitrogen in concentrations of less than 0.5%, within the temperature range of 800 to 1000°F and the pressure range of 1 to 15 atm. A bimolecular surface reaction between two adsorbed nitric oxide molecules is suggested by the rate equation, but it does not uniquely define the sequential steps in the reaction. One series of reaction steps for which Equation 15 is applicable is as follows:

$$NO + s \longrightarrow NOs \qquad (23)$$

$$2NOs \longrightarrow N_2 + 2Os \qquad (24)$$

$$2Os \longrightarrow O_2 + 2s \qquad (25)$$

In the above series of equations s is an empty active site on the surface of the catalyst and Ys is a site with adsorbed Y. Equation 24 is then

the rate-controlling step. The rate equation for this step which is listed as B2 in Table 6A assumes the form of Equation 15 if the term representing the adsorbed nitric oxide is small compared to other terms in the denominator.

Values of A were correlated as functions of temperature and pressure to give the following equation having the units of (gm moles NO converted)/(gm Cat)(hr)(atm^2).

$$A = E(39.7\ e^{-3080/T} - 17.32\ e^{-2740/T}\ \sqrt{P_{N_2}} + 3.18\ e^{-3010/T}\ P_{N_2}) \quad (26)$$

Here, E is related to an effectiveness factor and as indicated under Results is unity for Equation 20 and is a function of pressure as shown in Figure 16 for Equation 21. Log B was approximately a linear function of 1/T and was expressed as follows for both sets of data which were obtained.

$$B = 0.01348\ e^{11160/T}\ (atm^{-\frac{1}{2}}) \quad (22)$$

Equations 22 and 26 when used with Equation 15 correlate data for systems within the range of operating conditions described in this thesis.

For similarly reacting systems, therefore, the ratio of the catalyst weight divided by the feed rate of nitric oxide which is required to obtain a given conversion of nitric oxide can be obtained by using the following equation:

$$\frac{W}{F} = \frac{1}{A(P_{NO})_o^2}\left[\frac{X}{1-X} + B\sqrt{2(P_{NO})_o}\left(\frac{\sqrt{X}}{1-X} - \frac{1}{2}\ln\left|\frac{1+\sqrt{X}}{1-\sqrt{X}}\right|\right)\right.$$
$$\left. + \frac{B^2(P_{NO})_o}{2}\left(\ln|1-X| + \frac{X}{1-X}\right)\right] \qquad (17)$$

In applying Equation 17, additional information required is the operational variables and the value of E.

RECOMMENDATIONS

The following are recommendations based on the present research:

1. Further work using the present apparatus should be conducted, initially, to obtain additional information about the effects of pressure on the constant A of Equation 15.

2. Further studies of the temperature effect on the catalyzed reaction should be carried out at atmospheric pressure and at temperatures up to 2500°F, in a bench-scale quartz reactor.

3. The reactor is so constructed that, with slight modification, the pressure taps can be converted to sample taps. Therefore, the possibility of the reactor being used, as a differential reactor as well as an integral reactor should be investigated.

4. The addition and removal of catalyst can be facilitated by the use of flanged connectors at the ends of the reactor. A design for this item is presented in the APCD#3 logbook No. 2004.

REFERENCES

1. Bachman, P. W. and Taylor, G. B., J. Phys. Chem., 33, 447-455 (1929).

2. Briner, E., Meiner, C., and Rothen, A., J. Chim. Phys., 23, 609-620 (1926), (C.A. 20, 3372[9]).

3. Green, T. E. and Hinshelwood, C. N., J. Chem. Soc., 129, 1709-1713 (1926).

4. Muller, E. and Barck, H., Z. Anorg. Allgem. Chem., 129, 309-320 (1923), (C.A., 17, 3298[2]).

5. Schwab, G., Staeger, R., and Baumbach, H. H., Z. Physik. Chem., B21, 65-83 (1933), (C.A., 27, 3388[7]).

6. Uchida, S., J. Soc. Chem. Ind. (Japan), 30, 171-180 (1927), (C.A., 21, 2414[6]).

7. Zawadski, J. and Badzynski, T., Roczniki Chem., 11, 158-167 (1931), (C.A. 25, 3906[2]).

8. Zawadski, J. and Perlinsky, G., Compt. Rend., 198, 260-262 (1934), (C.A., 28, 2255[1]).

9. "Investigation of Catalytic Decomposition of Nitric Oxide," Armour Research Foundation of Illinois Institute of Technology, Chicago, Illinois, Feb. 21, 1957.

10. Fraser, J. M. and Daniels, F., J. Phys. Chem., 62, 215-220 (1958).

11. Briner, E. and Bouboff, N., Compt. Rend., 156, 228-230 (1913), (C.A., 7, 2523).

12. Briner, E. and Bouboff, N., J. Chim. Phys., 11, 597-631 (1914), (C.A., 8, 1530).

13. Briner, E., and Wroczynski, A., Compt. Rend., 149, 1372-1374 (1910), (C.A., 4, 853).

14. Granier-Mayence, J., Robin, J., and Robin, S., Compt. Rend., 236, 1011-1014 (1953), (C.A., 47, 3115g, 6250h).

15. Schener, O., Wien Ber (IIA), 123, 931-1068 (1914), (C.A., 10, 3011).

16. "Variable-Area Flowmeter Handbook," Fischer and Porter Company, Hatboro, Pennsylvania.

17. Smith, J. M., "Chemical Engineering Kinetics," 234-240, McGraw-Hill Book Co., Inc., 1956, New York.

18. "Physical and Thermodynamic Properties of Elements and Compounds," Chemetron Corp., 1958.

19. Yang, K. H., and Hougen, O. A., Chem. Eng. Prog., 46, 146-157 (1950).

20. Helfrey, P. F., Ph.D. Thesis, California Institute of Technology, 1957.

LIST OF FIGURES

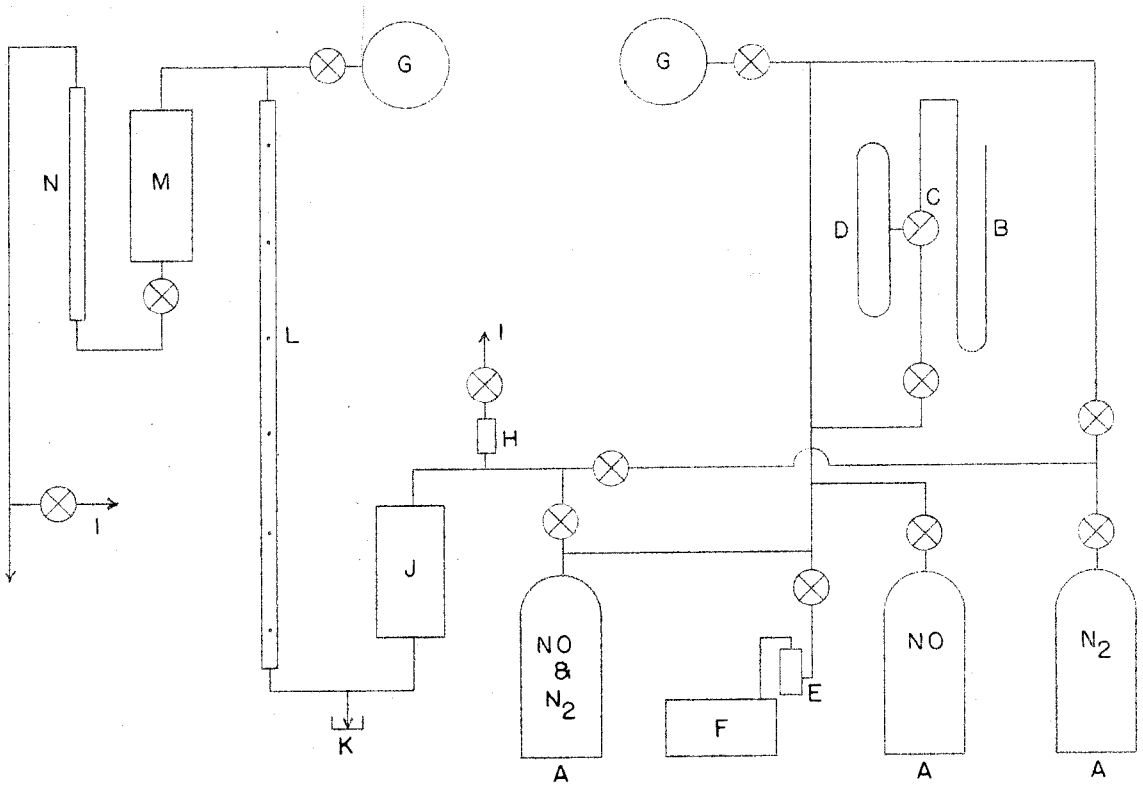

A - Compressed Gas
B - Manometer
C - Stopcock
D - McLeod Gauge
E - Trap
F - Vacuum Pump
G - Bourdon Gauge
H - Check Valve
I - Sample Port
J - Preheater
K - Safety Disc
L - Reactor
M - Cooler
N - Rotameter

Figure 1. Flow Diagram of Reactor Assembly

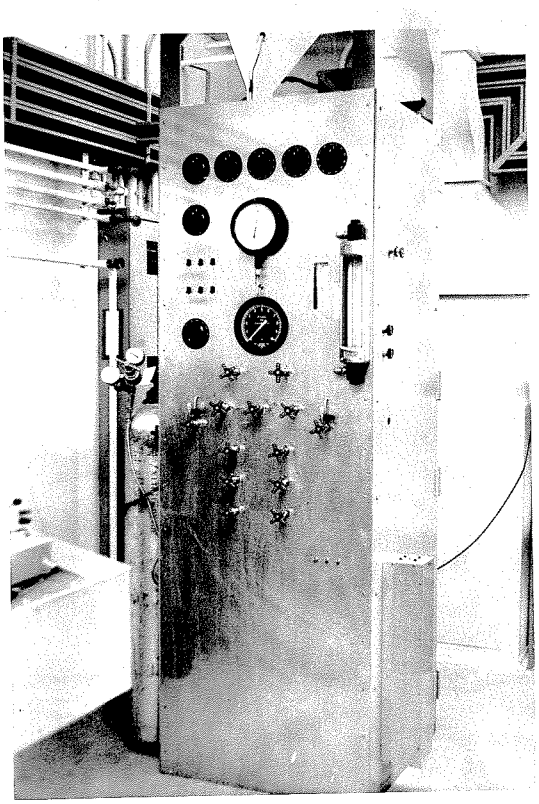

Figure 2. Exterior of Reactor Bay

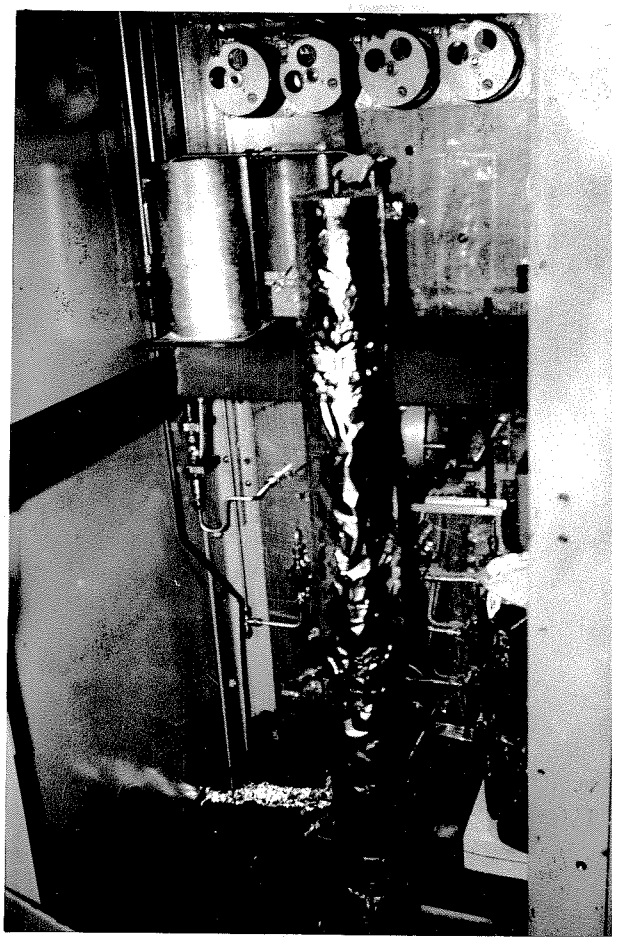

Figure 3. Interior of Reactor Bay

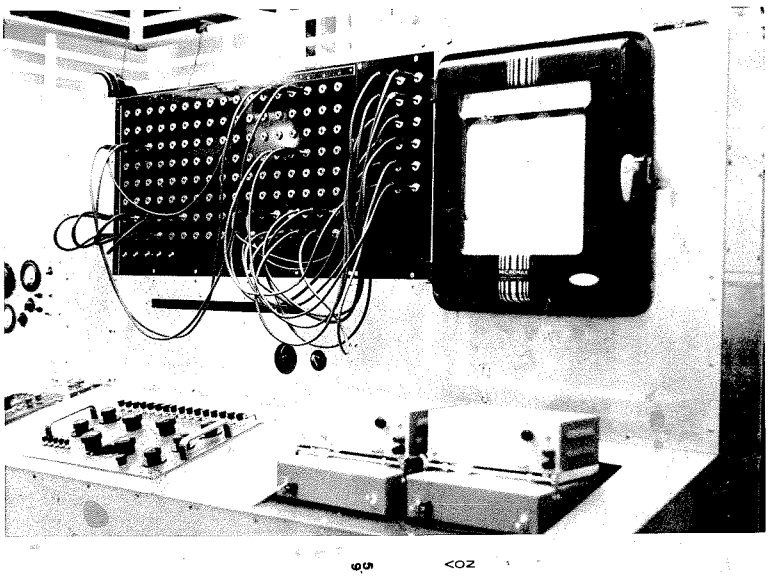

Figure 4. Instrument Bench

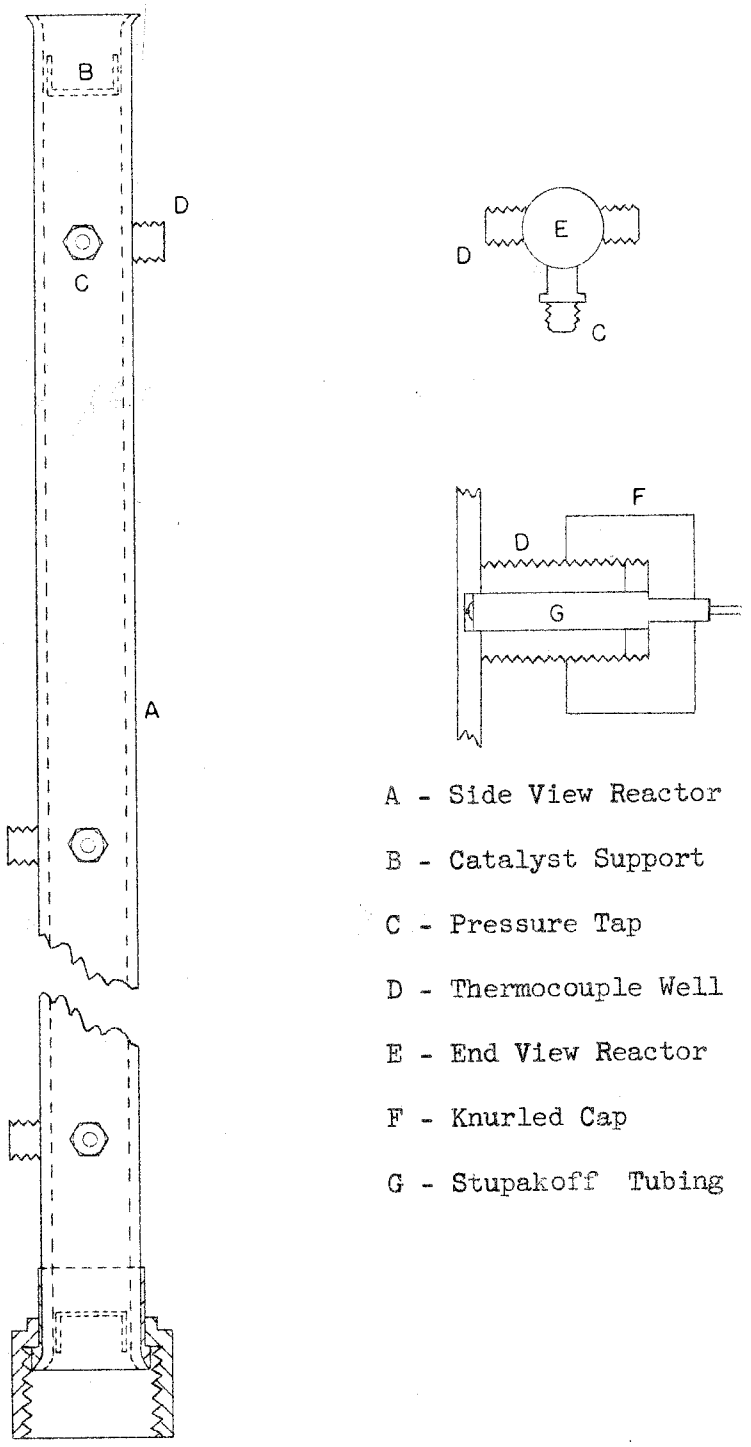

A - Side View Reactor

B - Catalyst Support

C - Pressure Tap

D - Thermocouple Well

E - End View Reactor

F - Knurled Cap

G - Stupakoff Tubing

Figure 5. Detailed Diagram of Reactor

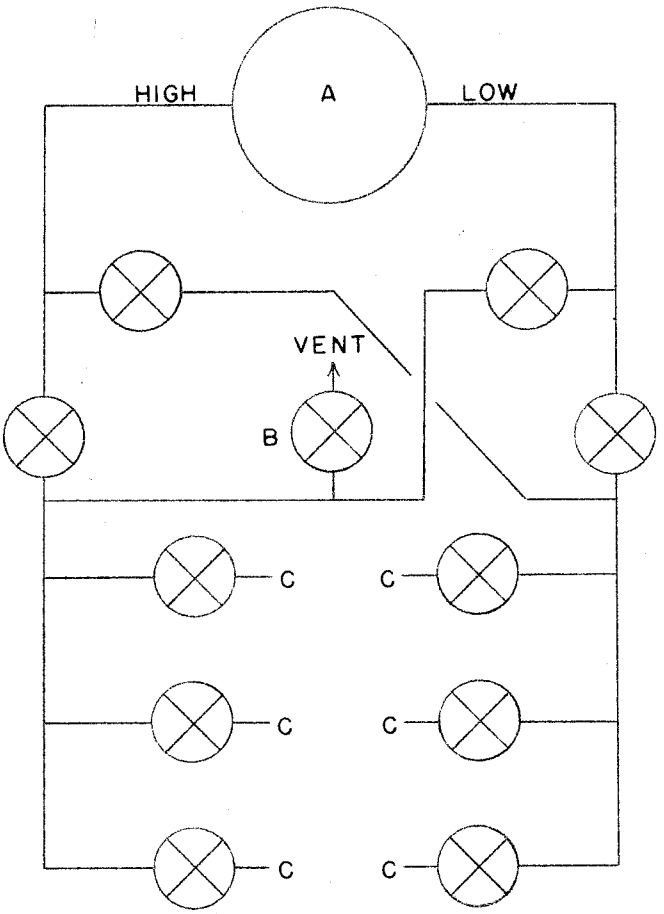

A - Differential Pressure Gauge
B - Stainless-Steel Needle Valve
C - Pressure Taps on Reactor

Figure 6. Differential Pressure Manifold

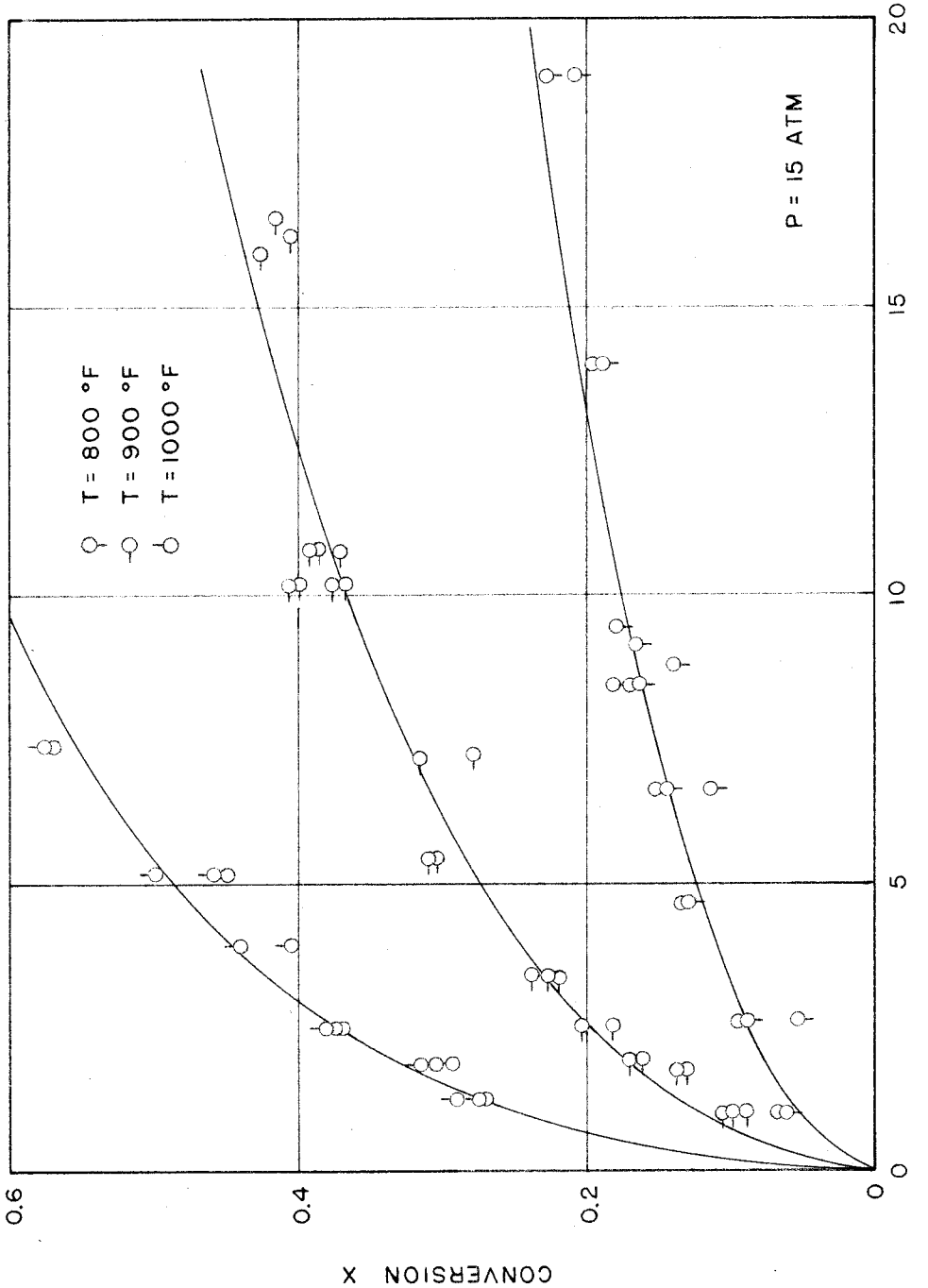

Figure 7. Conversion of NO vs W/F at 15 Atm for 0.432% Initial NO over a Catalyst Bed of 18.0 gm (the curves are plots of Equation 17)

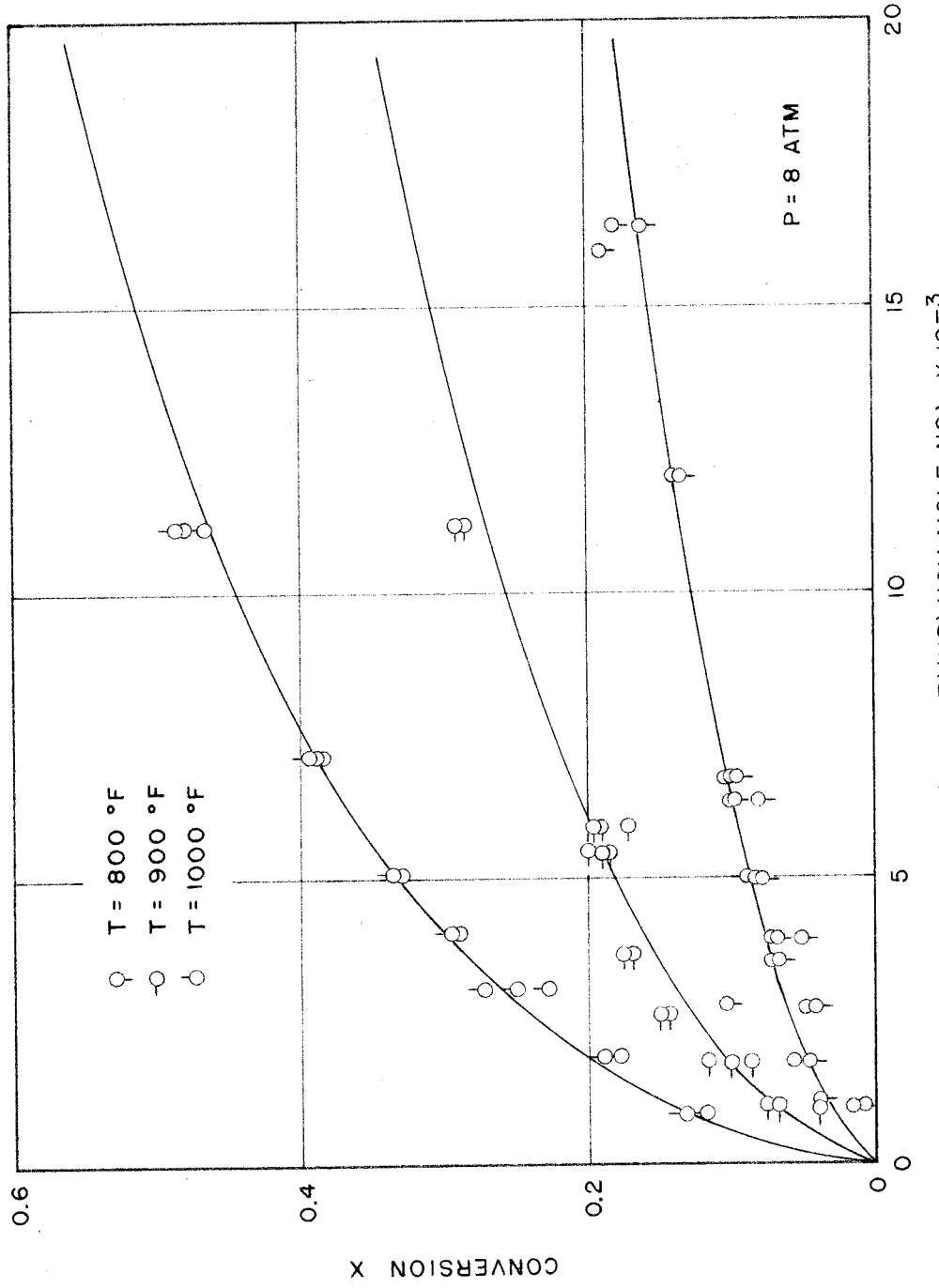

Figure 8. Conversion of NO vs W/F at 8 Atm for 0.432% Initial NO over a Catalyst Bed of 9.0 or 18.0 gm (the curves are plots of Equation 17)

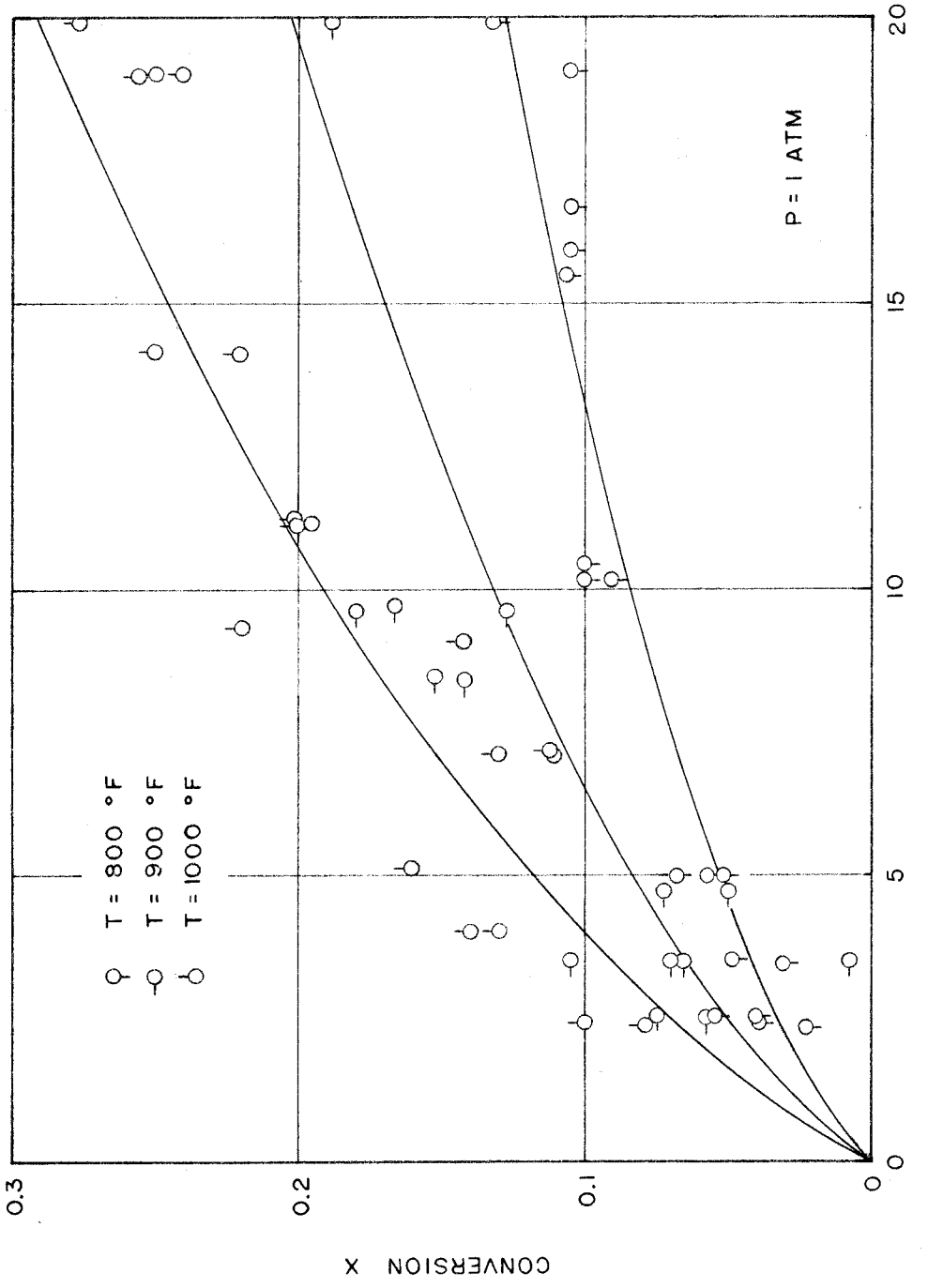

Figure 9. Conversion of NO vs W/F at 1 Atm for 0.432% Initial NO over a Catalyst Bed of 9.0 or 18.0 gm (the curves are plots of Equation 17)

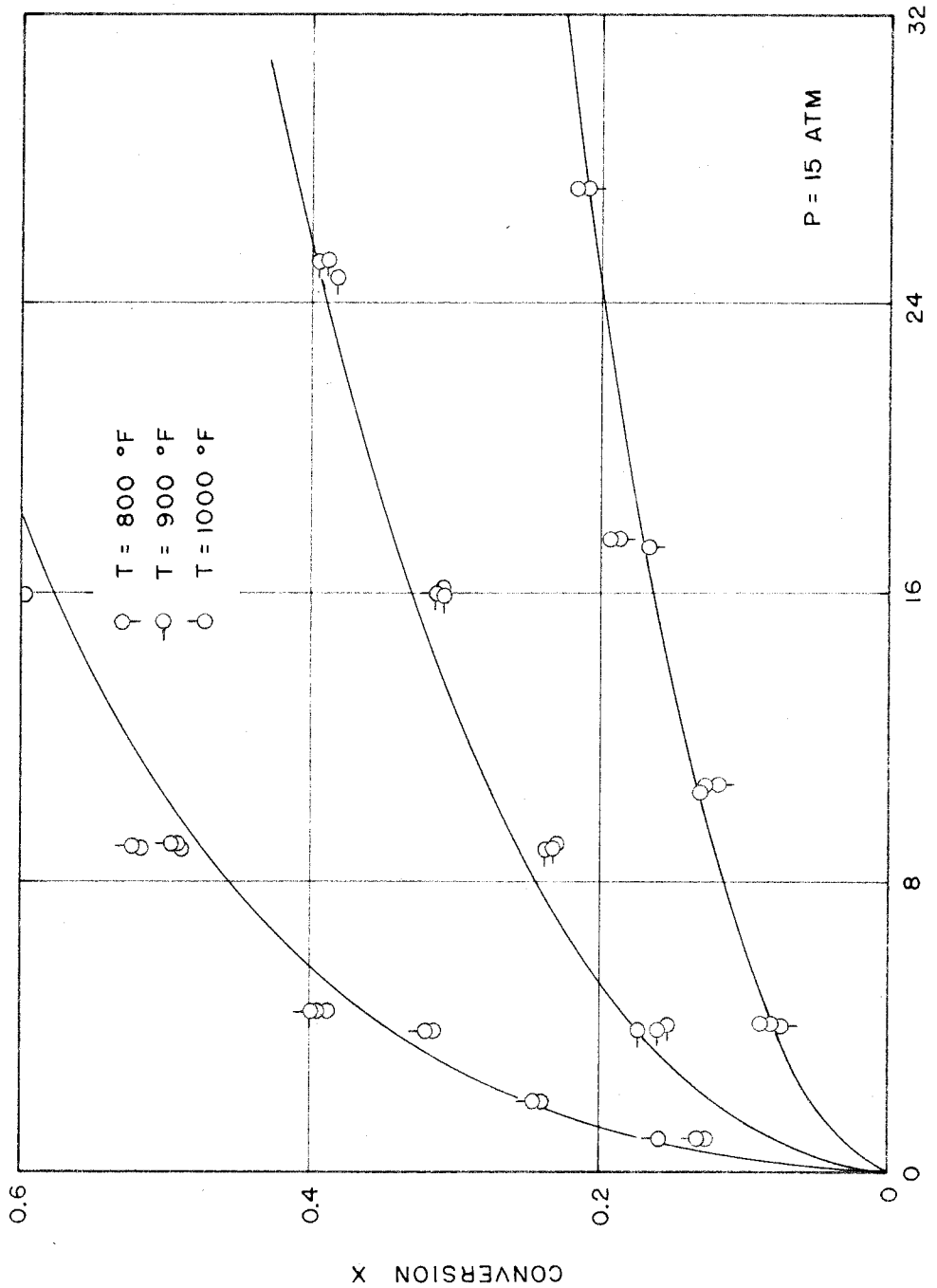

Figure 10. Conversion of NO vs W/F at 15 Atm for 0.404% Initial NO over a Catalyst Bed of 36.0 gm (the curves are plots of Equation 17)

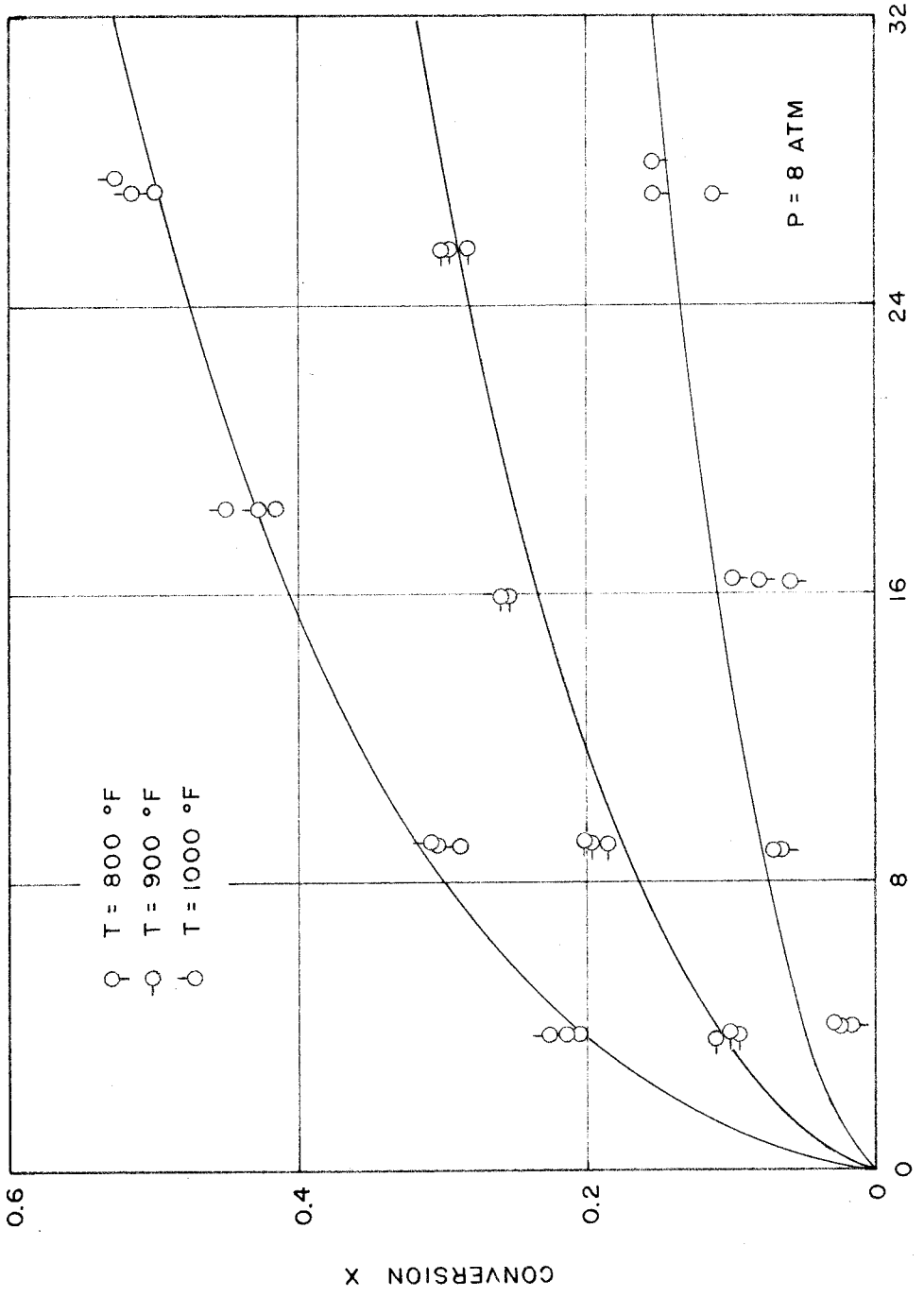

Figure 11. Conversion of NO vs W/F at 8 Atm for 0.404% Initial NO over a Catalyst Bed of 36.0 gm (the curves are plots of Equation 17)

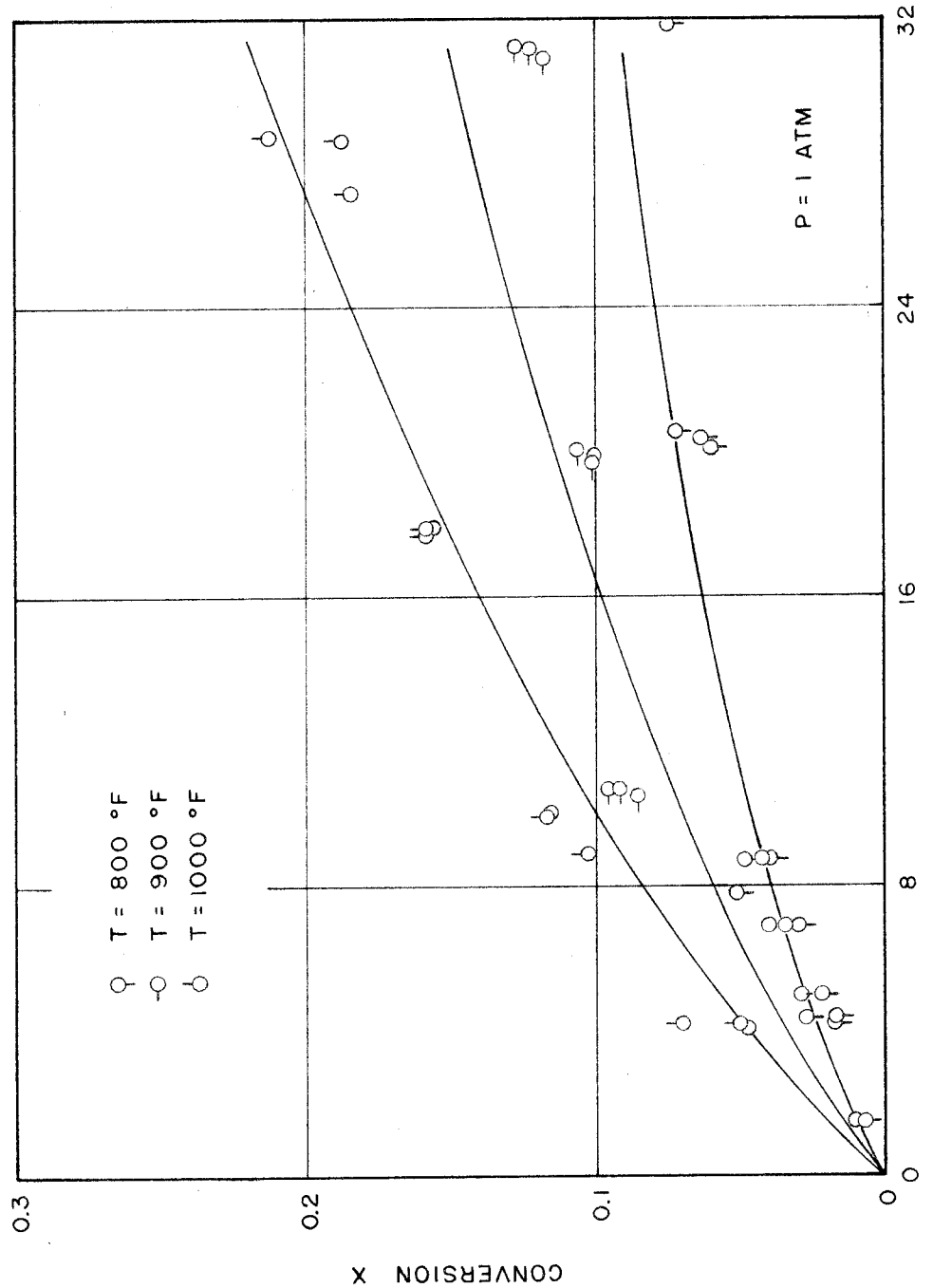

Figure 12. Conversion of NO vs W/F at 1 Atm for 0.404% Initial NO over a Catalyst Bed of 36.0 gm (the curves are plots of Equation 17)

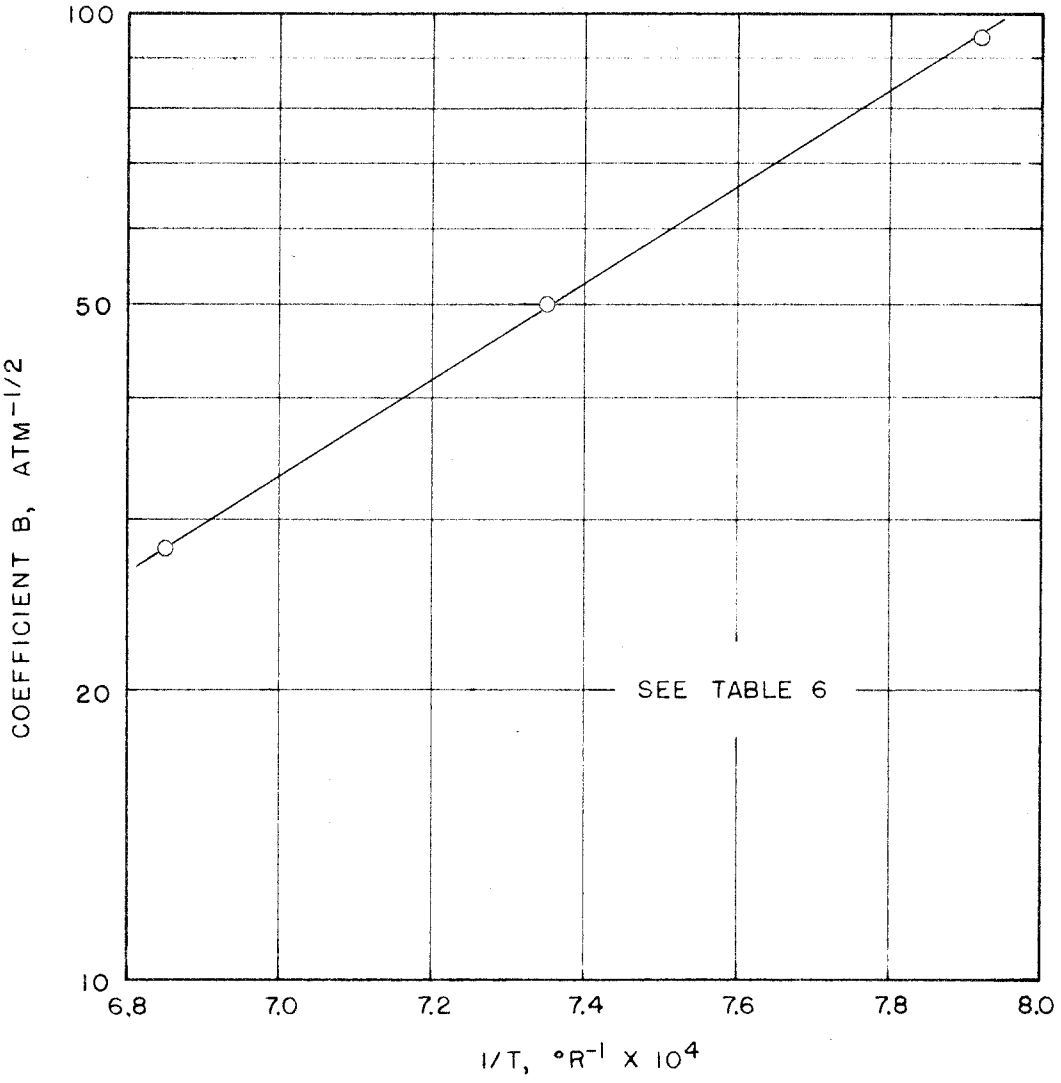

Figure 13. Log B vs 1/T for $r = \dfrac{A(P_{NO})^2}{(1 + B\sqrt{P_{O_2}})^2}$

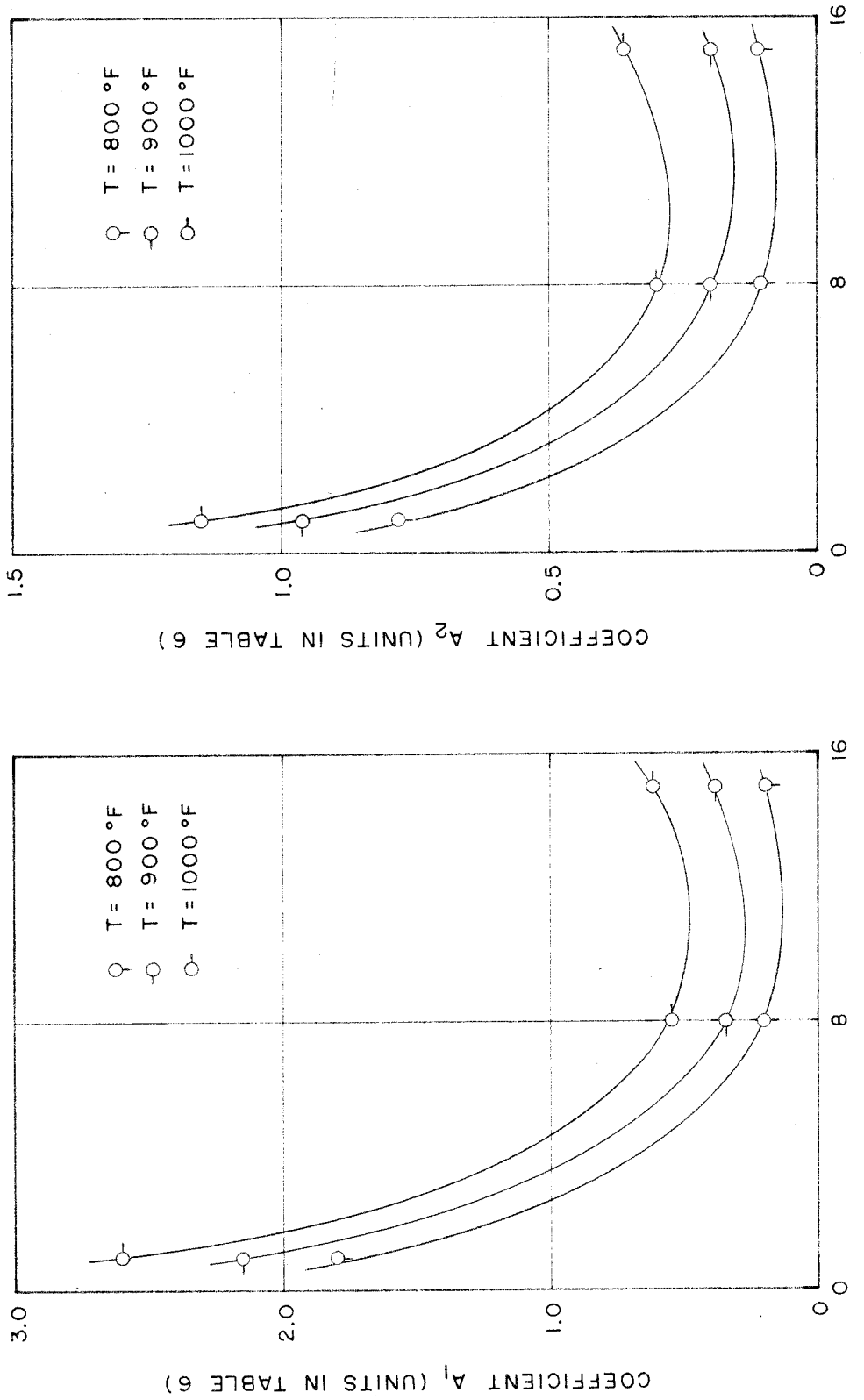

Figure 14. A vs P for $r = \frac{A(P_{NO})^2}{(1 + B\sqrt{P_{O_2}})^2}$

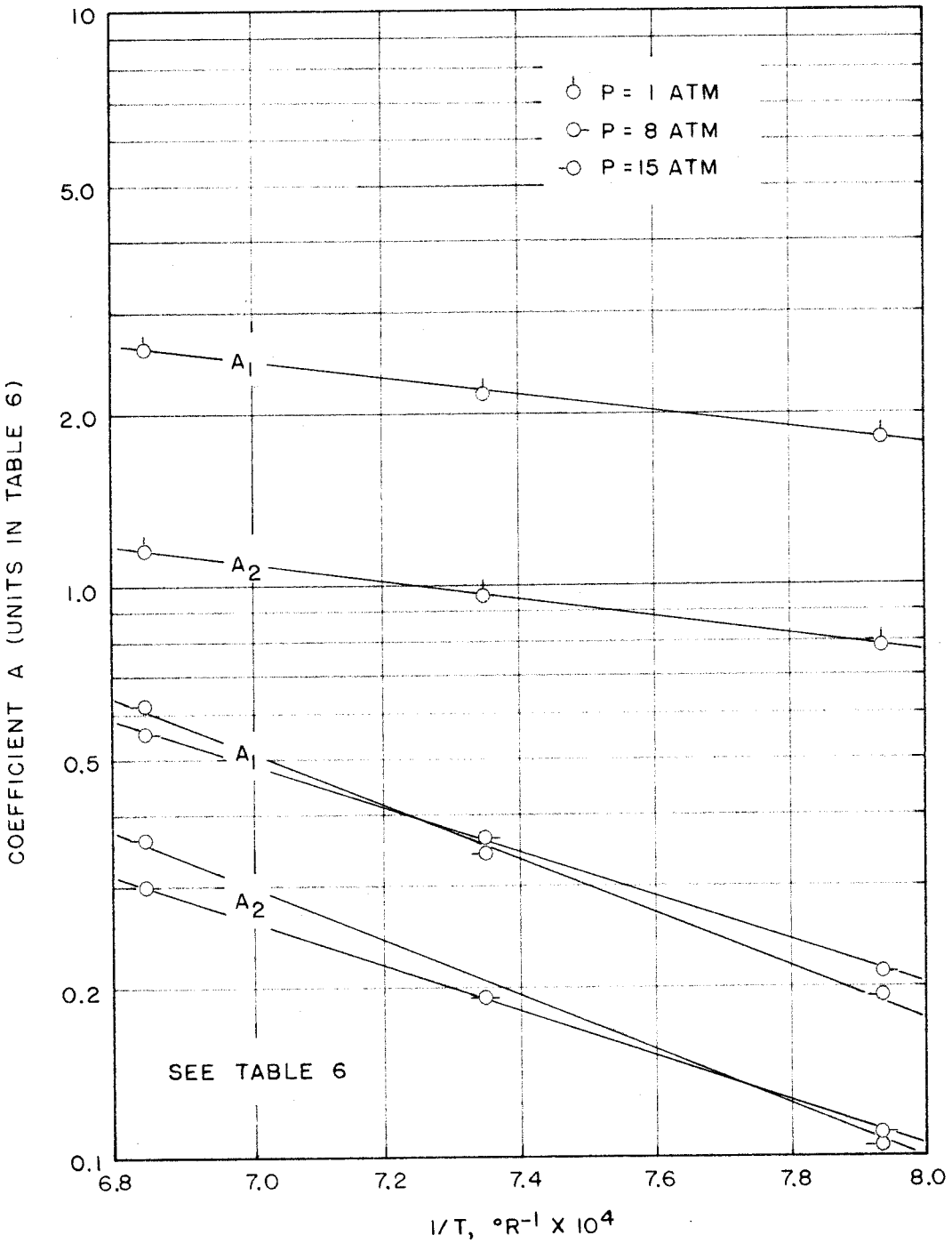

Figure 15. Log A vs 1/T for $r = \frac{A\,(P_{NO})^2}{(1 + B\sqrt{P_{O_2}})^2}$

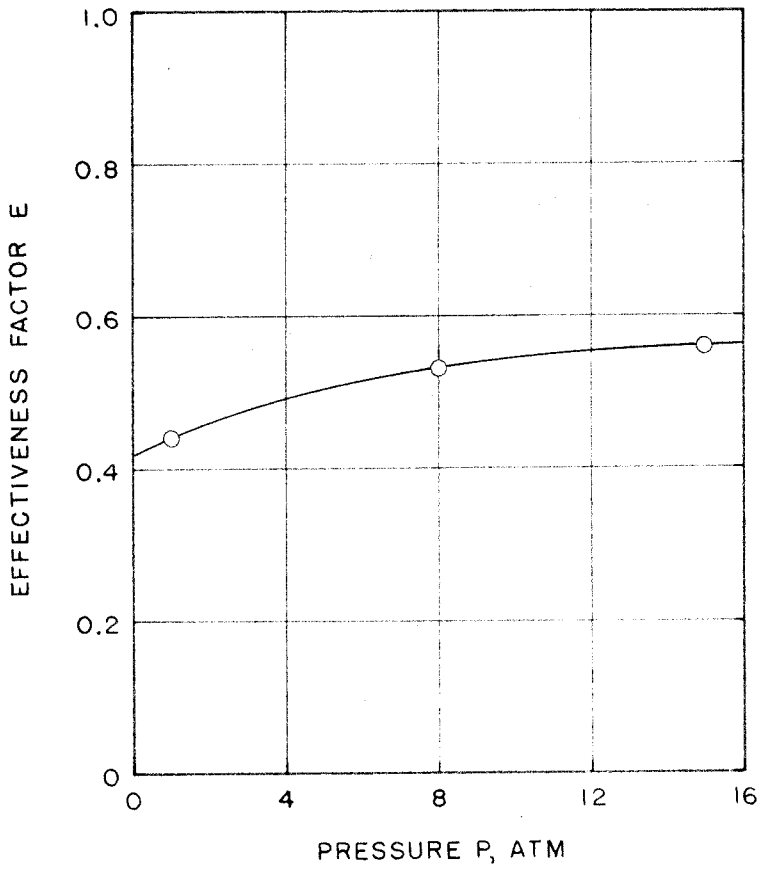

Figure 16. Relationship of Effectiveness Factor and Pressure

LIST OF TABLES

Table 1. Properties of the Girdler G-43 Catalyst

Data Obtained from the Catalyst Manufacturer:[a]

Surface area	188.4 sq meters/gm
Pore volume associated with a maximum pore diam of 800 A	0.27 cc/gm
Packed specific weight	68 ± 4 lb/ft^3

Composition:

Active Agents as Oxides	
Pt	0.1%
Ni	3.0
Carrier	
Fe_2O_3	0.07
Na_2O	0.02
SiO_2	0.10
SO_3	3.50
MgO	0.20
CaO	0.35
Al_2O_3	95.76

Measurements of Pellets:

Length	0.138 ± 0.004 in.
Diameter	0.1225 ± 0.0005 in.

Surface Area Measurement by Union Oil Company

167 sq meters/gm
172 sq meters/gm
} 2 runs

[a] Chemical Products Division of the Chemetron Corporation

Table 2. Data of G-43 Catalyst Beds in Reactor

Packing No.	No. of Pellets	Bed Height (in.)	Weights[a] (gm) Input	Output
1	500	8.0	20.05	17.97
2	250	4.0	10.14	8.99
3	1000	15.5	40.37	35.95
4	500	7.6	20.05	18.00

[a] Weight loss due to removal of moisture and dust

Table 3a. Computed Results of the Catalytic Decomposition of Nitric Oxide Using 18.0 gm of G-43 Catalyst

Pressure 0.975 ± 0.01 atm
Feed Composition 0.432% by volume of NO in N_2

Run No.	Temperature (°F)	Gas Feed Rate (gm/hr)	% NO Converted	W/F $\frac{(\text{gm Cat})(\text{hr})}{(\text{gm mole NO})} \times 10^{-2}$
1a	1003	1.89	33	619
b	1006	1.96	33	597
c	1005	1.89	31	619
2a	1001	3.49	28	335
b	1005	3.49	30	335
c	999	3.49	29	335
3a	1001	6.15	25	190
b	1000	6.15	24	190
4a	999	10.48	19.5	111
b	1000	10.48	20	111
c	1001	10.48	20	111
5a	1000	16.41	13	71.3
b	1003	16.41	11	71.3
c	1002	16.41	11	71.3
6a	1001	22.84	16	51.2
b	1001	23.05	19	50.7
c	999	23.05	20	50.7
7a	998	28.84	14	40.5
b	1005	28.84	13	40.5
c	1007	28.84	14	40.5
8a	999	12.71	14	91.9
b	1001	12.71	14	91.9
c	998	12.57	22	93.0
9a	1001	0.84	49	1395
b	1004	0.80	51	1456
c	1001	0.80	50	1456
10a	995	8.24	25	142
c	997	8.24	22	142
d	1001	8.24	22	142
25a	1002	5.73	27.6	204
b	1000	6.15	25.4	190
c	1001	5.73	27.6	204
26a	1001	3.14	33.7	372
b	1001	2.79	30.7	418
c	1001	2.79	31.9	418
27a	1003	12.08	17.1	96.7
b	1003	11.87	17.5	98.4
c	1002	11.87	17.1	98.4

Table 3a. (Cont.)

Run No.	Temperature (°F)	Gas Feed Rate (gm/hr)	% NO Converted	W/F $\frac{(\text{gm Cat})(\text{hr})}{(\text{gm mole NO})} \times 10^{-2}$
28a	1001	24.09	15.5	48.5
b	1002	24.09	12.7	48.5
c	1003	24.09	14.1	48.5
29a	1002	48.68	7.9	24.0
b	1002	48.05	10.5	24.3
c	1002	48.05	9.9	24.3
30a	899	2.79	13.9	419
b	899	2.79	15.5	419
c	898	2.93	12.1	399
31a	900	5.59	16.5	209
b	901	5.73	18.8	204
c	900	5.73	18.8	204
32a	899	12.15	18.0	96.0
b	901	12.15	12.8	96.0
c	900	12.08	16.7	96.7
33a	900	24.79	7.2	47.2
b	899	24.65	4.9	47.4
34a	900	1.40	19.3	837
b	898	1.40	20.8	837
c	900	1.40	18.1	837
35a	902	0.349	28.0	3347
b	901	0.349	25.9	3347
36a	899	33.52	1.4	34.9
b	901	33.87	7.1	34.5
c	900	33.87	11.2	34.5
47a	898	13.97	14.2	83.7
b	899	13.97	16.5	83.7
c	900	13.97	15.3	83.7
48a	899	32.69	11.5	35.8
b	898	33.52	10.5	34.9
c	902	33.87	6.6	34.5
49a	900	45.75	8.2	25.6
b	899	46.44	5.8	25.2
c	899	46.44	7.2	25.2
50a	901	2.37	25.4	492
b	897	2.37	25.0	492
37a	799	5.73	13.6	204
b	800	6.15	10.5	190
c	800	5.73	11.1	204

Table 3a. (Cont.)

Run No.	Temperature (°F)	Gas Feed Rate (gm/hr)	% NO Converted	W/F $\frac{(\text{gm Cat})(\text{hr})}{(\text{gm mole NO})} \times 10^{-2}$
38a	801	11.52	9.1	101
b	799	11.52	10.1	101
c	799	11.17	10.1	105
39a	799	23.40	5.8	50.0
b	798	23.40	6.8	50.0
c	799	23.75	5.2	49.2
40a	800	33.17	4.9	35.2
b	796	33.52	0.1	34.9
c	797	33.52	3.1	34.9
41a	802	48.54	3.9	24.1
b	798	48.89	2.3	23.9
42a	798	2.10	9.1	558
b	802	2.65	8.2	441
c	799	2.37	8.6	492
43a	797	0.349	22.2	3347
b	797	0.349	21.2	3347
44a	800	2.65	8.6	441
b	800	2.37	12.4	492
c	800	2.30	9.1	507
45a	801	7.54	10.7	155
b	799	7.33	10.5	159
c	799	6.98	10.5	167
46a	798	45.40	5.6	25.8
b	803	46.44	4.1	25.2
c	801	46.79	4.9	25.0
d	799	46.79	4.7	25.0

Table 3b. Computed Results of the Catalytic Decomposition of Nitric Oxide Using 18.0 gm of G-43 Catalyst

Pressure 8.0 ± 0.1 atm
Feed Composition 0.432% by volume of NO in N_2

Run No.	Temperature (°F)	Gas Feed Rate (gm/hr)	% NO Converted	W/F $\frac{(\text{gm Cat})(\text{hr})}{(\text{gm mole NO})} \times 10^{-2}$
18a	1001	16.41	38.8	71.2
b	1003	16.41	38.4	71.2
c	1005	16.41	39.4	71.2
19a	998	37.71	27.2	31.0
b	1000	37.71	25.0	31.0
c	1000	37.71	22.6	31.0
20a	1002	61.32	18.7	19.1
b	998	61.32	17.7	19.1
c	1000	61.46	17.1	19.0
21a	1002	10.48	48.0	111
b	1003	10.48	46.6	111
c	1005	10.48	48.6	111
22a	1003	5.38	58.2	217
b	1001	5.38	54.3	217
c	1002	5.38	54.3	217
23a	1003	2.10	71.8	558
b	1002	1.96	75.4	598
c	999	2.10	73.1	558
24a	1001	28.91	28.9	40.5
b	1003	28.63	29.3	40.8
c	1003	28.63	28.7	40.8
66a	904	3.14	39.6	372
b	898	3.14	42.4	372
c	901	3.14	41.0	372
67a	900	10.48	29.1	111
c	901	10.48	28.5	111
d	902	10.48	28.9	111
68a	899	19.90	19.3	59.7
b	899	19.56	17.1	59.7
c	903	19.56	19.1	59.7
69a	900	31.99	17.7	36.6
b	899	31.99	17.1	36.6
c	901	31.99	17.1	36.6
70a	898	44.70	15.1	26.2
b	899	44.70	14.9	26.2
c	902	44.70	14.6	26.2

Table 3b. (Cont.)

Run No.	Temperature (°F)	Gas Feed Rate (gm/hr)	% NO Converted	$\frac{W/F}{\frac{(gm\ Cat)(hr)}{(gm\ mole\ NO)}} \times 10^{-2}$
74a	899	5.38	33.1	217
b	899	5.10	32.7	229
c	897	5.38	32.7	217
56a	800	1.68	53.4	697
b	798	1.68	30.0	697
c	799	1.68	29.2	697
57a	801	7.33	19.2	159
b	799	7.12	18.0	164
c	800	7.12	16.1	164
58a	799	18.37	10.0	63.6
b	798	18.37	9.82	63.6
c	801	18.37	8.04	63.6
59a	800	29.68	6.88	39.4
b	799	29.68	7.26	39.4
c	799	29.68	5.30	39.4
60a	800	42.74	4.30	27.3
b	800	43.02	4.90	27.2
78a	798	23.40	8.40	50.0
b	801	23.26	8.80	50.3
c	799	23.40	7.70	50.0
79a	800	9.78	13.8	119
b	798	9.78	13.6	119
c	799	9.78	14.0	119
80a	801	5.31	16.1	220
b	802	5.10	16.55	230
c	799	5.10	16.55	230

Table 3c. Computed Results of the Catalytic Decomposition of Nitric Oxide Using 18.0 gm of G-43 Catalyst

Pressure 15.0 ±0.1 atm
Feed Composition 0.432% by volume of NO in N_2

Run No.	Temperature (°F)	Gas Feed Rate (gm/hr)	% NO Converted	W/F $\frac{(\text{gm Cat})(\text{hr})}{(\text{gm mole NO})}$ x 10^{-2}
11b	1004	3.49	83.8	326
c	1001	3.49	82.2	326
12a	997	16.41	57.0	71.3
b	998	16.41	57.6	71.3
c	1006	16.41	57.2	71.3
13a	999	22.84	44.8	51.2
b	1001	22.84	45.8	51.2
c	1002	22.84	49.5	51.2
14a	1001	29.82	40.6	39.2
b	1005	29.82	40.6	39.2
c	1001	29.82	44.0	39.2
15a	1000	46.79	37.4	25.0
b	1002	46.79	38.0	25.0
c	1003	46.79	36.8	25.0
16a	1002	93.10	27.4	12.6
b	997	94.28	27.0	12.4
c	1001	92.19	28.6	12.7
17a	1001	63.21	31.4	18.5
b	1002	63.06	29.2	18.5
c	1004	63.21	30.4	18.5
61a	898	5.10	48.1	229
b	895	4.54	47.6	258
c	900	4.54	47.4	258
62b	898	11.52	36.9	101
c	903	11.52	40.2	101
d	896	11.52	37.7	101
e	896	11.52	40.6	101
63a	899	21.65	30.9	54.0
b	901	21.65	30.7	54.0
c	899	21.65	30.7	54.0
64a	896	34.57	22.7	33.8
b	902	35.06	23.9	33.3
c	899	34.92	22.0	33.5
65a	898	46.44	18.2	25.2
b	901	46.23	20.4	25.3
c	903	46.23	18.2	25.3

Table 3c. (Cont.)

Run No.	Temperature (°F)	Gas Feed Rate (gm/hr)	% NO Converted	W/F $\frac{(\text{gm Cat})(\text{hr})}{(\text{gm mole NO})} \times 10^{-2}$
71a	899	7.05	41.4	166
b	900	7.19	40.4	162
c	899	7.33	42.5	159
72a	898	66.70	13.1	17.5
b	899	66.70	11.7	17.5
c	901	66.70	13.7	17.5
73a	902	3.14	47.1	372
b	903	2.65	47.9	440
c	897	2.93	48.1	399
51a	796	2.10	43.6	558
b	802	2.44	42.4	479
c	802	2.10	42.8	558
52a	803	6.15	20.7	190
b	803	6.15	22.7	190
c	802	6.15	22.7	190
53a	803	13.97	17.0	83.7
b	801	13.97	18.3	83.7
c	798	13.97	16.4	83.7
54a	800	25.49	13.0	45.9
b	800	25.49	13.0	45.9
c	800	25.49	13.4	45.9
55a	796	44.98	9.5	26.0
b	801	44.98	8.7	26.0
c	797	44.98	5.1	26.0
75a	802	17.67	11.5	66.0
b	802	17.46	15.4	66.9
c	798	17.60	15.2	66.0
d	800	17.46	14.7	66.9
76a	799	8.59	18.3	139
b	802	8.59	19.4	139
c	800	8.59	19.0	139
77a	800	3.84	26.0	304
b	799	3.84	25.6	304
c	800	3.84	26.2	304

Table 3d. Computed Results of the Catalytic Decomposition of Nitric Oxide Using 18.0 gm of G-43 Catalyst

Pressure 15.0 ±0.1 atm
Feed Composition 0.404% by volume of NO in N_2

Run No.	Temperature (°F)	Gas Feed Rate (gm/hr)	% NO Converted	$\frac{W/F}{\frac{(gm\ Cat)(hr)}{(gm\ mole\ NO)}} \times 10^{-2}$
175a	902	8.66	37.4	144
b	899	8.66	38.6	144
c	902	8.66	37.4	144
176a	900	17.46	27.7	71.7
b	896	17.46	27.5	71.7
c	902	17.67	31.6	70.9
177a	900	11.52	37.1	107
b	900	11.52	38.7	107
c	900	11.52	39.1	107
178a	900	64.95	16.9	19.4
b	900	64.95	16.2	19.4
c	900	65.65	16.6	19.0

Table 4a. Computed Results of the Catalytic Decomposition of Nitric Oxide Using 9.0 gm of G-43 Catalyst

Pressure 0.975 ±0.01 atm
Feed Composition 0.432 % by volume of NO in N_2

Run No.	Temperature (°F)	Gas Feed Rate (gm/hr)	% NO Converted	$\frac{W/F}{\frac{(gm\ Cat)(hr)}{(mole\ NO)}} \times 10^{-1}$
97a	1001	4.89	17.0	1195
b	1001	5.38	16.1	1088
c	1000	5.10	16.6	1149
98a	1001	15.71	13.2	372
b	1000	15.71	14.4	372
c	1000	15.57	14.3	376
99a	999	35.06	12.8	167
b	999	35.48	12.4	165
c	999	34.92	11.9	168
100a	999	59.36	9.9	98
b	999	59.36	11.1	98
c	1000	58.67	8.4	100

Table 4b. Computed Results of the Catalytic Decomposition of Nitric Oxide Using 9.0 gm of G-43 Catalyst

Pressure 0.975 ±0.01 atm
Feed Composition 0.404% by volume of NO in N_2

Run No.	Temperature (°F)	Gas Feed Rate (gm/hr)	% NO Converted	W/F $\frac{(\text{gm Cat})(\text{hr})}{(\text{mole NO})} \times 10^{-1}$
113a	901	8.59	9.0	728
b	900	8.59	8.8	727
c	900	8.38	9.4	745
d	898	9.08	8.6	689
114a	900	18.16	7.8	345
b	901	17.60	6.8	356
c	899	17.95	7.0	349
115a	902	35.76	4.6	175
b	902	34.92	3.4	179
c	901	35.20	3.8	178
116a	899	62.86	1.6	100
c	899	62.16	2.6	101
d	899	62.51	2.2	100
121a	802	9.08	4.1	688
b	800	8.03	5.2	778
c	799	7.19	7.2	870
122b	801	14.18	1.7	440
d	800	14.53	1.7	430
e	802	14.32	2.8	437
123a	800	9.08	3.0	688
b	801	9.08	3.4	688
c	800	8.73	2.6	716
124a	799	20.25	0.0	309
b	799	19.90	4.0	314
c	800	19.90	2.2	314
125a	800	39.81	0.6	157
b	800	40.16	1.1	156
c	801	40.86	1.1	153

Table 4c. Computed Results of the Catalytic Decomposition of Nitric Oxide Using 9.0 gm of G-43 Catalyst

Pressure 8.0 ± 0.1 atm
Feed Composition 0.432% by volume of NO in N_2

Run No.	Temperature (°F)	Gas Feed Rate (gm/hr)	% NO Converted	W/F $\frac{(\text{gm Cat})(\text{hr})}{(\text{mole NO})} \times 10^{-1}$
93a	1000	11.52	-	507
b	999	11.52	33.0	507
c	1002	11.52	33.2	507
d	1002	11.38	33.4	514
94a	1000	20.95	20.9	279
b	1002	20.95	21.6	279
c	1001	20.95	22.5	279
95a	999	62.86	11.8	93
b	999	61.95	11.8	94
c	1001	62.51	13.1	93
96a	1002	37.71	15.1	155
b	998	38.06	14.8	154
c	1002	37.92	15.5	154

Table 4d. Computed Results of the Catalytic Decomposition of Nitric Oxide Using 9.0 gm of G-43 Catalyst

Pressure 8.0 ± 0.1 atm
Feed Composition 0.404% by volume of NO in N_2

Run No.	Temperature (°F)	Gas Feed Rate (gm/hr)	% NO Converted	W/F $\frac{(\text{gm Cat})(\text{hr})}{(\text{mole NO})} \times 10^{-1}$
105a	901	6.98	21.5	895
b	896	6.98	21.5	895
c	899	6.98	20.3	895
106a	902	11.52	18.4	540
b	902	11.52	18.8	540
c	900	11.52	19.9	540
107a	901	35.27	10.1	177
b	901	34.92	8.7	179
c	902	34.92	11.8	179
108a	902	62.16	6.8	101
b	901	62.51	7.5	100
c	901	62.16	3.9	101
109a	799	9.22	10.4	679
b	803	9.22	10.2	679
c	801	9.08	9.6	688
110a	800	17.67	6.7	354
b	800	17.46	10.6	359
c	802	17.67	7.3	354
111a	801	35.48	4.7	176
b	801	35.27	5.7	177
c	798	35.27	8.1	177
112a	801	62.02	0.4	101
b	805	62.02	4.0	101
c	800	62.02	1.6	101

Table 4e. Computed Results of the Catalytic Decomposition of Nitric Oxide Using 9.0 gm of G-43 Catalyst

Pressure 15.0 ± 0.1 atm
Feed Composition 0.404% by volume of NO in N_2

Run No.	Temperature (°F)	Gas Feed Rate (gm/hr)	% NO Converted	W/F $\frac{(\text{gm Cat})(\text{hr})}{(\text{mole NO})} \times 10^{-1}$
101a	998	6.98	52.3	895
b	998	6.98	51.7	895
c	999	6.98	49.8	895
102a	1000	13.97	38.7	448
b	1000	13.97	39.8	448
c	1002	13.97	39.6	448
d	997	14.11	38.9	444
103a	1001	31.78	24.5	197
b	1000	31.78	24.3	197
c	998	31.78	23.8	197
104a	1000	62.86	13.2	100
b	1000	63.21	12.6	99
c	1000	63.07	15.8	99
117a	900	7.89	27.9	791
b	900	7.54	28.5	829
c	901	7.89	29.9	791
118a	900	13.97	22.3	448
b	901	13.97	22.9	448
c	900	13.97	22.0	448
119a	900	26.82	14.8	233
b	901	26.82	15.0	233
c	901	27.24	14.6	230
120a	900	62.16	10.0	101
b	900	62.16	8.9	101
c	899	63.55	10.6	99
d	901	63.55	8.7	99
126a	797	6.63	17.9	942
b	798	7.12	13.9	877
c	800	6.84	16.6	913
127a	801	16.06	19.4	669
b	801	15.92	12.4	705
c	800	15.92	10.5	705
128a	801	30.38	6.7	206
b	800	30.38	5.5	206
c	799	30.38	10.5	206
129a	800	62.51	6.3	100
b	800	62.51	6.7	100
c	800	61.95	7.1	101

Table 5a. Computed Results of the Catalytic Decomposition of Nitric Oxide Using 36.0 gm of G-43 Catalyst

Pressure 0.975 ± 0.01 atm
Feed Composition 0.404% by volume of NO in N_2

Run No.	Temperature (°F)	Gas Feed Rate (gm/hr)	% NO Converted	W/F $\frac{(\text{gm Cat})(\text{hr})}{(\text{mole NO})} \times 10^{-2}$
150a	999	6.63	19.2	377
b	999	6.63	19.2	377
c	1000	6.63	20.2	377
151a	1000	9.22	18.4	271
b	1000	8.73	21.2	286
c	1000	8.73	18.6	286
152a	1000	13.97	15.6	179
b	1001	13.97	15.8	179
c	1001	14.11	15.8	177
153a	1000	28.15	10.3	88.8
b	1002	27.80	11.5	89.9
c	999	27.94	11.7	89.5
154a	1000	60.55	5.0	41.3
b	998	61.25	4.7	40.8
c	1000	60.55	7.7	41.3
145a	900	5.59	16.3	447
b	901	5.59	14.0	447
c	901	5.94	15.5	421
146a	900	23.75	8.5	105
b	900	23.26	9.6	107
c	900	23.40	9.2	107
147a	899	12.71	10.2	197
b	900	12.57	10.0	199
c	900	12.43	10.6	201
148a	900	64.95	8.6	38.7
b	899	64.74	7.3	38.7
c	899	63.90	8.3	39.0
149a	898	8.10	13.0	309
b	900	8.03	14.0	311
c	901	8.03	13.4	311
170a	800	5.73	8.6	437
b	800	5.73	10.2	437
171a	800	7.54	7.6	331
b	800	7.82	7.4	320
c	799	7.54	7.8	331

Table 5a. (Cont.)

Run No.	Temperature (°F)	Gas Feed Rate (gm/hr)	% NO Converted	W/F $\frac{(\text{gm Cat})(\text{hr})}{(\text{mole NO})} \times 10^{-2}$
172a	801	12.43	5.9	201
b	800	12.22	6.3	204
c	801	12.15	7.2	205
173a	800	28.63	4.1	87.3
b	800	28.63	4.3	87.3
c	800	28.63	4.9	87.3
174a	799	50.49	1.6	49.4
b	800	50.56	2.9	49.4
c	799	50.56	2.2	49.4

Table 5b. Computed Results of the Catalytic Decomposition of Nitric Oxide Using 36.0 gm of G-43 Catalyst

Pressure 8.0 ± 0.1 atm
Feed Composition 0.404% by volume of NO in N_2

Run No.	Temperature (°F)	Gas Feed Rate (gm/hr)	% NO Converted	W/F $\frac{(\text{gm Cat})(\text{hr})}{(\text{mole NO})} \times 10^{-2}$
135a	1001	6.43	54.4	389
b	1003	6.15	55.4	407
c	1002	6.63	56.6	377
136a	1000	9.22	50.0	271
b	999	9.22	51.6	271
c	1001	9.08	52.7	275
d	1002	8.94	49.1	280
137a	1000	66.70	22.6	37.5
b	1001	66.70	20.5	37.5
c	1000	66.35	21.3	37.7
138a	999	13.62	45.0	184
b	1000	13.62	41.6	184
c	1000	13.62	42.7	184
139a	1001	27.59	28.7	90.6
b	1000	27.59	30.5	90.6
c	1000	27.59	30.7	90.6
140a	901	6.15	35.9	407
b	901	6.15	36.1	407
c	901	6.01	35.7	416
141a	901	9.78	28.2	256
b	902	9.78	30.0	256
c	899	9.78	29.6	256
142a	901	15.71	25.4	159
b	901	15.71	25.4	159
c	900	15.71	25.8	159
143a	901	27.59	19.8	90.6
b	900	27.59	18.5	90.6
c	900	27.59	20.1	90.6
144a	899	65.65	10.1	38.1
b	900	66.70	11.1	37.5
c	901	66.00	10.1	37.9
d	900	65.86	9.5	38.0
165a	800	6.29	13.7	398
b	800	6.29	15.4	398
c	800	6.29	14.7	398

Table 5b. (Cont.)

Run No.	Temperature (°F)	Gas Feed Rate (gm/hr)	% NO Converted	W/F $\frac{(\text{gm Cat})(\text{hr})}{(\text{mole NO})} \times 10^{-2}$
166a	800	8.94	15.4	280
b	800	9.22	15.4	271
c	800	9.22	11.2	271
167a	801	15.36	5.8	163
b	800	15.36	7.9	163
c	800	15.23	9.7	164
168a	800	28.29	5.2	88.4
b	799	28.29	6.9	88.4
c	799	28.29	6.6	88.4
169a	798	62.16	2.7	40.1
b	800	62.16	1.5	40.1
c	800	62.16	2.5	40.1

Table 5c. Computed Results of the Catalytic Decomposition of Nitric Oxide Using 36.0 gm of G-43 Catalyst

Pressure 15.0 ± 0.1 atm
Feed Composition 0.404% by volume of NO in N_2

Run No.	Temperature (°F)	Gas Feed Rate (gm/hr)	% NO Converted	W/F $\frac{(\text{gm Cat})(\text{hr})}{(\text{mole NO})} \times 10^{-2}$
130a	997	10.48	70.3	239
b	1000	10.48	71.6	239
c	1000	10.48	71.4	239
131a	1000	6.98	76.3	358
b	1000	6.84	75.9	365
c	1001	6.63	76.3	377
132a	1001	15.50	61.4	159
b	1000	15.50	60.1	159
c	1003	15.50	60.6	159
133a	1001	27.94	49.3	89.5
b	1000	27.94	48.9	89.5
c	1001	27.94	49.3	89.5
134a	1000	64.60	31.3	38.7
b	1000	64.60	31.5	38.7
c	1000	64.60	31.8	38.7
155a	901	6.84	44.5	365
b	900	6.98	44.5	358
c	899	6.98	45.3	358
156a	899	9.92	38.8	252
b	899	10.13	38.2	247
c	900	9.92	39.4	252
157a	899	15.71	30.8	159
b	900	15.50	30.8	161
c	900	15.64	31.0	160
158a	899	27.73	23.0	90.2
b	900	27.94	23.0	89.5
c	900	27.94	23.6	89.0
159a	901	62.16	15.3	40.1
b	899	62.86	17.3	39.7
c	899	62.86	15.7	39.7
160a	800	6.43	25.5	389
b	801	6.43	25.1	389
c	799	6.43	24.3	389
161a	800	9.22	21.6	271
b	800	9.22	20.9	271
c	800	9.22	21.4	271

Table 5c. (Cont.)

Run No.	Temperature (°F)	Gas Feed Rate (gm/hr)	% NO Converted	W/F $\frac{(\text{gm Cat})(\text{hr})}{(\text{mole NO})} \times 10^{-2}$
162a	799	14.46	16.6	173
b	800	14.32	19.3	175
c	799	14.32	18.7	175
163a	800	23.75	12.9	105
b	801	23.54	12.6	106
c	799	23.47	11.8	107
164a	800	62.16	7.5	40.1
b	800	61.81	8.9	40.5
c	800	62.50	8.1	40.1

Table 6. Calculated Results of A and B for $r = \frac{A(P_{NO})^2}{(1+B\sqrt{P_{O_2}})^2}$

Temperature (°F)	B ($atm^{-\frac{1}{2}}$)
1000	28
900	50
800	94

	Temperature (°F)					
	1000		900		800	
Pressure (atm)	A_1	A_2	A_1	A_2	A_1	A_2
15	0.62	0.36	0.36	0.19	0.19	0.11
8	0.55	0.30	0.34	0.19	0.21	0.105
1	2.6	1.15	2.15	0.96	1.8	0.78

$$A = \frac{(\text{gm moles NO})}{(\text{gm cat})(\text{hr})(\text{atm}^2)}$$

Subscripts

1 - Results for studies with 9.0 and 18.0 gm of catalyst (high conversion data)

2 - Results for studies with 36.0 gm of catalyst (low conversion data)

Part I

APPENDICES

LIST OF FIGURES

LIST OF TABLES

APPENDIX I

PRELIMINARY REACTOR TESTS

Test of Wall Effect

In the initial experiments to determine wall effects, the reactor was packed with 22.8 gm of type-304 stainless-steel turnings. Information regarding the properties of type-304 stainless-steel used to fabricate the feed lines and reactor is presented in Table 1A. At atmospheric pressure and at temperatures up to 1100°F, it was found that the decomposition of nitric oxide at an initial concentration of 0.432% by volume in nitrogen was negligible.

Several preliminary tests were also made at pressures of 8 and 15 atm and at a reactor temperature of approximately 1000°F. These results presented in Table 2A helped to determine the minimum rate of the feed stream for which the contributions to the decomposition of nitric oxide from wall effects and homogeneous reactions were negligible. For these tests, the reactor was empty.

Tests of Catalysts

A variety of materials with potential to catalyze the decomposition of nitric oxide was selected on the basis of a report by the Armour Research Foundation (9) and suggestions from several catalyst manufacturers. Samples were obtained, and testing was confined to pelleted catalysts in the form of 1/8-in. cylinders. The catalysts as described in Tables 3A and 4A were subjected to comparable tests in an effort to select the one most suitable for further studies.

For the tests of comparative activity, the charges of catalyst to the reactor each consisted of 500 of the 1/8-in. cylinders. Each charge was heated in place for a minimum of one day at a temperature of about 1100°F and with a low rate of flow of dry nitrogen at atmospheric pressure. Following the conditioning period, the catalyst bed was subjected to a feed stream containing 0.432% nitric oxide in nitrogen at a temperature of approximately 1000°F and at several pressures which are listed in Table 5A. The percentage decreases in quantity of nitric oxide are also listed in Table 5A.

Table 1A. Properties of Type-304 Stainless Steel Used in the Reactor Assembly and Turnings

Specific Weight	0.29 lb/in.^{3}
Coefficient of Thermal Expansion	11.0 x 10^{-6} in./in./°F (68 to 1500°F)
Max Temp of Usability	1500°F
Creep Strength	1% flow in 10,000 hrs at 19,000 lb/in.^{2} and 1000°F

Composition	% by weight
Carbon	0.08 Max
Manganese	2.00
Silicon	1.00
Chromium	18.00 - 20.00
Nickel	8.00 - 11.00

Dimensions of Turnings Put into Reactor

Width	50% were 0.040 in. 50% were 0.055 in.
Thickness	0.005 in.
Total Weight	22.8 gm

Table 2A. Results of Reactor Wall Tests

(0.495-in. I.D. Empty Reactor)

Feed Composition = 0.432% by Volume of NO in N_2

Temperature (°F)	Reactor Pressure (psig)	Gas Feed Rate (gm/hr)	% NO Converted
998	205	10.5	0
1000	207	10.5	0
1004	205	10.5	0
997	205	10.5	4
992	205	15.7	2
996	204	15.7	0
999	207	5.4	0
1002	205	5.4	0
1006	205	5.4	0
1005	204	5.4	0
1004	205	3.5	2
1004	205	3.5	0
1005	205	3.4	2
1008	103	1.9	4
1002	106	2.1	6
995	106	2.1	5
987	106	3.5	0
997	105	3.5	0
1009	105	3.5	2
1014	104	3.5	0
1000	104	5.7	0
1000	104	5.7	0
1008	103	5.7	0

Table 3A. Catalysts Tested in Studies of Decomposition of NO in Presence of N_2

Catalyst	Nominal Composition
G-33A	Nickel Oxide (36%) on Alumina
G-43	Platinum (0.1%), Nickel (3%) on Alumina
T-306	Molybdic Oxide (10-12%) on Alumina
T-308	Palladium (0.05%) on Alumina
T-309	Platinum (0.10%) on Alumina
T-310	Nickel Oxide (10-12%) on Alumina
T-312	Nickel Oxide (10-12%), Copper Oxide (1% Cu) on Alumina
V-0301	V_2O_5 (10%) on Alumina

Note: The G and T catalysts were obtained from the Chemical Products Division of the Chemetron Corporation.

The V catalyst was obtained from the Harshaw Chemical Company.

Table 4A. Physical Characteristics of Catalysts Tested[a]

Catalyst	Surface Area (sq meters/gm)	Pore Volume (cc/gm)	Specific Weight (lb/ft^3)
G-33A	91.4	0.11	65 ± 4
G-43	188.4	0.27	68 ± 4
T-306	192	0.27	65 ± 4
T-308	210	0.28	
T-309	215	0.27	
T-310	195	0.27	65 ± 4
T-312	198	0.27	65 ± 4
V-0301[b]	-	-	

[a] Data were obtained from the Chemical Products Division of the Chemetron Corporation

[b] No data available

Table 5A. Results of Preliminary Catalyst Tests in the Decomposition of NO in the Presence of N_2

Feed Composition 0.432% by volume of NO in N_2

Test	Catalyst	Reactor Temp (°F)	Flow Rate (gm/hr)	Pressure (psig)	Wt of Cat (Out) (gm)	% NO Converted[a]
7A	G-33A	1028	7.0	-	30.8	-
B		1030	10.5	-		48 ± 6
8A	"	1015	7.0-7.3	-		23 ± 1
9A	"	1023	17.0	-		0
B		1016	11.2	-		4
10A	"	1011	17.1	235		69 - 83
B	"	1010	17.5	232		
11A	G-43	1021	7.7-8.0	-	18.2	33.5 ± 1.0
B		975	4.8	-		20.5
12	"	1017	4.7-4.9	-		25 ± 2
13A	"	1007	11.0	230		56 ± 3
B		1011	11.5	225		52 ± 2.5
14	T-306	970	4.2-4.4	-	20.4	0
15A	"	1000	3.3	-		2 ± 2
B		1012	1.8	-		2 ± 2
16	"	1022	8.9-9.2	225-230		0
17A	T-310	1036	4.2-4.9	-	21.3	0
B		980	3.5	-		0
18A	"	1020	3.5	200		49 ± 3
B		1023	8.0	218		42 ± 2
19	"	1046	2.1-2.7	95-100		2
20A	T-312	998-1006	3.5-4.5	-	21.7	0
21A	"	1030-1045	2.4	210-215		19 ± 3

Table 5A. (Cont.)

Test	Catalyst	Reactor Temp (°F)	Flow Rate (gm/hr)	Pressure (psig)	Wt of Cat (Out) (gm)	% NO Converted[a]
22A	T-308	985-990	-	-	20.8	26 ± 3
B		1015-1025	2.4	-		23 ± 2
23A	"	983-997	2.1-2.4	-		22 ± 4
24A	T-308	1000-1005	1.9-2.4	200	20.8	58
B		1000-1005	7.5	210		22 ± 4
25A	"	1015-1060	2.1	100-110		26 ± 4
26A	T-309	1004-1018	2.1	-	16.6	35
B		1003-1014	5.2-5.6	-		23 ± 3
27A	"	997-1015	8.0	202-203	16.6	53 ± 2
B		1002-1015	12.2	201		46 ± 1
C		1020-1023	12.2	200		50 ± 2
28A[b]	V-0301	1010-1032	1.7-2.0	-	21.6	9 ± 3
B		1019-1034	0.84-1.1	-		8 ± 2
29A	"	1016-1017	2.17-5.4	200		3.0 ± 1
30A	G-33	1019-1026	1.8-2.0	-	21.1	43.5
B		1018-1024	4.7-4.9	-		23 ± 2
31A	"	1009	7.5	218		90 ± 1
B		1012-1025	14.8	212		71 ± 2
32A	"	1018-1021	7.0-7.5	-		17 ± 1
B		1020	2.8-2.9	-		41 ± 0.5
33A	"	1019-1023	17.1	205-210		73 ± 7
34A	G-43	1018-1020	8.0-8.2	-	17.9	21 ± 2
B		1025	2.3-2.6	-		38 ± 2
35A	"	1018-1023	16.4	202-205		51 ± 3
B		1014-1017	10.5	200		56 ± 2
C		1018-1027	3.1-3.3	-		33 ± 1

[a] Each test represents several samples, and results for change in concentration of NO are arithmetic averages of the several samples

[b] Test 28: High attrition, pellets broken down on removal from reactor

APPENDIX II

RATE EQUATIONS FOR THE HETEROGENEOUS DECOMPOSITION OF NITRIC OXIDE

In postulating models for the decomposition of nitric oxide, the overall step for each model involved the bimolecular reaction of two nitric oxide molecules. The assumptions involved in deriving rate equations for the various models were:

1. The reverse reaction for the overall decomposition

$$2NO \longrightarrow N_2 + O_2$$

was negligible.

2. The gaseous mixtures behaved as perfect gases.
3. The adsorption and reaction-rate constants were functions only of temperature.
4. Diffusion steps were always rapid and at equilibrium. As stated under Discussion, this was observed experimentally.
5. Only one of the possible chemical steps was rate controlling while all the others were at equilibrium. Adsorption was considered as a chemical step in the derivations.
6. The law of mass action applied to all reactions including those in which active sites on the catalyst were involved.

In Table 6A are presented the sequential reaction steps for several reaction models, which are lettered A to E. Opposite each step is the resulting equation for the rate of conversion of nitric oxide if that step were rate controlling.

Also, based upon the above set of assumptions, two generalized rate equations were derived and are presented in Table 7A. For the

equation in I, the controlling step was the surface reaction between two adsorbed nitric oxide molecules. For the equation in II, the controlling step was the surface reaction between one adsorbed and one gaseous nitric oxide molecule.

From these generalized equations, the several rate equations for surface reactions in Table 6A can be obtained by eliminating from the denominator those species which are not adsorbed according to the proposed model. For example, A_2 and B_2 can be obtained from the equation in I of Table 7A.

Table 6A. Postulated Reaction Steps and Corresponding Rate Equations

	Reaction Step	Rate Equation
A1.	$NO + s \longrightarrow NOs$	$r_{A_1} = \dfrac{k_{A_1}(P_{NO})}{(1 + K_{N_2}P_{N_2} + K_{O_2}P_{O_2})}$
2.	$2NOs \longrightarrow N_2s + O_2s$	$r_{A_2} = \dfrac{k_{A_2}(P_{NO})^2}{(1 + K_{O_2}P_{O_2} + K_{N_2}P_{N_2} + K_{NO}P_{NO})^2}$
3.	$N_2s \longrightarrow N_2 + s$	$r_{A_3} = k_{A_3}$
4.	$O_2s \longrightarrow O_2 + s$	$r_{A_4} = k_{A_4}$
B1.	$NO + s \longrightarrow NOs$	$r_{B_1} = \dfrac{k_{B_1}(P_{NO})}{(1 + K_O \sqrt{P_{O_2}})}$
2.	$2NOs \longrightarrow N_2 + 2Os$	$r_{B_2} = \dfrac{k_{B_2}(P_{NO})^2}{(1 + K_{NO}P_{NO} + K_O \sqrt{P_{O_2}})^2}$
3.	$2Os \longrightarrow O_2 + 2s$	$r_{B_3} = k_{B_3}$
C1.	$NO + s \longrightarrow NOs$	$r_{C_1} = \dfrac{k_{C_1}(P_{NO})}{(1 + K_{O_2}P_{O_2})}$
2.	$NOs + NO \longrightarrow N_2 + O_2s$	$r_{C_2} = \dfrac{k_{C_2}(P_{NO})^2}{(1 + K_{NO}P_{NO} + K_{O_2}P_{O_2})}$
3.	$O_2s \longrightarrow O_2 + s$	$r_{C_3} = k_{C_3}$
D1.	$NO + s \longrightarrow N + Os$	$r_{D_1} = \dfrac{k_{D_1}(P_{NO})}{(1 + K_{O_2}P_{O_2} + K_O \sqrt{P_{O_2}})}$
2.	$2N \longrightarrow N_2$	

Table 6A. (Cont.)

	Reaction Step	Rate Equation
3.	$2Os \longrightarrow O_2s + s$	$r_{D_3} = \dfrac{k_{D_3}(P_{NO})^2/(P_{N_2})}{(1 + K_{O_2}P_{O_2} + P_{NO}\sqrt{K'/P_{N_2}})^2}$
4.	$O_2s \longrightarrow O_2 + s$	$r_{D_4} = k_{D_4}$
E1.	$NO + s \longrightarrow N + Os$	$r_{E_1} = \dfrac{k_{E_1}(P_{NO})}{(1 + K_{O_2}P_{O_2})}$
2.	$NO + Os \rightarrow N + O_2s$	$r_{E_2} = \dfrac{k_{E_2}(P_{NO})^2/(P_{N_2})^{\frac{1}{2}}}{(1 + K_{O_2}P_{O_2} + K_{NO}P_{NO}\sqrt{K_3/P_{N_2}})}$
3.	$N + N \longrightarrow N_2$	
4.	$O_2s \longrightarrow O_2 + s$	$r_{E_4} = k_{E_4}$

s = an empty active site

Ys = an active site with adsorbed Y

K_Y = adsorption equilibrium constant for Y

Table 7A. Generalized Rate Equations for Bimolecular Surface Reactions

I. Surface reaction between two adsorbed NO molecules for the rate controlling step: $2NOs \longrightarrow$ products

$$r = \frac{k_I(P_{NO})^2}{(1 + K_{NO}P_{NO} + K_{N_2}P_{N_2} + K_N\sqrt{P_{N_2}} + K_{O_2}P_{O_2} + K_O\sqrt{P_{O_2}})^2}$$

II. Surface reaction between one adsorbed and one gaseous NO molecule for the rate controlling step: $NOs + NO \longrightarrow$ products

$$r = \frac{k_{II}(P_{NO})^2}{(1 + K_{NO}P_{NO} + K_{N_2}P_{N_2} + K_N\sqrt{P_{N_2}} + K_{O_2}P_{O_2} + K_O\sqrt{P_{O_2}})}$$

By assuming that certain of the terms in the denominator are negligible in comparison to other terms, the above equations can be modified. The equation which best fits the data obtained in the decomposition studies was obtained in this manner from I.

$$r = \frac{k_{I_1}(P_{NO})^2}{(1 + K_O\sqrt{P_{O_2}})^2}$$

The constants, k_{I_1} and K_O, in the above equation were represented as A and B in the main body of the text since these constants were correlated as empirical functions of temperature and pressure.

APPENDIX III

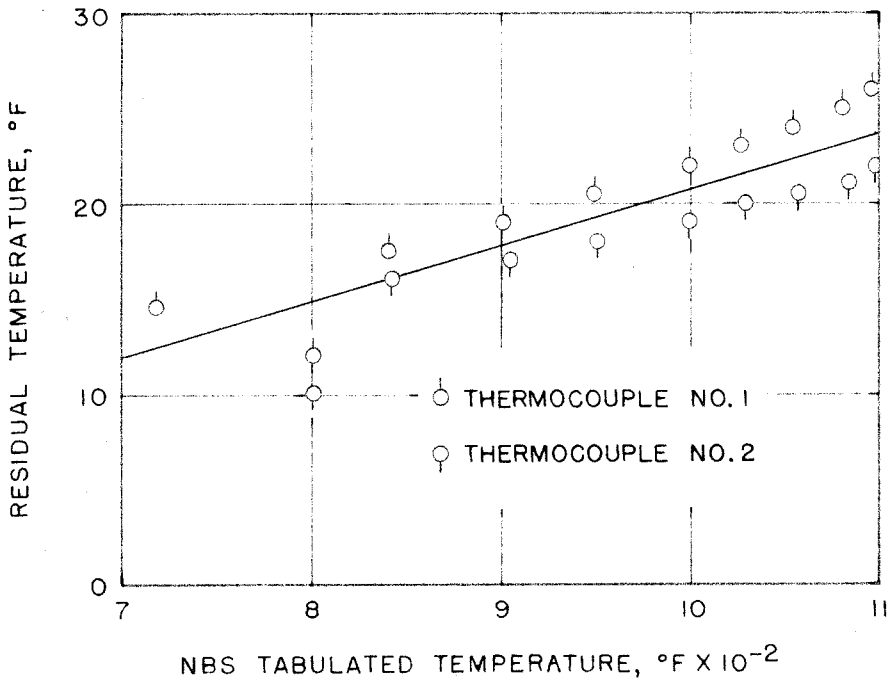

Figure 1A. Residual Temperature versus NBS Tabulated Temperatures of Chromel-Alumel Thermocouples

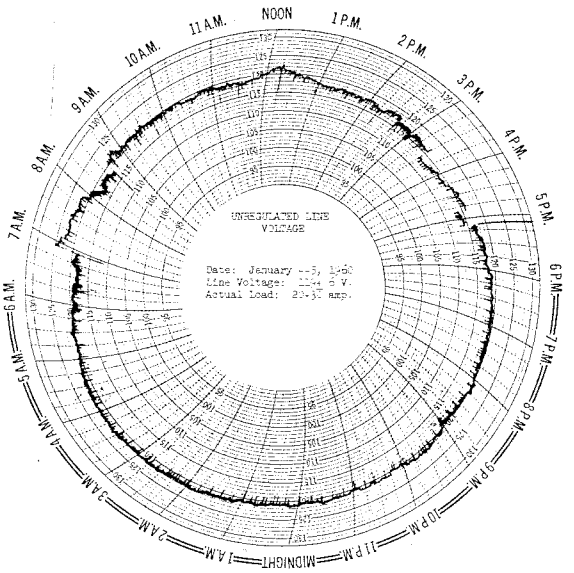

Unregulated Line Voltage

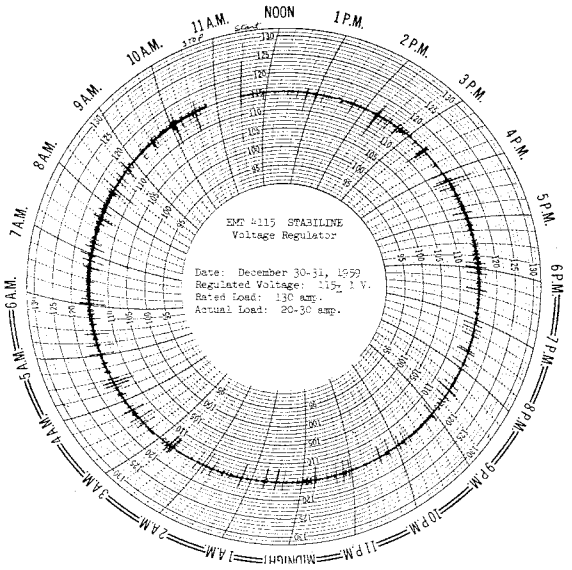

Regulated Line Voltage

Figure 2A. Record of Line Voltage to Reactor

Table 8A. Chromel-Alumel Thermocouple Calibration

Temperature NBS Thermocouple[a] (°F)	Thermocouple #1 Table Temp[b] (°F)	Thermocouple #1 △[c] (°F)	Thermocouple #2 Table Temp (°F)	Thermocouple #2 △ (°F)
733	718.5	14.5	-	-
813	801	12	803	10
858	840.5	17.5	842	16
922	903	19	905	17
969	948.5	20.5	951	18
1016	994	22	997	19
1049	1026	23	1029	20
1078	1054	24	1057.4	20.5
1105	1080	25	1084	21
1123	1097	26	1101	22

[a] NBS Calibration Test 146382a

[b] Emf reading of thermocouple was converted to temperature according to NBS Circular 561

[c] Here, △ is the difference between the NBS thermocouple temperature and the temperature obtained from NBS Circular 561 corresponding to the emf of the thermocouple

Table 9A. Equilibrium Data for the Decomposition of Nitric Oxide

$$2NO \rightleftharpoons N_2 + O_2$$

$$K_P = \frac{P_{N_2} P_{O_2}}{(P_{NO})^2} \qquad \text{(perfect gases)}$$

Temperature (°F)	$\log_{10} K_P$	K_P
1000	10.340	2.19×10^{10}
900	11.198	1.58×10^{11}
800	12.190	1.549×10^{12}

Assume initially for a total pressure of 1 atm:

$$P_{N_2} = 0.995 \text{ atm}$$
$$P_{NO} = 0.005 \text{ atm}$$

Temperature (°F)	$(P_{NO})_{equilibrium}$ (atm)
1000	3.37×10^{-7}
900	1.26×10^{-7}
800	4.01×10^{-8}

Part II

A CHROMATOGRAPHIC APPARATUS AND TECHNIQUE FOR THE ANALYSIS OF NITRIC OXIDE IN NITROGEN

INTRODUCTION

In the past, one of the major deterrents to the study of the catalytic decomposition of nitric oxide was the lack of accurate and rapid analyses for reaction species. That difficulty partially accounts for the limited amount of published information about the decomposition. Practically all the methods of analyses which were used depended, in part, upon the oxidation of nitric oxide to nitrogen dioxide.

For example, in a simple method, Bachman and Taylor (1) measured the extent of decomposition of nitric oxide by observing the decrease in pressure in a constant volume reactor which was thermostated near room temperature. The decrease in pressure was caused by the oxidation of the remaining nitric oxide by a product of its decomposition:

$$2NO \longrightarrow N_2 + O_2 \qquad (1)$$

$$2NO + O_2 \longrightarrow 2NO_2 \qquad (2)$$

Further decrease in volume occurred because of the following equilibria:

$$2NO_2 \rightleftharpoons N_2O_4 \qquad (3)$$

$$NO + NO_2 \rightleftharpoons N_2O_3 \qquad (4)$$

More recently, spectrophotometry techniques have been used (2,3). These methods also require the oxidation of nitric oxide to nitrogen dioxide; and in some instances, additional oxygen and ozone are added

to the product stream to assure complete oxidation of the nitric oxide.

Chemical and colorimetric methods of analyses for the oxides of nitrogen also exist, but the time required for the analyses is generally excessive. This necessitates having many sample containers which greatly increases the probability of errors. Likewise, the value of any given series of kinetic runs usually cannot be appraised even qualitatively for a period of time which may be as much as 1 to 2 days. Thus considerable time is lost if the results of the analyses uncover defects in the reactor, in the sampling systems or in the analytical procedures.

Two chromatographic methods for the analysis of nitric oxide in nitrogen have been developed recently (4,5). Silica gel is used in both instances as the column packing, but the methods of operation differ. Szulczewski (4) used 40-60 mesh dried silica gel in a column at dry ice-acetone temperatures and measured the separated components, nitrogen and nitric oxide by means of a thermal conductivity detector. Smith (5), however, operated his column at room temperature and measured the nitric oxide by difference. Smith's column consisted of 2 sections of silica gel separated by a layer of iodine pentoxide, which served to oxidize the nitric oxide to nitrogen dioxide. This oxidation product was adsorbed in the second section which was downstream from the iodine pentoxide, and hence did not leave the column. Since nitrogen was not separated from nitric oxide in the first section, the difference in peaks obtained from each of the silica gel sections gave the relative amount of nitric oxide present in the initial sample.

The present study was conducted in order to develop a rapid chromatographic technique for the analysis of nitric oxide in concentrations of less than 0.5% in nitrogen, wherein the column would be operated at or above room temperature. The plan was to separate the nitric oxide from the nitrogen and measure it directly by means of a thermal conductivity detector.

SUMMARY OF EXPERIMENTAL WORK

In the initial phases of this research, the feasibility of using a gas-solid or gas-liquid chromatographic technique for the analysis of the reactants and products of the catalytic decomposition of nitric oxide was explored. Chromatographic equipment was constructed and several column packings were tested for their ability to separate nitric oxide from nitrogen in a reproducible manner. These columns are listed in Table 2.

It was found that silica gel when treated and operated under the conditions discussed under Experimental Procedure met the requirements as an analytical tool for the system under consideration. Specifically, this system was a gas mixture composed of nitric oxide in nitrogen at concentrations of less than 0.5% by volume.

APPARATUS

Chromatography columns and detection devices which were used in this research were placed in a steel cabinet with a height of 8 ft and a square cross section measuring 3 ft on a side. The cabinet was lined with Fiberglas and was used as a constant-temperature air bath.

The cabinet space was divided in half by a vertical panel with openings at the top and bottom for air circulation. An electric blower, a bank of refrigeration coils and a thermostatically-controlled heater were installed in the bottom opening. A 15-ft length of 3/16-in. stainless-steel tubing filled with mercury was looped back and forth across the top opening. The mercury-filled tubing served as a temperature-sensing device and switch which controlled the electrical energy to the cabinet heater by activating an electronic relay. Proper adjustment of Freon flow through the refrigeration coils and of the voltage across the heater allowed control of the cabinet temperatures between 29 and 31°C to $\pm$ 0.2°C regardless of exterior temperatures or individual column temperatures. The blower provided enough circulation so that both sections of the cabinet were kept to within 0.25°C of one another.

On the exterior, the cabinet was divided into four sections, each with two doors: an upper small door for sample insertion and a lower large door for repairing and interchanging columns. With this arrangement, four columns could be operated simultaneously. Other details of the cabinet and accessories have been described by Rinker (6).

On one side of the cabinet were located most of the instruments

and controls as shown in Figure 1. These included an amplifier, bridge circuits for the detector, gas manifolds, rotameters, voltage recorders, variable resistors for control of direct current to the detectors, a cabinet for several 2-volt storage batteries, an ice bath for thermocouple reference junctions, and variacs which were used to control voltage to the cabinet heater and to the individual chromatography columns.

The column used for the separation of nitric oxide from nitrogen was constructed of type-304 stainless-steel tubing, and had a length of 8 ft, an O.D. of $\frac{1}{4}$ in., and a 0.035-in. wall. It was packed with either 35-48 or 48-60 mesh Davison No. 912 silica gel. This column was double looped to an overall length of approximately 4 ft and was placed inside a Pyrex tube which had a length of 4 ft and an O.D. of 1 in. The entire length of the glass tube was wrapped with Nichrome wire to give a heating element with a resistance of 25 ohms. Another Pyrex tube of the same length but with an O.D. of $1\frac{1}{2}$ in. was placed over the heater tube as shown in Figure 2, and was insulated with a combination of Fiberglas and aluminum foil. A similar unit with a 4-ft column of silica gel was used as the buffer column. These assemblies were connected inside the chromatograph cabinet, as shown in Figures 3 and 4, to a dual-thermistor thermal conductivity cell. Tygon tubing and $\frac{1}{4}$-in. copper tubing were used to connect the columns to rotameters and to the source of helium.

Figure 4 shows the path of gas flow through the columns. The helium purchased from Air Reduction was delivered from the cylinder at

10 psig by means of an automatic regulator. After flowing through a needle valve and a Tri-flat rotameter, the gas then passed in sequence through the buffer column, one side of the detector cell, the sample insertion section or a bypass, the separation column, the other side of the detector cell, and finally through the exit rotameter.

A line diagram of the thermal conductivity cell, which was constructed from a block of type-304 stainless-steel, is shown in Figure 5. The reference thermistor was offset from the direct line of gas flow in order to damp the effects of pressure fluctuations caused by the turning of stopcocks in the sampling system. All inlet and outlet connections were made of $\frac{1}{4}$-in. stainless-steel tubing. Thermistors were held in place by screw-type followers which compressed Teflon and neoprene gaskets around the thermistor sheaths. Surrounding the cylindrical block of stainless-steel and its connecting tubes was a brass water jacket which insulated the cell from temperature fluctuations in the cabinet. Wires leading from the thermistors were insulated from the cell by covering them with polyethylene tubing.

The thermistors in the conductivity cell were a pair of Fenwal G 106-GB32P8 probes matched to within 1% at 100°C. Since they are a part of the detector bridge network outlined in Figure 6, they were connected to the network by means of shielded cable. In operation, the measuring thermistor was used to detect changes in the thermal conductivity of the gas stream as its composition varied. These changes created a temperature variation in the thermistor bead which, because of its high negative coefficient of resistivity (over 3.5% per °C),

caused a measurable unbalance in the bridge circuit. This unbalanced voltage was recorded on a Varian recorder which had a full scale deflection of 10 mv.

Direct current which passed through the bridge circuit and energized the thermistors was supplied by four 2-volt batteries which were placed in series to provide an output of 8 volts. The current from the batteries was measured by an ammeter with a 0 - 100 ma scale while the current through the detecting thermistor in one leg of the bridge was measured with a more sensitive 0 - 30 ma ammeter.

To obtain measurable deflections for mixtures in which some components were in extremely low concentrations, the component signals were either attenuated or amplified. A 10-turn 10-K Helipot was used as an attenuator and was adjusted to give a 50-fold decrease in the output signal. By means of a two-way switch, either an attenuated or a full scale signal could be obtained. This signal was then fed to a second switching system which allowed its amplification by means of a Kintel Model 111 D.C. Amplifier. Also inserted in the amplifier circuit was a filter network which removed electrical noise from signals before their entrance into the recorder.

The Varian recorder was operated at a chart speed of 2 in. per min when recording data and at speeds of less than 16 in. per hr when checking drift of the base line and stability of the output signal. Data curves obtained on the recorder chart were integrated by means of a Lietz Model 236 Optical Planimeter.

Gaseous samples for analysis were taken in a sampling device which is shown in Figure 7. The glass sampler was fitted with a 12/5 ball joint at one end and a matching socket joint at the other. By means of butterfly clamps the sampler was easily attached or removed from the sampling sections of the chromatograph or the reactor. Special three-way stopcocks, each with a single bore for connecting any pair of the three legs arranged 120° apart, were used to avoid dead spaces in which air could be entrapped during the flush cycle. Three similar portable gas samplers were available and were used successively during the experiments. The volumes of the legs in each of the sample valves were calibrated by filling each leg separately with mercury and weighing the amount of mercury required. By noting the temperature at which the legs were filled, the volumes were calculated from the density and weight of the mercury. Results of these calibrations are tabulated in Table 1.

Copper-constantan thermocouples were used to measure temperatures in the cabinet and the columns. Two thermocouples were placed on both sides of the central panel in the cabinet. A second pair was attached to the top and bottom of the chromatography column. There were provisions in the unit for the eventual use of 20 pairs of thermocouples. A mercury thermometer was also placed in the cabinet for rough measurement of temperature.

EXPERIMENTAL PROCEDURE

Chromatography Column Selection

Columns constructed from 8-mm glass tubing or $\frac{1}{4}$-in. stainless-steel tubing were packed with a variety of adsorbents. Before use, each of the columns was dried in place for at least 12 hr by the passage of dry helium at approximately 150°C. These columns were tested at three different temperatures within the range of 30 to 125°C with various mixtures of nitric oxide, nitrogen dioxide and nitrogen. The mixtures consisted of 0.1%, 0.25% and 0.5% by volume of nitric oxide in nitrogen and 0.25% nitrogen dioxide in nitrogen and were all purchased from Matheson. These percentages were not always as specified, because the subsequent calibration by Matheson for two cylinders of 0.500% showed that the compositions were 0.404 and 0.436%, respectively. Other mixtures were made using prepurified nitrogen, pure nitric oxide, pure nitrogen dioxide and/or proportionate amounts of the above-mentioned binary mixtures. Tests of reproducibility were made using the Matheson-prepared mixtures. Each column was evaluated on the basis of its ability to quantitatively and reproducibly separate the three molecular species. This evaluation is discussed under Results.

Operation of Chromatography Unit

The chromatography column, chosen for the present work, was packed with 60-80 mesh silica gel and required a conditioning period of 2 to 3 days before quantitative separations of nitric oxide from nitrogen were obtained. This involved drying the silica gel, in place, with a low

flow of helium for 20 to 24 hr at temperatures of 150 to 200°C. Following the drying period, the column was treated with at least five 2.8-cc samples of nitric oxide and two or three 1.9-cc samples of nitrogen dioxide at the operating temperature range of 60 to 85°C. Conditioning of the column with nitrogen dioxide as well as with nitric oxide was necessary in order to obtain a separation of nitric oxide from nitrogen. After this separation was achieved for samples containing 0.5% nitric oxide, more of the same type of samples were passed through the column until reproducibility of separation and of the relative peak areas was attained. The column was then ready for quantitative analysis.

Operating conditions of the chromatography unit were as follows:

Inlet helium pressure at 25°C	10 psig
Helium flow rate at 25°C and 1 atm	45 cc/min
Cabinet temperature	30.0 ± 0.2°C
Thermal conductivity cell temperature	30.0 ± 0.2°C
Column heater voltage	32.5 ± 0.5 volts
Column temperature (top)	85 ± 2°C
Column temperature (bottom)	68 ± 2°C
Current in detector bridge	18 ma
Current in sensing element	8.5 ma
Recorder chart speed	2 in./min
Recorder sensitivity for N_2 peak (full scale)	500 mv
Recorder sensitivity for NO peaks unamplified (full scale)	10 mv
amplified (full scale)	0.5 mv

Starting procedures for the chromatograph consisted initially of switching on the power to the cabinet blower, heaters, and relay-controlled thermostat and then adjusting the cabinet variac to 125 volts. Next, the column variac and helium flow were adjusted to the proper settings. When the cabinet reached its control temperature, refrigerant was circulated through the cooling coils, and the cabinet variac was then adjusted to give equal heating and cooling cycles. Finally, power from the batteries was supplied to the thermistors, and the Varian recorder was switched on.

Samples were not introduced into the column until a steady base-line response was obtained at the most sensitive scale necessary for the analysis. In other words, if an amplification of 20 was used in part of the analysis, the base-line response was checked for steadiness at that amplification. With a steady base line, several calibration samples were analyzed until the results of the analysis were reproducible. Also, before and after each series of reactor samples were passed through the column, several calibration samples were analyzed, and these were used as a basis for calculating the concentrations of nitric oxide in the reactor samples.

Ordinarily, the unit was left on control during the time between experiments unless this interval exceeded several days. At the end of every experiment, however, the thermistor current and recorder were turned off and a slight static pressure of helium was left in the column. When the column was not in use for a period of more than 2 days, the entire chromatograph system was turned off with the exception of the

power to the column heater. The variac setting of the column heater was increased 3 to 5 volts and the static helium pressure in the column was maintained at 2 to 5 psig with no flow.

RESULTS

Chromatography Column Selection

A variety of adsorbents as noted in Table 2 was tested in order to find a column packing which would reproducibly effect the separation of nitric oxide, nitrogen dioxide and nitrogen. Helium was used as the carrier gas, but in a few of the tests hydrogen was used. The tests with hydrogen, however, were too few and therefore inconclusive.

A column packed with a molecular sieve (Column No. 3, Table 2) separated oxygen, nitrogen and the nitrogen oxides; but reproducible results were not obtained at any temperature. Column No. 5 containing silica gel coated with sulfuric acid absorbed the nitrogen dioxide at all temperatures with more complete removal of the dioxide at the higher temperatures but with no separation of the nitric oxide from nitrogen. Column No. 11 containing activated vanadia strongly oxidized nitric oxide in the temperature range studied with a resultant color change in the vanadia.

None of the columns in the preliminary tests, with the exception of silica gel, effected a good separation of all three components. The gel, although separating nitric oxide, nitrogen dioxide and nitrogen gave non-reproducible peaks for the nitrogen dioxide.

Since the silica gel appeared to be the most suitable of the adsorbents, it was used in additional experiments to optimize column parameters such as mesh size, column temperature and pressure, carrier-gas flow rate, and the sample size. The optimum conditions which

provided an acceptable analysis of the nitric oxide-nitrogen system are listed in Experimental Procedure.

Silica Gel Column

Representative results of the analysis of nitric oxide in nitrogen are presented in Table 3. For continuous operation of the chromatography unit, the reproducibility of the relative peak areas was found to be within $\pm$ 4% for mixtures containing 0.1 to 0.5% nitric oxide by volume. When the unit was shut down between experiments, it was found that identical operating conditions were not attained from one experiment to the next without adjustment of controls. This resulted in a change in relative peak areas without affecting the reproducibility so that recalibration with a standard nitric oxide-nitrogen mixture was necessary.

The elution time of the nitric oxide varied with its concentration. Figure 8 which presents elution curves of an unamplified and an amplified nitric oxide peak shows that as the concentration decreased the elution time increased. This phenomenon may possibly be attributed to overloading of the column or to the fact that at higher concentrations, equilibration between the phases is more rapid. The elution time, when taken as the interval between the insertion of a sample and the appearance of a peak, was approximately 90 sec for the nitrogen and varied from 165 to 200 sec for the nitric oxide, at concentrations ranging from 0.5 to 0.1% by volume, respectively.

Figure 8 also shows that considerable tailing of the nitric oxide peak occurred for a 2.8-cc sample. Similar tailing was obtained for

samples as small as 1.0 cc. This phenomenon, which was probably due to adsorption of the nitric oxide on silica gel, was of such significance that extreme care was exercised in obtaining a non-drifting base line for area measurements. This was especially important for concentrations of nitric oxide near the minimum value for which amplification was necessary. Hence, samples were introduced only when the base line was steady at the highest recorder sensitivity used in the analysis.

The areas of the resulting peaks were measured very carefully with a planimeter. Since the perimeter-to-area ratios of the peaks were high, the probability for planimeter errors was increased. An area could be reproducibly measured with the planimeter to plus or minus the last digit on the vernier. This gave a maximum deviation of about $\pm$ 2% for the smallest area measured.

It was also found in the experiments that a negative temperature gradient in the direction of carrier-gas flow improved the separation of the nitric oxide from nitrogen. Separation was incomplete, however, for a gradient imposed in the opposite direction. The negative temperature gradient was a natural one due to convection and was subject to slight variation whenever the column was removed and repacked. Component separations were not measurably affected by these variations in the temperature gradient on the column.

DISCUSSION

Sources of Error

Several sources of error in the chromatographic analyses and the precautions which were taken to minimize them are discussed as follows:

1. Temperature Fluctuations - There were three kinds of temperature fluctuations:
   a. Variations in the column temperature resulting from line-voltage fluctuations in the column heater. Without voltage control, the column temperature varied as much as $\pm$ 3°C over a period of 10 hr.
   b. Inherent variations in the cabinet temperature because of the limitations in the on-off type of control thermostat. In some experiments this fluctuation was as high as $\pm$ 0.25°C.
   c. Accidental variations in the cabinet temperature resulting from opening of the cabinet doors.

   These fluctuations in temperature created variations in the detector response and hence brought about base-line drift.

   In order to help decrease temperature fluctuations in the column, an electro-mechanical voltage regulator was installed to supply constant voltage within $\pm$ 1 volt to the column heater. This regulation proved to be entirely satisfactory.

The inherent variations in cabinet temperature could not be eliminated but fortunately were negligible at ordinary detector sensitivities. At detector signal amplifications higher than 50, however, base-line variations became increasingly significant.

If the small cabinet doors were not opened for more than 5 sec, the resultant temperature fluctuation in the cabinet was quickly damped out or was insufficient to cause base-line drift. Hence, samples were introduced into the column in a period of less than 5 sec.

2. Thermistor Current Fluctuations - A drift in the electrical current supplied to the thermistor also created a base-line drift and was attributed to the discharging of the storage cells in the bridge circuit. The storage cells were rated at 20 amp-hr; and although the current load of the bridge circuit was only 18 ma, it was necessary to recharge the cells at least once a month. Immediately after recharge, however, it was necessary to allow current flow through the bridge for several hours in order to obtain a steady current and thus a non-drifting base line.

3. Flow Rate Fluctuations - Changes in helium flow during a sample analysis were detected on the rotameters and were generally attributed to leaks resulting from poor sampler attachment or improperly greased stopcocks and ball joints.

Such leakage gave partial loss of sample from the column. Therefore, extreme care was taken in greasing all ground-glass joints. Too much grease also made precise analysis difficult because the excess lodged in the stopcock bores and then absorbed nitric oxide from the samples.

Even without leaks, large changes in helium flow past the thermistors caused base-line drift. By carefully adjusting the helium flow with a pressure regulator, these changes were eliminated as long as no adjustments were made during an analysis.

4. Improper Sampling Procedure - Since samples from the reactor were obtained by allowing the product stream to flow through the sampler, it was necessary to allow sufficient time for flushing in order to obtain a representative sample. Also, prior to elution of the sample in the column, at least 5 min were required to flush air out of the by-pass arm and through the column. If the flushing was not complete, the contaminant remaining was primarily air, which eluted with the nitrogen in the sample and also oxidized part of the nitric oxide to higher oxides. The errors in analysis resulting from each of these effects were additive, with a consequent decrease in nitric oxide concentration. Higher oxides were undetectable.

By taking precautions to minimize or eliminate the above errors, it was usually possible to obtain analyses which were reproducible to

± 4% for mixtures containing 0.1 to 0.5% nitric oxide in nitrogen.

Hypothetical Model of Separation

The silica gel column was developed as a method for the quantitative analysis of nitric oxide-nitrogen mixtures in which the concentration of nitric oxide was less than 0.5%. Since this was the primary objective, no studies were made to determine the reason for the rather specific conditioning procedure required to activate the silica gel.

By noting the effects of each step in the conditioning procedure, however, a hypothetical model of the activation process was proposed. Starting with a fresh column of silica gel, the first few samples of pure nitric oxide showed a definite successive increase in the quantity of the oxide eluted. This indicated that nitric oxide was being adsorbed. Subsequent samples of 0.5% nitric oxide in nitrogen were then apparently eluted from the column quantitatively, but the nitric oxide was only partially separated from the nitrogen. It was only after the injection of nitrogen dioxide into the column that separation of the nitric oxide and nitrogen occurred. From these results it was assumed that some nitric oxide and nitrogen dioxide were tightly held to the surface of the silica gel by physical or chemical bonding. It was further assumed that nitrogen dioxide was oriented on the silica gel surface in such a position that it formed a weak complex with the nitric oxide and retarded its progress through the column.

The weakly bonded complex was assumed to be a nitrogen sesquioxide molecule which supposedly has the following structure (7):

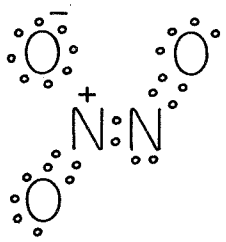

This structure required that the nitrogen dioxide be adsorbed on the surface in such a way that either one or both of the oxygens were bonded to the silica gel and hence exposed the nitrogen to a passing nitric oxide molecule. Pictorially, the orientation would appear as shown below:

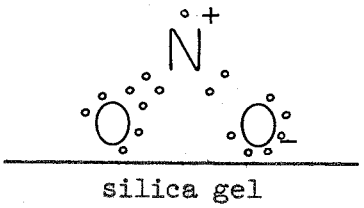

Bond distances of the nitric oxide molecule suggested resonance between two electronic structures (8).

Although the second structure had an unfavorable charge distribution, the similarity of their structural stability allowed the assumption of complete resonance. Thus, if the adsorption of nitrogen dioxide occurred as shown in the hypothetical model, there existed an attractive force between the adsorbed nitrogen dioxide and the gas phase nitric oxide. This weak bonding was sufficient to permit the separation of the small amounts of nitric oxide from nitrogen by the formation

of adsorbed nitrogen sesquioxide. The bond was subsequently broken and re-formed during the elution process.

CONCLUSIONS

A chromatographic method has been developed for the analysis of a binary gas mixture containing nitric oxide in nitrogen at concentrations of 0.1 to 0.5% by volume. A thermal conductivity cell incorporating a matched pair of thermistors and coupled with an amplification system was used to detect the species separated by the silica gel column. A continuous record of the thermistor response thus made possible the quantitative measurement of the amount of nitric oxide present in nitrogen. Reproducibility of this measurement was possible to within $\pm$ 4%.

The stepwise procedure of conditioning the silica gel column, which included addition of nitrogen dioxide, was important in obtaining reproducible analyses.

REFERENCES

1. Bachman, P. W. and Taylor, G. B., J. Phys. Chem., 33, 447-455 (1929).

2. "Investigation of Catalytic Decomposition of Nitric Oxide," Armour Research Foundation of Illinois Institute of Technology, Chicago, Illinois, Feb. 21, 1957.

3. Fraser, J. M. and Daniels, F., J. Phys. Chem., 62, 215-220, (1958).

4. Szulczewski, D. H. and Higuchi, T., Anal. Chem., 29, 1541-1543 (1957).

5. Smith, R. N., Swinehart, J., and Lesnini, D. G., Anal. Chem., 30, 1217-1218 (1958).

6. Rinker, R. G., Ph.D. Thesis, California Institute of Technology, 1959.

7. Ingold, C. K. and Ingold, E. H., Nature, 159, 743-744 (1947).

8. Pauling, L., "The Nature of the Chemical Bond," 2nd ed., 266-267, Cornell Univ. Press, Ithaca, N. Y., 1948.

LIST OF FIGURES

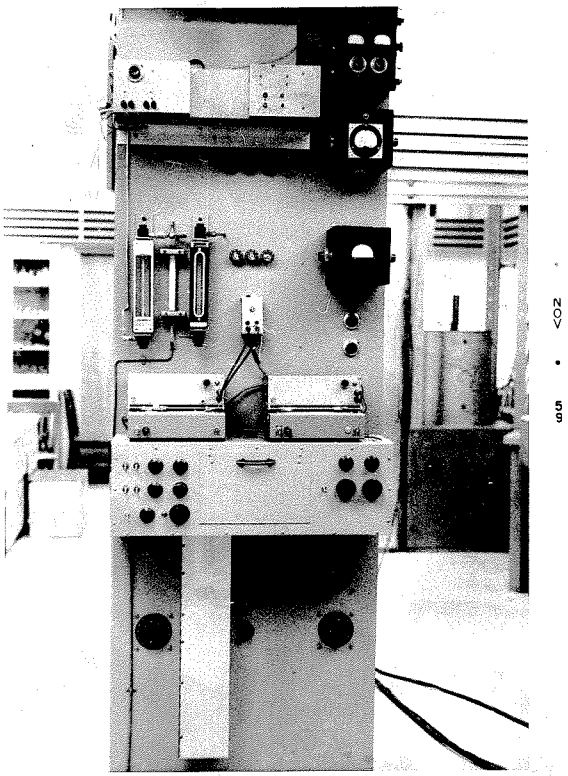

Figure 1. Instrument Panel of Chromatography Unit

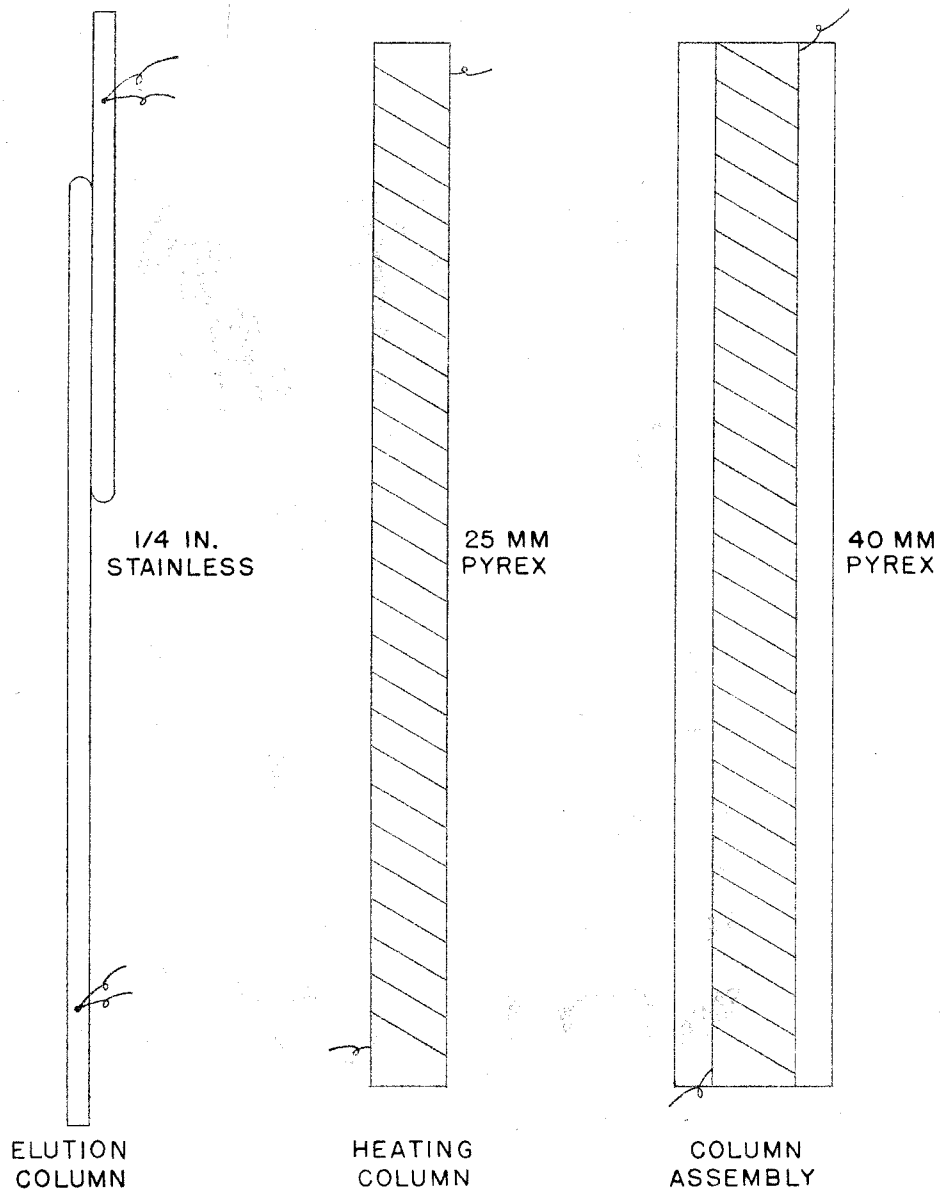

Figure 2. Details of Elution Column

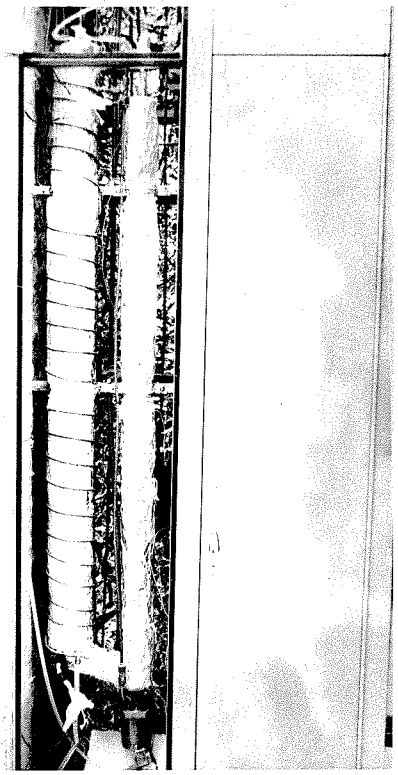

Figure 3. Column Assembly Inside the Chromatography Unit

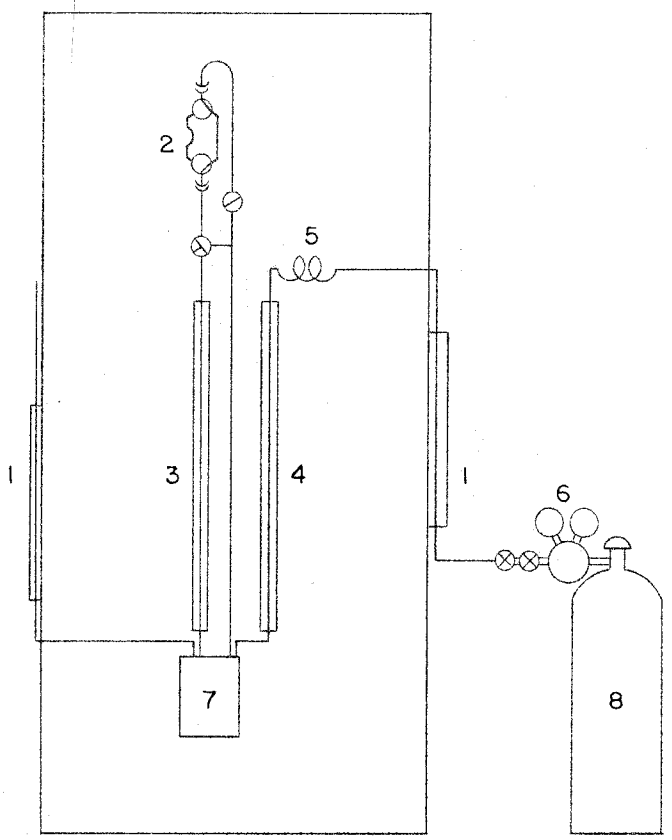

1. Rotameter
2. Gas Sampler
3. Elution Column
4. Buffer Column
5. Gas Conditioner
6. Gas Regulator
7. Conductivity Cell
8. Compressed Helium

Figure 4. Flow Diagram of Chromatography Apparatus

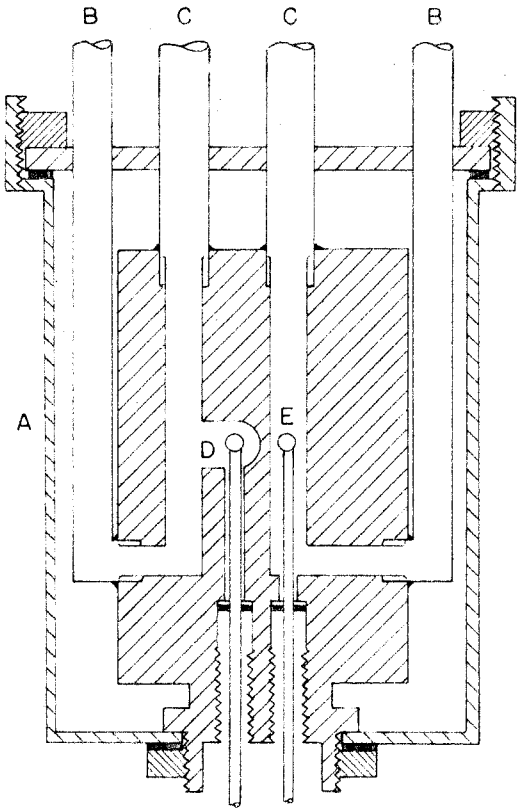

A - Water Jacket
B - Gas Outlet
C - Gas Inlet
D - Reference Thermistor
E - Measuring Thermistor

Figure 5. Line Diagram of Thermal Conductivity Cell

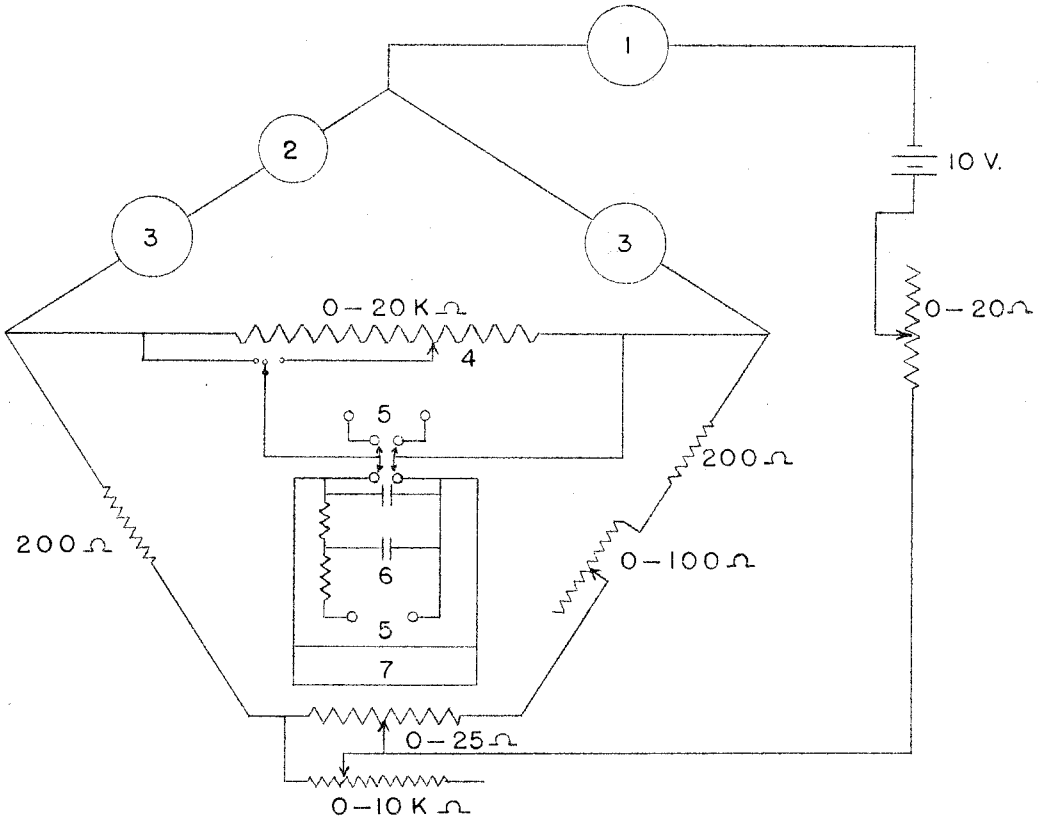

1. Ammeter (0-100 ma)
2. Ammeter (0-30 ma)
3. Matched Thermistors (2000 ohms at 25°C)
4. Attenuation (10-turn Helipot)
5. Amplifier Connections
6. Filter Network
   Capacitors (20 microfarads)
   Resistors (10 K ohms)
7. Varian Recorder (10 mv full scale)

Figure 6. Bridge Circuit for the Thermal Conductivity Detector

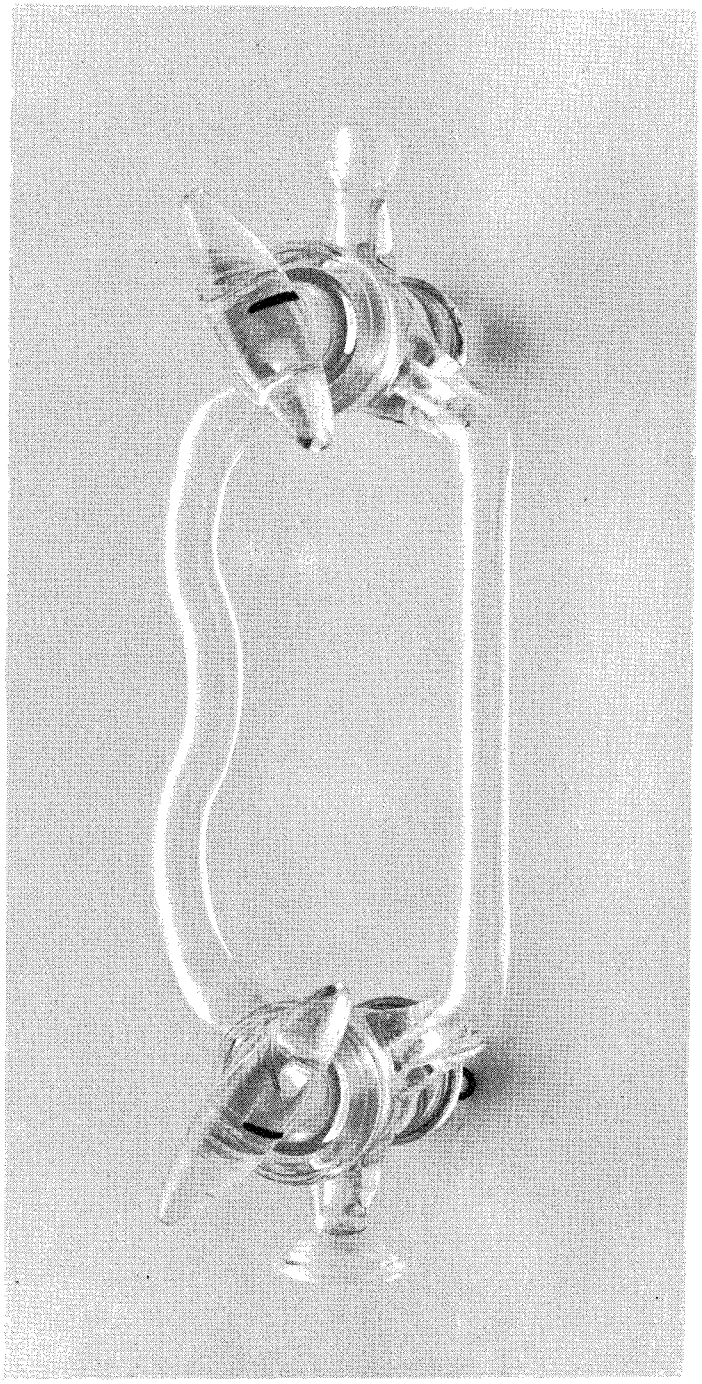

Figure 7. Portable Gas Sampler

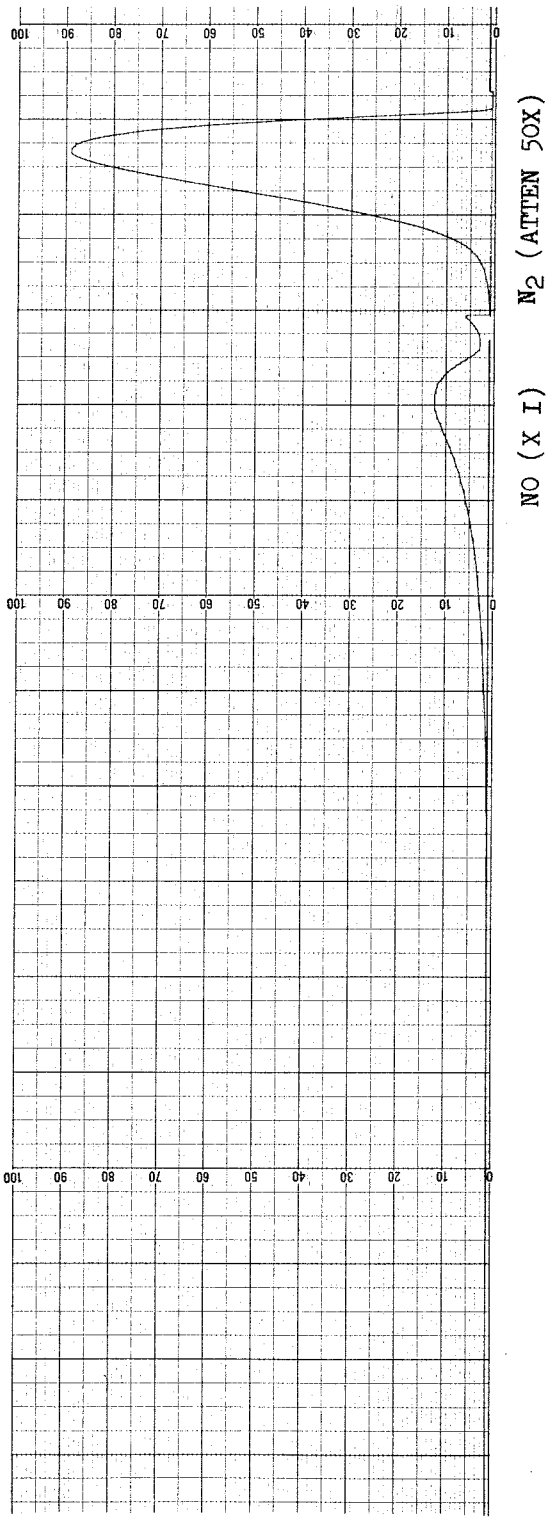

Figure 8. Elution Curves for NO and N_2

LIST OF TABLES

Table 1. Volumes of Gas Samplers

Sampler No.	Volume of Straight Leg (cc)	Volume of Curved Leg (cc)
IV	1.96	2.78
V	1.89	2.90
VI	1.93	2.76

Table 2. Chromatography Columns Tested

No.	Column Length (ft)	Mesh Size	Packing
1	4	60-80	Silica Gel Davison #912
2	4	35-48	Activated Alumina
3	4	35-48	Molecular Sieves Linde 13x
4	4	35-48	Silica Gel with 10% by weight of Kel F. Packing slightly brown due to traces of carbon.
5	4	60-80	Silica Gel with 25% by weight of 98% H_2SO_4
6	4	60-80	Silica Gel with 25% by weight of Kel F
7	4	60-80	Acid washed Dicalite
8	4	10-30	Johns-Manville "Chromosorb"
9	4	48-60	Vanadia oxidation catalyst Davison #903 (nonactivated)
10	4	35-48	"Chromosorb" with 25% by weight of Kel F
11	4	60-80	Vanadia oxidation catalyst (activated at 800°F for 3 hours)
12	4	60-80	Same as 11 purged with NO to reduce V_2O_5
13	4	35-48	Celite with 25% by weight of $FeSO_4$
14	12	60-80	Silica Gel
15	4	35-48	Celite with Fe_2O_3 dusted on the surface
16	4	35-48	Celite mixed with powdered TiO_2
17	12	35-48	Silica Gel
18	8	48-60	Silica Gel
19	8	35-48	Silica Gel

Table 3. Representative Results of NO - N_2 Analyses

Source Sample	Column Temperature		Helium Flow Rate	Area of NO / Area of (NO+N_2)	Elution Times[b]	
(Tank No.)	Top (°C)	Bottom (°C)	(cc/min)[a]	(%)	N_2 (Sec)	NO (Sec)
1.	85	70	40.4	0.158	99	197
			39	0.152	98	193
			45	0.168	94	196
2.	82-83	67	42	0.544	90	168
			45	0.542	90	169
			45.5	0.542	90	173
			43	0.554	88	172
			45	0.555	89	172
			42	0.554	89	172
2.	83.5-84.5	66.5-68	47	0.575	86	162
			45.5	0.549	89	168
			45.5	0.554	89	168
			46	0.544	89	165
			45.5	0.540	89	165
2.	86.5	69.5	45.5	0.549	89	168
			45.5	0.538	89	168
			45	0.570	90	179
2	87	70	46	0.556	92	177

[a] Flow rate based on 1 atm and 25°C

[b] Elution time is interval of time between sample insertion and appearance of peak

Part III

KINETICS AND MECHANISM OF THE AIR OXIDATION OF THE DITHIONITE ION ($S_2O_4^{=}$) IN AQUEOUS SOLUTION

[Reprinted from the Journal of Physical Chemistry, **64**, 573 (1960).]

KINETICS AND MECHANISM OF THE AIR OXIDATION OF THE DITHIONITE ION ($S_2O_4^=$) IN AQUEOUS SOLUTION

By Robert G. Rinker, Thomas P. Gordon, David M. Mason,[1] Roy R. Sakaida and William H. Corcoran

Chemical Engineering Laboratory, California Institute of Technology, Pasadena, California

Received September 16, 1959

A study of the air oxidation of sodium dithionite was conducted in aqueous solution which was 0.1 *M* in sodium hydroxide. The concentration of the dithionite was measured as a function of time at 30, 40, 50 and 60°. Initial concentrations varied from 5×10^{-3} to 20×10^{-3} *M*. Under conditions in which diffusion of air was not controlling it was found that the oxidation was half order with respect to dithionite and first order with respect to molecular oxygen. The half order mechanism was attributable to the presence of the SO_2^- radical ion as an intermediate.

Introduction

Probably the earliest air oxidation study of dithionite was conducted by Meyer[2] in 1903. He studied the oxidation of sodium dithionite by observing the oxygen uptake in shaken flasks containing aqueous dithionite solution. His results showed that the products of reaction were sulfite and sulfate. He proposed a primary reaction to be

$$H_2S_2O_4 + H_2O + O_2 = H_2SO_4 + H_2SO_3 \quad (1)$$

Also, he found that a competing reaction was

$$2H_2S_2O_4 + 2H_2O + O_2 = 4H_2SO_3 \quad (2)$$

From the over-all reaction rates, he computed first-

(1) Division of Chemical Engineering, Stanford University, Stanford, California.

(2) J. Meyer, *Z. anorg. Chem.*, **34**, 43 (1903).

order rate constants but found that they drifted over a wide range.

Bassett and Durrant[3] in 1927 studied the reaction between dithionite and molecular oxygen. Their explanation of the oxidation mechanism was based upon arguments that dithionite exists in three isomeric forms. Each isomer was believed to decompose in a way such that all of the observed reaction products could be explained by one or more of the mechanisms. Although Bassett and Durrant's work is of considerable value as a compilation of experimental observations of dithionite reactions, subsequent work has invalidated their interpretations.

Nicloux[4] in 1933 was interested in determining the over-all stoichiometry of the reaction between dithionite and oxidizing agents of varying strengths. With a comparatively weak oxidizing agent such as silver ion, the dithionite was oxidized to sulfite. With molecular oxygen, an equimolar mixture of sulfite and sulfate was formed. Finally, with a very strong oxidizing agent, sulfate was the only product. No experimental details were given. The results of Lynn[5] suggested that the atmospheric oxidation of $Na_2S_2O_4$ proceeded according to a first-order mechanism with respect to dithionite and that the rate increased with temperature. He stated that the over-all stoichiometry was described by the equation

$$Na_2S_2O_4 + O_2 + H_2O = NaHSO_4 + NaHSO_3 \quad (3)$$

An examination of his data at 50° showed that the oxidation rate increased with an increase in air flow which meant that the diffusion rate of oxygen was a contributing factor. Without correcting for diffusion his results for the actual oxygen–dithionite reaction were, therefore, only approximate. His experiments did show that in the presence of 0.1 *M* sodium bisulfite the oxidation rate was extremely high. In the presence of 0.1 *M* sodium hydroxide the rate was inhibited, and the reaction proceeded smoothly.

Experimental

Apparatus.—The air oxidation of the sodium dithionite was carried out in a glass reactor with a volume of approximately 600 cc. Air was bubbled at a rate of 2500 to 3000 cc./min. into the reaction mixture near the bottom of the reactor through a medium-coarse glass frit which could be inserted or removed through a standard-taper opening on the reactor. During the reaction, the frit was always immersed in the liquid contents.

Before the air entered the frit, it was passed first through an Alundum-stone trap to remove suspended solids and aerosols, next through a molecular-sieve dryer, and finally through a temperature-conditioning coil. The air flow was measured by means of a wet-gas meter placed on the downstream side of the reactor.

Mixing was accomplished by means of a glass stirrer having two impellers. The stirrer was supported and sealed through a mercury-in-glass bearing. Stirring speeds could be varied up to 1100 revolutions per minute, which was the speed used throughout the experiments.

The reactor and the temperature-conditioning coil were thermostated in a 28-liter water-bath, which maintained the temperature within ± 0.02°. Heaters in the water-bath were energized by an electronic-relay circuit which in turn received its signal from a mercury-expansion switch immersed in the water.

(3) H. Bassett and R. G. Durrant, *J. Chem. Soc.*, **2**, 1401 (1927).
(4) M. Nicloux, *Compt. rend.*, **196**, 616 (1933).
(5) S. Lynn. Ph.D. Thesis, California Institute of Technology, 1954.

Samples were taken from the reactor through an opening in the top. A syringe needle or pipet was inserted into the reacting mixture, and the sample then was removed.

Commercial-grade nitrogen was the source of supply for the oxygen-free atmosphere required in preparing the sample of fresh sodium dithionite to be charged to the reactor. The nitrogen contained approximately 0.01% oxygen by volume and this amount proved excessive. Hence, most of the oxygen was removed by passing the nitrogen through two scrubbing towers in series. Each contained 0.2 *M* chromous chloride solution in 1.0 *N* hydrochloric acid. Acid and water vapors were subsequently removed by passing the nitrogen through a 0.1 *M* sodium hydroxide solution and then through a calcium chloride dryer.

Concentration of Dithionite as a Function of Time.—Chemically pure sodium dithionite (Baker Chemical Company, Batch No. 3712, Lot No. JTB6113) was the starting point for the source of dithionite ions. In preparing the dithionite for a typical run, approximately 25 g. of the powder was placed in an oxygen-free flask into which a stream of oxygen-free nitrogen had been passed for several minutes. Then, approximately 100 cc. of distilled water, free of oxygen and carbon dioxide, was injected into the flask through a rubber serum-bottle-cap. The mixture was heated to 60° with constant agitation until a saturated solution was obtained. With great care to avoid contact with oxygen, a 60-cc. sample of the saturated solution was withdrawn with a syringe and injected into a side-armed test-tube already filled with nitrogen. The tube with its contents then was cooled to 0° in an ice-bath while maintaining the pressure of the nitrogen constant at slightly above one atmosphere. At the lower temperature the liquid became supersaturated with sodium dithionite. With sufficient agitation, crystals of $Na_2S_2O_4 \cdot 2H_2O$ were formed. Again, with great care, practically all the liquid was removed from the tube leaving the white crystals settled at the bottom. Approximately 4 cc. of distilled water at 0° and free of carbon dioxide and oxygen was injected into the tube to wash the crystals. This washing process was repeated once again to obtain reasonably pure crystals. The final saturated solution with a volume of approximately 20 cc. was used to supply the reactor with an initial concentration of dithionite.

Before injection of the dithionite, the reactor was filled with 505.0 cc. of 0.1 *M* sodium hydroxide solution. The reactor was then immersed in the water-bath and allowed to reach steady conditions of temperature, stirring rate and air flow. The time of initial air flow was noted in order to account for evaporation losses from the reactor. At steady conditions, 5.00 to 15.00 cc. of the saturated dithionite solution, depending upon the initial concentration desired, was injected into the reactor. Since the delivery times of large syringes are of the order of several seconds, the time at which half of the sample was injected was taken as the initial time of the reaction.

Without delay, 1.00 or 2.00 cc. samples were removed from the reactor with a calibrated syringe and injected into 150-cc. flasks containing a mixture of 50 cc. of 0.1 *M* potassium hydroxide and 15 cc. of methyl alcohol. Also, the flasks contained a nitrogen atmosphere which was maintained during titration. The solutions in the titration flasks were stirred magnetically. The time at which half the sample from the reactor had been injected into a titration flask was recorded as the injection time.

The concentration of dithionite in the titration flasks was determined by titration with a standardized aqueous solution of methylene blue having a concentration in the range of 9.0×10^{-4} to 9.3×10^{-4} *M*.

Usually, the total time required to obtain a sample and titrate it was 40 sec. At the maximum temperature of 60° and at the minimum initial concentration of 5×10^{-3} *M*, the time for completion of the reaction was a minimum. Under these conditions, at least five titrations were accomplished before the end of the reaction.

As soon as all the dithionite had been oxidized, the air-flow was stopped, and the time was noted. The reactor was removed from the water-bath, and the volume of its contents was measured. A material balance, coupled with the knowledge of the air-flow rate and the assumption that the exit air was saturated with water vapor, made it possible to calculate the loss of water by evaporation prior to and during the reaction.

In the analysis of the dithionite samples, the methylene blue was reduced quantitatively on an equimolar basis from

an intense blue color to an almost colorless leuco-form. It was found in agreement with Lynn's work,[5] that the leuco-form was relatively insoluble in water at room temperature; and unless it was dissolved, it apparently adsorbed unreacted methylene blue during the titration. This resulted in a lowered over-all rate of reaction because of the time required for the dithionite to diffuse to the solid surface before reaction could occur. The purpose of the addition of the methyl alcohol in the titration flasks was to dissolve the solid leuco-compound and hence speed up the titrations. When titrated quickly, any thiosulfate and sulfite present in a sample did not interfere in the reaction between dithionite and methylene blue for the temperature range 0–30°. The end-point was sharp and was attained rapidly at room temperature.

Standardization of the methylene blue was done according to the method of Welcher[6] and Kolthoff.[7] Briefly, the methylene blue was titrated into a standard water-solution of 0.005 *M* picrolonic acid which was buffered at a *p*H of about 6. Periodic removal of the dark green product, methylene blue picrolonate, from the water phase was necessary in order to detect the end-point. This was accomplished by extraction of the methylene blue picrolonate with chloroform. Neither the picrolonic acid nor the methylene blue was soluble in the chloroform. Near the end-point. only 2 or 3 drops of methylene blue were titrated into the acid between successive extractions with chloroform. The end-point occurred when a blue color persisted in the water phase after addition of one drop of methylene blue, but with no color in the chloroform phase. When carefully applied, this method gave results accurate to ±0.5% compared with ±2% for the classical iodine-precipitation method.[8]

Solubility of Dithionite at 0°.—A solution of sodium dithionite saturated at 0° was prepared as described in the previous section. The saturation concentration of the dithionite, however, far exceeded the desired value for titrations with reasonable volumes of methylene blue. Therefore, 5.00 cc. of the saturated solution was injected through a serum-bottle cap into a 1-liter vessel which contained 500.0 cc. of 0.1 *M* sodium hydroxide maintained under a nitrogen atmosphere and at a temperature of 0°. Several 2.00-cc. samples of the resulting solution were titrated with methylene blue under conditions similar to those stated in the previous section. From these results, the solubility of the dithionite at 0° was calculated.

End-Products of the Dithionite Oxidation Reaction.—A knowledge of the types and quantities of the oxidation products of dithionite was important in determining a mechanism for the reaction. For the qualitative tests, a decomposed sample of dithionite was prepared by adding 0.20 g. of the purified powder to 100 cc. of 0.1 *M* sodium hydroxide solution through which air was bubbled until a test showed no reduction of methylene blue. A sample of the reaction mixture was acidified with hydrochloric acid to a *p*H of about 2, then lead acetate was added. A white precipitate resulted which indicated the absence of sulfide from the mixture. For the conditions here of small amounts of chloride ion, a black precipitate of lead sulfide would have appeared had sulfide been present. Another sample, when mixed with potassium triiodide at a *p*H of about 5, decolorized the iodine, indicating the presence of thiosulfate and/or sulfite. Still another sample at that *p*H was treated with barium chloride to remove sulfite and sulfate, if present, as barium sulfite and barium sulfate. The white precipitate was filtered. The filtrate was then titrated with potassium triiodide which showed a positive test for thiosulfate. Treatment of the precipitate with strong hydrochloric acid resulted in the evolution of sulfur dioxide to give a positive test for sulfite. The fact that a portion of the precipitate was essentially unattacked by an excess of acid showed the presence of sulfate as barium sulfate.

The procedure for the quantitative analysis was based upon the results of the qualitative findings. The principal ions of interest were sulfite, sulfate and thiosulfate. Any complexes of these ions or the presence of other ions were considered highly unlikely or in concentrations too low to be detected. The quantitative results substantiate this assumption.

Samples for quantitative analysis were taken from two sources, both of which were different from the source used in the qualitative analysis. The first source was contained in a flask which originally was charged with 500 cc. of 0.1 *M* sodium hydroxide at 30° and with 7 cc. of saturated dithionite solution. Oxygen entered the liquid bulk only by molecular diffusion through the surface of the liquid. This mixture was checked for completion of dithionite oxidation before other components were studied. The second source was contained in the reactor following a usual run at 30° as described previously.

In both cases, the method of analysis for end-products was the same. Four separate analyses were made on four separate samples from each source. These were: (1) iodometric titration to determine the sum of the concentration of thiosulfate and sulfite; (2) iodometric titration to determine only the concentration of thiosulfate; (3) barium chloride titration to determine the sum of the concentration of sulfite and sulfate; (4) barium chloride titration to determine only the concentration of sulfate.

In the iodometric analysis for the sum of the sulfite and thiosulfate, a 10 to 25-cc. sample was buffered with a solution which was 0.5 *M* in sodium acetate and 0.4 *M* in acetic acid. Usually, a volume of the buffer solution equal to the volume of the sample was added to give a constant *p*H of about 5. Using a starch end-point, the solution was titrated with a standardized solution of approximately 0.01 *N* triiodide. In case of excess addition of triiodide, back-titration was done with a standard thiosulfate solution which was approximately 0.01 *N* in thiosulfate.

In the iodometric analysis for only the thiosulfate ion, a 10 to 25-cc. sample was buffered to a *p*H of about 5. To this was added a volume of 37 weight % formaldehyde in water equal to about half the volume of the sample. The purpose of the formaldehyde was to form a complex with the bisulfite according to the reaction

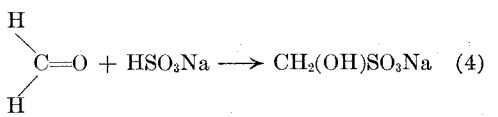

$$\begin{matrix} H \\ \diagdown \\ C{=}O \\ \diagup \\ H \end{matrix} + HSO_3Na \longrightarrow CH_2(OH)SO_3Na \quad (4)$$

The mixture was stirred for 15 minutes at room temperature to allow sufficient time for the complexing to occur. The unreacted thiosulfate then was determined with the standard triiodide solution.

The use of barium chloride in a titration method to determine sulfate was suggested in the literature by Fritz and Freeland.[9] This method depends upon a color change in the indicator Alizarin Red-S which acts as an adsorption indicator in the presence of a barium sulfate precipitate. In solution the alizarin anion was yellow; but on the surface of suspended barium sulfate and in the presence of excess barium ion, the alizarin complexed with the barium ion to give a red color to the suspended solid. In using the procedure outlined by Fritz and Freeland, however, the method was limited to concentrations of sulfate greater than 20×10^{-3} *M*. It was necessary, then, to modify the procedure in applying it to the concentrations of sulfate down to 4×10^{-3} *M*. After several tests, it was noted that the limit of detection of sulfate was determined by the amount of precipitate available for adsorption of alizarin. Too small a quantity of precipitate, although colored red with complexed alizarin, was not perceptible through the yellow color of the alizarin in solution. Therefore, by adding a quantity of semi-colloidal barium sulfate suspended in methyl alcohol to the titration mixture, it was possible to detect the end-point with an accuracy of 1 or 2%. A further improvement in detecting the end-point was to pass an intense light beam through the suspension during the titration. This aided in bringing out color changes more sharply.

To determine the sum of the sulfite and sulfate concentration by the above method, it was first necessary to oxidize the sulfite to sulfate by means of the triiodide ion. The amount of triiodide needed was determined by a starch end-point; but there was some uncertainty as to the effects of the starch on the subsequent sulfate titration. Therefore, it was decided to avoid using the starch by first running a blank to determine the exact triiodide requirement and then adding

(6) F. J. Welcher, "Organic Analytical Reagents," D. Van Nostrand Co., New York, N. Y., 1948.

(7) I. M. Kolthoff and G. Cohn, *J. Biol. Chem.*, **148**, 711 (1943).

(8) J. Rosin, "Reagent Chemicals," D. Van Nostrand, New York, N. Y., 1937.

(9) J. S. Fritz and M. Q. Freeland, *Anal. Chem.*, **26**, 1593 (1954).

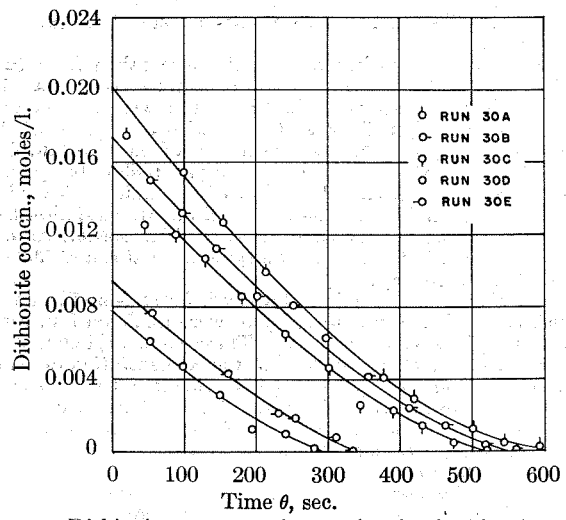

Fig. 1.—Dithionite concentration *vs.* time in air oxidation at atmospheric pressure and 30°.

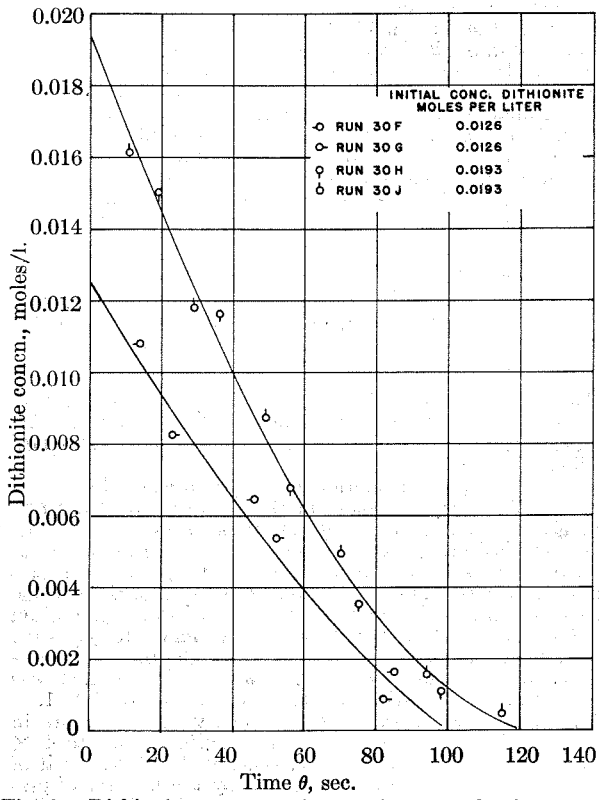

Fig. 2.—Dithionite concentration *vs.* time at 30° using pure oxygen at atmospheric pressure.

the same amount in the absence of starch to a fresh sample buffered at a *p*H of about 5 as specified above. Following the oxidation of the sulfite, the buffered solution was acidified to a *p*H of about 3.5 with 20 weight% acetic acid. The volume of acetic acid required was about equal to the volume of the original sample. Then methyl alcohol containing a semi-colloidal suspension of barium sulfate was added in an optimal amount equal to 38% by volume of the final mixture. With constant stirring, 90% of the estimated 0.1 *M* barium chloride requirement was added rapidly followed by 3 to 5 drops of 0.020 weight % alizarin-red solution. The final titration was performed slowly with an interval of 3 to 5 sec. between drops of barium chloride solution.

Finally, in determining the concentration of sulfate alone, the sulfite was complexed by addition of formaldehyde. The subsequent barium chloride titration was not affected adversely by the presence of the formaldehyde.

All the standard solutions used in the foregoing analyses were prepared and standardized according to the procedures outlined by Swift.[10]

Results

Rate Studies.—Rate data obtained at 30° are shown in Fig. 1, in which the concentration of dithionite in moles per liter is plotted against time in seconds. A tabulation of these data along with results at 40, 50 and 60° is available.[11] Initial concentrations of dithionite ranged from 5×10^{-3} to 20×10^{-3} mole/liter. The rate of change of concentration was large in the initial stages but decreased continuously and rapidly as the concentration decreased.

In the determination of the order of the reaction with respect to dithionite, the oxygen concentration was held constant for a given temperature. Only for those experiments in which the order with respect to oxygen was to be determined was the oxygen concentration varied. Still maintaining atmospheric pressure, pure oxygen was used as a replacement for air to give nominally a fivefold increase in oxygen concentration. For an assumption of Henry's law, the concentration ratio of dissolved oxygen in equilibrium with the pure gas at atmospheric pressure to dissolved oxygen in equilibrium with air at atmospheric pressure would be 4.8. This same ratio was assumed for the very dilute dithionite solutions in which the total gas pressure was at the atmospheric level. For the equipment used, this method of varying the partial pressure of the oxygen in the gas phase was preferred to a method in which the total pressure on the system would have been varied.

It was found experimentally that the initial rate of the reaction was increased by a factor of 5 when pure oxygen was substituted for air, all other conditions remaining the same. Therefore, the reaction was believed to be first order with respect to molecular oxygen. Figure 2 shows rate data obtained at 30° when pure oxygen was bubbled through the system with the total pressure being atmospheric. Those results have also been tabulated.[11] The figure may be compared with Fig. 1 for the case in which air was used.

Two procedures were available for analyzing the data in the determination of initial rates. An initial concentration could have been established by use of solubility data obtained as explained in Experimental Procedure. Also an initial concentration could have been obtained by extrapolation of the concentration–time curve back to zero time. Inasmuch as sampling of the reactor was usually begun only 30 to 50 sec. after zero time, the use of the extrapolation technique was satisfactory. The extrapolation method was preferred because of the need for exact control of equilibrium conditions in the event that the solubility data were used.

(10) E. H. Swift, "Systematic Quantitative Analysis," Prentice-Hall, New York, N. Y., 1939.

(11) R. G. Rinker, T. P. Gordon, D. M. Mason, R. R. Sakaida and W. H. Corcoran, Am. Doc. Inst., Washington 25, D. C., Document 6104 (1959). A copy of this document may be secured by citing the document number and by remitting $2.50 for photoprints or $1.75 for 35 mm. microfilm. Advance payment is required. Make checks or money orders payable to: Chief, Photoduplication Service, Library of Congress.

After the initial concentration was determined by extrapolation, initial rates were obtained by plotting slopes of concentration–time curves as a function of time for each initial concentration. Extrapolation to zero time produced the initial rates. These compared satisfactorily with the values obtained by drawing tangents to the concentration–time curves at zero time.

From a knowledge of the initial rates and concentrations, the order n of the reaction with respect to dithionite was obtained. The relationship used in this determination applied at time zero was

$$-\frac{dC}{d\theta} = k_c[C]^n \qquad (5)$$

in which C is the concentration of dithionite in moles per liter; θ is the time in seconds; and k_c is the specific reaction rate constant which includes the constant concentration of oxygen.

A plot of log C *vs.* log $(-dC/d\theta)$ for initial conditions is shown in Fig. 3 for runs at 30°, and the data have been recorded[11] along with those obtained at 40, 50 and 60°. The slopes of the best straight lines through the points at each temperature were calculated to be 0.50 ± 0.04, which was near enough to 0.5 to indicate that the reaction was one-half order with respect to dithionite. The purpose of obtaining n for conditions at zero time was to eliminate any possible effects of reaction products or side reactions in masking the true order of the initial reaction. A discussion of these effects is given later in the section on Product Analysis.

The integrated form of equation 5 was used to obtain values of k_c as a function of time, and the unsmoothed data were used in the computations. Integration of equation 5 gives

$$k_c = \frac{2}{\theta}\left[C_0^{1/2} - C^{1/2}\right] \qquad (6)$$

It was found that k_c calculated from equation 6 drifted slightly as a function of time when calculated for various points up to 50% completion of the reaction, but the variation was smooth and linear. A typical plot for data at 30° is shown in Fig. 4, and tabulations of these results together with those at 40, 50 and 60° have been made.[11] The curves for k_c, when extrapolated to time zero, converge to a range of values well within experimental accuracy. Because the values for k_c varied with reasonable smoothness the procedure of using unsmoothed data in the calculation appeared satisfactory. Figure 4 also shows a value of $k_{c_{av}}$, which is the arithmetic average of k_c at zero time and includes the concentration of oxygen. The oxygen dependence can be eliminated, however, by dividing $k_{c_{av}}$ by the saturation concentration of oxygen, which for the dilute solutions studied here was taken as the saturation concentration in pure water.[12] That calculation was made, and the resulting value of specific reaction rate at zero time and independent of the oxygen concentration was designated as k_c^0. Its value at 30° is listed in Fig. 4 and also in Table I with values at 40, 50 and 60°.

(12) N. A. Lange, "Handbook of Chemistry," 7th edition, Handbook Publishers, Inc., Sandusky, Ohio, 1949.

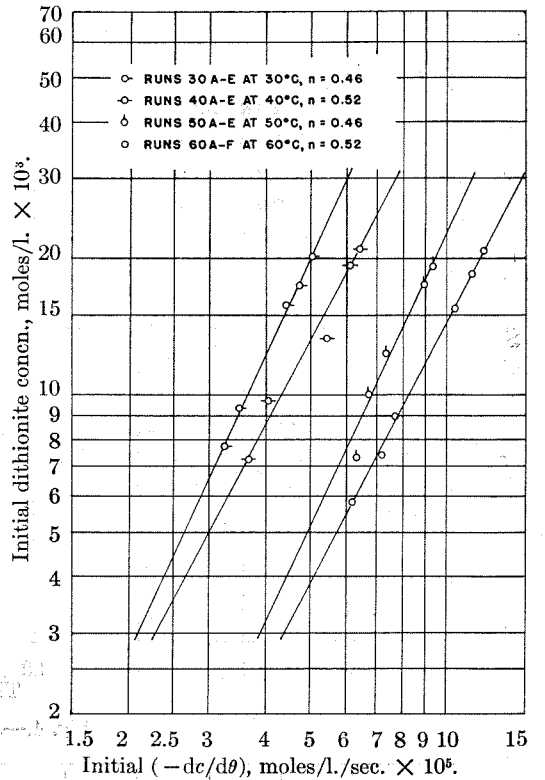

Fig. 3.—Log C *vs.* log $(-dc/d\theta)$ for initial conditions at 30, 40, 50 and 60° at atmospheric pressure.

TABLE I

MEAN VALUES OF k_c^0, SPECIFIC REACTION CONSTANT AT ZERO TIME AND INDEPENDENT OF OXYGEN CONCENTRATION

t, °C.	k_c^0, (moles/l.)$^{-1/2}$ sec.$^{-1}$
30	0.151
40	.214
50	.372
60	.565

A correlation of the rate constants with temperature was made by use of the Arrhenius equation. The simple form of the equation was used where

$$k_c^0 = Ae^{-\Delta E/RT} \qquad (7)$$

The constants were evaluated by use of a plot of the data in Table I. A value of 9.3 kcal./mole was obtained for ΔE, and the frequency factor was found to be 7.2×10^5 (moles/l.)$^{-1/2}$ sec.$^{-1}$.

Product Analyses.—Table II lists the experimental results for the analyses of end products. As indicated in the Experimental Procedure, data were obtained from reactions conducted in flasks and in the reactor vessel. For the reactions conducted in the flasks, the molal ratio of sulfite to sulfate was found to be 2.3. In the case of the analyses of the end products in the reactor, the ratio was more nearly 3.0. Such a large difference between the two ratios was due primarily to the difference in reaction time. Whereas the flask reactions required approximately 29 hours for completion, the reactor runs were completed

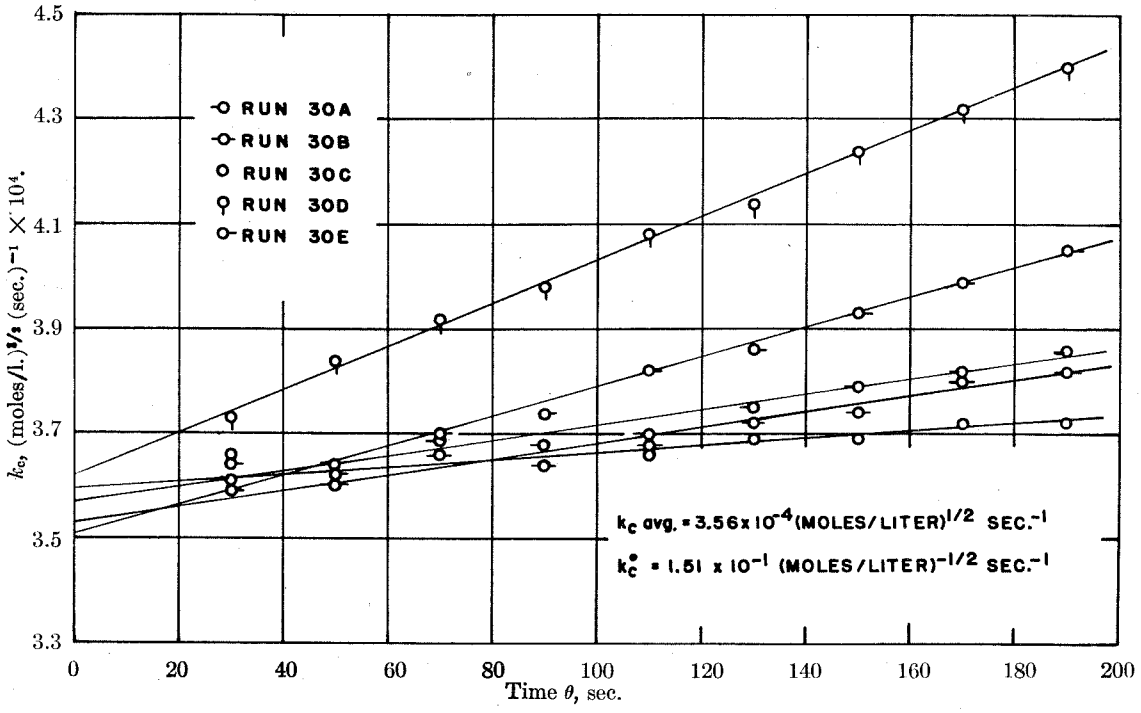

Fig. 4.—k_c *vs.* time at 30°.

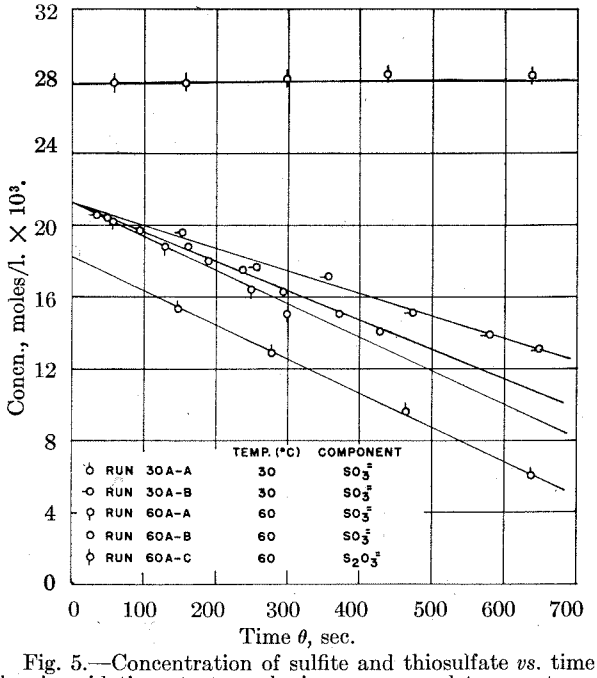

Fig. 5.—Concentration of sulfite and thiosulfate *vs.* time in air oxidation at atmospheric pressure and temperatures of 30 and 60°.

in about 300 seconds. During the relatively long time in the flasks, the oxidation of sulfite to sulfate was undoubtedly significant. In comparison to the rate of dithionite oxidation, under identical conditions, the oxidation of pure sulfite was quite slow as may be noted by comparing Fig. 1 with Fig. 5. This lower rate was also observed when at the completion of dithionite oxidation the air flow was allowed to continue for 10 to 15 minutes with no significant change in the sulfite–sulfate ratio. There was no real assurance, however,

TABLE II

END PRODUCT ANALYSES

Air oxidation of dithionite at room temperature and atmospheric pressure, concentrations in moles per liter

		Run EP-A[a]	Run EP-B[b]	Run EP-C[b]
Initial	$[S_2O_4^=]$	10.30×10^{-3}	9.50×10^{-3}	10.10×10^{-3}
Final	$[SO_4^=]$	5.72×10^{-3}	4.16×10^{-3}	4.26×10^{-3}
Final	$[SO_3^=]$	13.14×10^{-3}	13.16×10^{-3}	11.90×10^{-3}
Final	$[S_2O_3^=]$	1.60×10^{-3}	0.42×10^{-3}	1.00×10^{-3}
Final	$\frac{[SO_3^=]}{[SO_4^=]}$	2.3	3.16	2.78

[a] Reaction time of 29 hr. in non-stirred flasks. [b] Experiments conducted with agitation and air flow so that diffusion was not controlling. Analysis for EP-B was corrected for 8.8% thermal decomposition and that for EP-C for 21%.

that in the presence of dithionite ions or transient intermediates the sulfite oxidation was not catalyzed. Indeed, the oxidation of sulfite to sulfate by molecular oxygen has been shown to be catalyzed by free radicals.[13] The presence of appreciable amounts of sulfate in the reaction products suggests that catalysis was occurring. The observed ratio of sulfite to sulfate of 3 to 1 sets an upper limit of 25% conversion of sulfite to sulfate by catalyzed air oxidation.

As shown in Table II, thiosulfate in small but measurable quantities was also among the products. There seems to be no explanation of its formation unless it is assumed that a secondary reaction involving thermal decomposition occurred simultaneously with the air oxidation. As the product of a secondary reaction, it accounted for nearly 10% of the dithionite disappearance for a temperature of 30°. This is based upon the stoichiometry of the thermal decomposition in which the two major products are sulfite and thiosulfate. Prob-

(13) H. N. Alyea and H. L. J. Backstrom, *J. Am. Chem. Soc.*, **51**, 90 (1929).

ably the secondary reaction was the greatest single factor contributing to the drift in the rate constant k_c.

The stability of thiosulfate in the basic solution and in the presence of molecular oxygen was established by the absence of sulfide and tetrathionate in the end products, and also by the fact that the thiosulfate concentration in the flask reactions remained constant up to 100 hours after the depletion of the dithionite. Further evidence for the very slow oxidation of thiosulfate was obtained when a 0.028 M solution was subjected to the same conditions of temperature, stirring, and air flow in the reactor that existed for dithionite oxidations. No significant oxidation was measured for times up to 15 minutes as may be seen in Fig. 5. Data for runs at both 30 and 60° have been recorded.[11]

Diffusion Effects.—As stated in the experimental procedure, the rate of air or oxygen discharge through the frit into the reacting mixtures was varied from 2500 to 3000 cc./min. Preliminary tests showed, however, that an air rate of only 1200 cc./min. was sufficiently high to oxidize the dithionite independently of the air rate. Therefore, reproducibility of tests was not affected by variable air rates greater than 1200 cc./min. The rate of stirring (approximately 1100 r.p.m.) in the reactor was rapid enough to maintain an isothermal, homogeneous mixture. A stirring rate of only 800 r.p.m., coupled with an air rate of 1200 cc./min. gave the same results within experimental error as a stirring rate of 1100 r.p.m. and an air rate of 2500 cc./min., all other conditions being the same. Figure 6 shows the effects of stirring rate and air flow in the dithionite oxidation, and tabular data are also available.[11] In the figure, the concentration of dithionite as a function of time for the same initial concentration at 60° and a stirring speed of 800 r.p.m. is shown for different air rates. As the air rate increased to 1200 cc./min., the curves moved close to an asymptotic curve which established the lower limits of operation. Data obtained at 2500 cc./min. and 1100 r.p.m. are shown for comparison. The fact that the curves of Fig. 6 differed indicated that diffusion of oxygen to a point in the system was a controlling factor in the rate of oxidation for air rates less than the asymptotic value of 1200 cc./min. at the stirring speed of 800 r.p.m. In the oxidation of the dithionite, the greatest demand for oxygen occurred at the highest temperature, which was 60°, and at the maximum initial concentration of dithionite, which was approximately 20×10^{-3} M. The tests represented by Fig. 6 were performed at nearly the extreme conditions of demand, as noted above, except that the initial concentration was only 12×10^{-3} M. The experimental data for the runs at concentrations higher than 12×10^{-3} M were consistent with data obtained for runs below this concentration. It was therefore assumed that for the air rates and stirring speeds used throughout the experimental work the diffusion of oxygen was not a controlling factor.

Effects of Ionic Strength.—Data obtained at 60°, as shown in Fig. 7 and recorded elsewhere,[11] show that the rate of reaction did not change upon

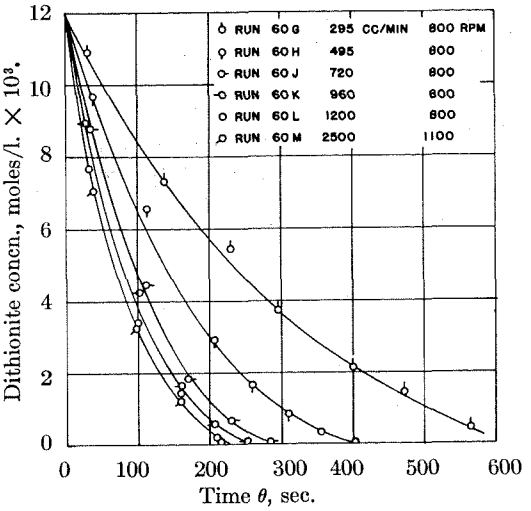

Fig. 6.—Effects of air flow and stirring rate on concentration of dithionite as function of time in oxidation at atmospheric pressure and 60°.

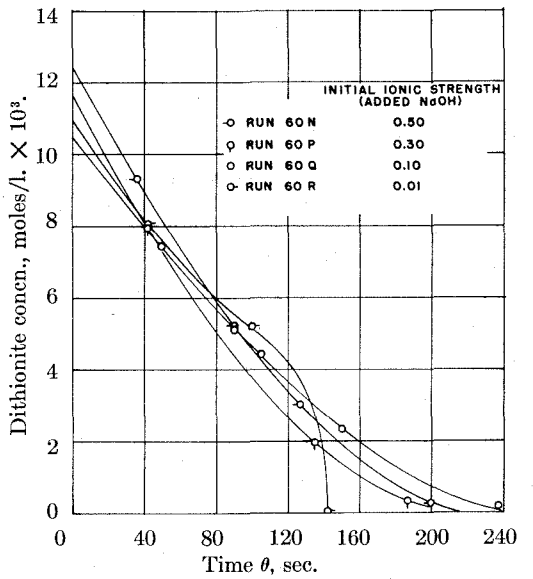

Fig. 7.—Effects of ionic strength in air oxidation of dithionite at atmospheric pressure and 60°.

increasing the concentration of sodium hydroxide, and hence the ionic strength, by factors of three and five. The result in that figure for an experiment conducted in 0.01 M sodium hydroxide appears anomalous. It is almost certain that the different course of reaction resulted from thermal decomposition when the hydrogen ion which was generated neutralized the sodium hydroxide.

***p*H and Effects of Metal Ions.**—The *p*H of the dithionite solutions changed approximately from 13 to 12.8 for the highest initial concentration of 20×10^{-3} M. This change indicated that hydrogen ion was generated as one of the products of reaction. No detailed study of the variation in *p*H was made for the air oxidation of dithionite.

No careful study was made to determine the effects of metal ions on the oxidation of dithionite. It was observed, however, in a qualitative way, that mercury in minute quantities caused the reaction to become erratic. A reasonable suggestion

is that the mercury reacted to form complexes such as $Hg(SO_3)_2^{=}$.

Solubility Studies.—In measurements of the solubility of sodium dithionite in water at 0°, the average value of 11 determinations was found to be 13.20 g. per 100 g. of water with a standard deviation of 1.08 g. per 100 g. of water or about 8%. Yost[14] lists a value of 12.85 g. per 100 g. of water at 1°, and Rao and Patel[15] list 11.86 g. per 100 ml. of solution at 0°. Neither of those experimenters give any limits of error.

Discussion

A mechanism which satisfies the established order of reaction with respect to dithionite and oxygen and in which the initial step was dissociation of dithionite[16] is given as

$$S_2O_4^{=} \rightleftarrows 2SO_2^{-} \qquad (8)$$

$$SO_2^{-} + O_2 \longrightarrow \text{Products} \qquad (9)$$

The first step which is shown as equation 8 reaches equilibrium rapidly, and the second step presented as equation 9 is relatively slow and thus rate determining. Thus the observed reaction rate may be described as

$$r_{obsd} = k_2[SO_2^{-}][O_2] \qquad (10)$$

where r_{obsd} is the reaction rate in moles per liter per second; k_2 is the specific rate constant in moles-liters-seconds units; $[SO_2^{-}]$ is the concentration of SO_2^{-} in moles per liter, and $[O_2]$ that of oxygen in moles per liter.

A relationship between the observed experimental specific reaction rate constant, k_c^0, and the rate constant given in equation 10 may be obtained by noting the rapid achievement of equilibrium for the reaction given in equation 8 and the rate-determining character of the reaction given by equation 9. For equation 8 the equilibrium constant may be written as

$$K_c = \frac{[SO_2^{-}]^2}{[S_2O_4^{=}]} = \frac{k_1}{k_{-1}} \qquad (11)$$

In this relationship K_c has the units of moles/liter. If the value for the quantity $[SO_2^{-}]$ obtained from equation 11 is substituted in equation 10, the rate expression may be written as

$$r_{obsd} = k_2K_c^{1/2}[S_2O_4]^{1/2}[O_2] \qquad (12)$$

The experimentally determined rate constant, k_c^0, is then related to k_2 and K_c by the expression

$$k_c^0 = k_2K_c^{1/2} \qquad (13)$$

As noted in the section on Results the variation of k_c^0 with temperature permitted the calculation of an Arrhenius activation energy of 9.3 kcal./mole and a frequency factor of 7.2×10^5 (moles/l.)$^{-1/2}$ sec.$^{-1}$. If it is assumed that the rate-determining step involved an electron transfer to form O_2^{-} and SO_2, the observed activation energy of 9.3 kcal./mole would appear high. Uri[17] has correlated data for a number of exothermic electron-transfer-reactions and found typical activation energies to lie between 0 and 5 kcal./mole. The experimentally observed value of 9.3 kcal./mole, however, does include a contribution from the equilibrium step described by equation 8. If approximate values of frequency factors obtained from Frost and Pearson[18] are used, order-of-magnitude calculations can be made for the limiting contributions of the equilibrium and rate-determining steps to the observed activation energy. The calculations are

$$k_c^0 = k_2K_c^{1/2} = \frac{k_2k_1^{1/2}}{k_{-1}^{1/2}} \qquad (14)$$

Then in the Arrhenius form, equation 14 may be rewritten as

$$A_c^0e^{-\Delta E_c^0/RT} = A_2e^{-\Delta E_2/RT}\left[\frac{A_1e^{-\Delta E_1/RT}}{A_{-1}e^{-\Delta E_{-1}/RT}}\right]^{1/2} \qquad (15)$$

If the logarithm is taken of both sides, equation (16) results

$$\ln A_c^0 - \frac{\Delta E_c^0}{RT} = \ln A_2 - \frac{\Delta E_2}{RT} + {}^1/_2 \ln\left(\frac{A_1}{A_{-1}}\right) - {}^1/_2\left[\frac{(\Delta E_1 - \Delta E_{-1})}{RT}\right] \qquad (16)$$

A combination of terms then gives

$$\Delta E_c^0 - RT\left[\ln\frac{A_c^0}{A_2} - {}^1/_2 \ln\frac{A_1}{A_{-1}}\right] = \Delta E_2 + {}^1/_2(\Delta E_1 - \Delta E_{-1}) \qquad (17)$$

Frost and Pearson suggest a value of 10^6 to 10^7 (moles/l.)$^{-1/2}$ sec.$^{-1}$ for A_2, 10^{13} sec.$^{-1}$ for A_1, and 10^5 to 10^6 (moles/l.)$^{-1/2}$ sec.$^{-1}$ for A_{-1}. If the value of 9.3 kcal./mole is substituted for ΔE_c^0 and a rounded value of 7×10^5 (moles/l.)$^{-1/2}$ sec.$^{-1}$ for A_c^0, then

$$\Delta E_2 + {}^1/_2(\Delta E_1 - \Delta E_{-1}) = 15 \text{ kcal./mole} \qquad (18)$$

These order-of-magnitude calculations place limits on the value of ΔE_2 and $(\Delta E_1 - \Delta E_{-1})$ as

$$0 \leqslant \Delta E_2 \leqslant 15 \text{ kcal./mole} \qquad (19)$$
$$0 \leqslant (\Delta E_1 - \Delta E_{-1}) \leqslant 30 \text{ kcal./mole}$$

If a mean value is assumed for ΔE_2 based on Uri's[17] values of 0–5 kcal./mole, for an electron-transfer reaction, a rough estimate can be made of K_c and k_2 in the equation given above. If a value of 3 kcal./mole is assumed for ΔE_2, then K_c is found to be 8×10^{-11} mole/l. and k_2 is therefore 2×10^4 (moles/l.)$^{-1}$ sec.$^{-1}$. These values for K_c and k_2 are, at best, order-of-magnitude estimates.

The order of reaction of the air oxidation with respect to dithionite and molecular oxygen determines the composition of the transition state in the rate-determining step. That is, the activated complex must consist of one molecule of SO_2^{-} and one molecule of O_2. Further information about the geometry of the activated complex or the products which result from its decomposition cannot be inferred with certainty from the present data. Knowledge of the composition of the transition state and the composition of the end products does, however, place a reasonable limit on the number of mechanisms which might be proposed for the intermediate steps. Two

(14) D. M. Yost and H. Russell, "Systematic Inorganic Chemistry," Prentice-Hall, Inc., New York, N. Y., 1944.

(15) M. R. A. Rao and C. C. Patel, *Proc. Nat. Inst. Sci. India*, **19**, 211 (1953).

(16) R. G. Rinker, T. P. Gordon, D. M. Mason and W. H. Corcoran, THIS JOURNAL, **63**, 302 (1959).

(17) N. Uri, *Chem. Revs.*, **50**, 375 (1952).

(18) A. A. Frost and R. G. Pearson, "Kinetics and Mechanism," John Wiley and Sons, Inc., New York, N. Y., 1953.

possibilities are suggested immediately for the rate-determining step

$$SO_2^- + O_2 \rightleftharpoons \text{complex A} \xrightarrow{k_2} SO_4^- \quad (20)$$

or

$$SO_2^- + O_2 \rightleftharpoons \text{complex B} \xrightarrow{k_2} SO_2 + O_2^- \quad (21)$$

It is not inconceivable that both of these mechanisms could occur. Both free radical intermediates, SO_4^- and O_2^-, have ample precedent in the literature.[17] End product analysis does, however, exclude the mechanism given in equation 20 from being the only mechanism by which the activated complex is decomposed. Subsequent steps would almost certainly be of the type

$$SO_4^- + SO_2^- \longrightarrow SO_4^= + SO_2 \quad (22)$$

which would lead to a sulfite-to-sulfate ratio of unity in the reaction products. The mechanism given by equation 21 leads to a series of free-radical intermediates of hydrogen peroxide. The following series of reactions may be written as a suggestion

$$S_2O_4^= \rightleftharpoons 2SO_2^-$$

$$SO_2^- + O_2 \rightleftharpoons \text{complex B} \xrightarrow{k_2} SO_2 + O_2^-$$

$$SO_2^- + O_2^- \xrightarrow{k_3} SO_2 + O_2^=$$

$$O_2^= + H_2O \xrightarrow{k_4} HO_2^- + OH^-$$

$$HO_2^- + SO_3^= \xrightarrow{k_5} SO_4^= + OH^- \quad (23)$$

$$HO_2^- + SO_2^- \xrightarrow{k_6} SO_3^= + OH$$

$$OH + SO_2^- \xrightarrow{k_7} SO_2 + OH^-$$

$$SO_2 + OH^- \xrightarrow{k_8} SO_3^= + H^+$$

$$1/2SO_3^= + 1/4O_2 \xrightarrow{k_9} 1/2SO_4^=$$

These equations lead to the observed over-all stoichiometry and by suitable choice of kinetic constants could be shown to be kinetically consistent. The summation of the scheme is that the peroxide intermediates which are formed on a mole for mole basis by the decomposition of dithionite can react either with sulfite molecules already formed to form sulfate or with SO_2^- radical ions to form more sulfite and regenerate peroxide intermediates. Since the concentration of sulfite ions in solution greatly exceeds that of SO_2^- ions after the first second of the reaction, the preponderance of sulfite rather than sulfate in the products requires that $k_6 >> k_5$ in the above scheme. A steady-state concentration of intermediates need not be postulated in this hypothetical analysis.

Acknowledgment.—Funds for this research on dithionite chemistry were mainly provided through a general grant from the Shell Companies Foundation. In addition, fellowship support was given by the Union Carbide Corporation and the Monsanto Chemical Company. The help of all is gratefully acknowledged.

PROPOSITIONS

1. The catalytic decomposition of NO should be studied with helium as the inert gas.

   a. The effect of pressure can be studied without being affected to any great extent by the adsorption of the inert gas.

   b. The relative importance of N_2 and NO as adsorbed components on the catalyst surface can be clarified.

2. The heat loss from a wire located axially in a thermostated tube through which gas passes in laminar flow at steady state is given by:

$$q = \frac{2\pi Lk(t_w - t_t)}{\ln D_t/D_w} = I^2R$$

The equation was found to apply to within 2% (1) for wire temperatures up to 120°C and for gas and tube temperatures maintained at about 25°C. With use of the above equation, the minimum concentration of a component detectable in a thermal conductivity cell, as used in a gas chromatography apparatus can be calculated.

NOMENCLATURE

D - Diameter
I - Current Through Wire
k - Thermal Conductivity of the Gas
L - Length of Wire
q - Rate of Heat Transfer
R - Resistance of Wire
T - Temperature

Subscripts
t - tube
w - wire

3. In the chromatographic analysis of mixtures containing NO, NO_2 and N_2, there are several phenomena that require further study and experimentation.

   a. A hypothetical mechanism for NO-N_2 separation on silica gel is presented in the thesis. The following studies are proposed to test this mechanism: Close control in the variation of column conditioning procedures, tagged nitrogen exchange,

and a study of the orientation of an NO_2 molecule on the surface of silica gel.

b. Although NO_2 is separable from NO and N_2 by using silica gel, the resulting elution peak is not quantitatively reproduced. It is, therefore, suggested that attempts be made to reduce NO_2 to NO by means of a reducing column which precedes a silica gel column. Mixtures of small amounts of NO_2 in N_2 as well as NO and NO_2 in N_2 can then be analyzed.

4. A study of the polymerization of olefins and dienes with ($S_2O_4^{=}$) as a catalyst may prove to be of interest.

5. The fitting of equations to data points is often done by least squares methods. In some cases, attempts are made to fit equations with interrelated constants to experimental data. A least squares program for use with a digital computer should be written to include such interrelated constants.

6. Flare fittings are commonly used to connect metal tubing. When the flare fittings and tubing are fabricated from stainless steel, the use of ductile metal gaskets will substantially facilitate the construction of unions which are to maintain pressures above 50 psi.

7. A syringe needle for blood sampling and transfusion should be so constructed that, for a patient who periodically needs frequent blood sampling within short periods of time, the needle can be left in the patient's arm.

8. It is proposed that a study be made of the physiological effects of various gaseous substitutes for N_2 in the atmosphere to determine whether or not mental and/or physical activities can be increased or decreased.

9. The sole purpose for the existence of red cells is for the transport of oxygen and carbon dioxide by means of hemoglobin (2). Exchanges of the gases in the capillaries occur simply by diffusion with the concentration gradient of the gases as the driving force. Since the cell, itself, is extant only for containing hemoglobin in distinct units, it is proposed that effort be directed towards the synthesis of substitute red cells.

10. Oftentimes it is found necessary to reinsert a typed page into a typewriter. A simple guide should be attached to or adjustment be made to the sheet-alignment bar of a typewriter such that pages can be replaced identically with minimum effort or guesswork. A half-space device should also be available to facilitate the typing of consistent subscripts.

REFERENCES

1. Peterson, A. C., Madden, A. J., and Piret, E. L., Ind. Eng. Chem., 46, 2038-2040 (1954).

2. "A Symposium on the Blood and Blood-Forming Organs," 83, The University of Wisconsin Press, Madison, 1939.